Progress in Sensory Devices of Pesticides, Pathogens, Coronavirus, and Chemical Additives and Hazards in Food Assessment: Food Safety Concerns

M. A. Shenashen[a], M. Y. Emran[a], A. ELSabagh[b], M. M. Selim[b], A. Elmarakbi[d], S. A. El-Safty [a,*]

[a] National Institute for Materials Science (NIMS), 1-2-1 Sengen, Tsukuba-shi, Ibaraki-ken 305-0047, Japan

[b] Department of Field Crops, Faculty of Agriculture, Siirt University, 56100, Kezer Campus/Siirt/TURKEY

[c] Al-Aflaj College of Science and Human Studies, Prince Sattam Bin Abdulaziz University, Al-Aflaj, 710-11912, Saudi Arabia

[d] Faculty of Engineering and Environment, Northumbria University, Newcastle upon Tyne, NE1 8ST, UK

*Correspondence: sherif.elsafty@nims.go.jp; https://samurai.nims.go.jp/profiles/sherif_elsafty

Content ***Page***

Abstract

Food intake gives vitality and supplements to support humans and other living organisms. Food safety and contamination problems associated with food hygiene, storage, chemical additives, enzymes, bacteria, and pesticides are crucial issues because of their direct influence on the health of humans and even animals. New monitoring technologies should be developed for potential food safety and significant environmental benefits. To date, the ultrasensing, early detection, and real- and on-time monitoring of vital reactive species, biomolecules, chemicals, and hazardous agents are important in ensuring food quality. With significant advances in the engineering of sensory devices, the progressive development of accurate quantity screening, early explicit monitoring and assessment, and real-time detection analysis can support the standard food quality through the full control of an extraordinary food safety test. Progress in numerous auto-examining appraisals, sensing protocols, and tools of (i) reactive species and chemical additives associated with human metabolism and various nutritional and industrial processes of foods, including ascorbic acid (AA), H_2O_2, uric acid (UA), and nitrite and sulfite anions; (ii) extremely organic and inorganic hazards such as heavy metals and bisphenol A; and (iii) food adulteration, pesticides, pathogenic microorganisms are a key challenge for food safety concerns. To date, evidence supporting the possibility of transmitting coronavirus disease 2019 (COVID-19) infection through food products is unavailable. However, in a report on an outbreak in mid-June 2020 in China, food contamination with the causative agent of COVID-19 pandemic, SARS-CoV-2, was discovered. Thus, sensory protocol devices for monitoring the SARS-CoV-2 antigen associated with food products is urgently needed for the future perspective progress in health. As such, we provide details in advanced sensor development in the monitoring, analysis, and evaluation sectors for food safety applications. We also report on next-generation

nano/microscale wearable sensor devices that can wirelessly provide relevant healthy and safety food information data. This review gives evidence that the powerful engineering of mobile food sensor devices is an ongoing acquisition, offering considerable future avenues to the perspective in-home healthcare of aging individuals.

Keywords: food safety, monitoring, assessment; food reactive species; bacteria; pesticides; wearable touchscreen sensor devices; COVID-19; food healthcare

1. Introduction

Food safety remains one of the most vital issues worldwide because the presence of hazardous species or even urgent additives with risky levels of food poses a real risk to food safety and healthcare. The World Health Organization (WHO) pointed out that foodborne diseases negatively affect the economies of underdeveloped countries. In developing countries, food safety is linked to many different diseases and disorders, such as diarrhea, which leads to about 3 million deaths [1-3]. Therefore, food safety has been recorded as a high priority by the WHO. However, according to a report of the Centers for Disease Control and Prevention, approximately 48 million Americans consume contaminated food and that 3,000 die of foodborne diseases in the United States [2, 3].

With the increasing interest in the food industry, high-quality products with high safety rates have become urgently needed. Therefore, food and quality control systems should be established to meet food safety requirements and maximize the financial profits of food companies. In food markets, many major companies have to ensure the improvement of a quality assurance and controlled production line to avoid losses because of sanctions, product withdrawal, and customer trust loss in brand names [4]. Nanotechnology offers enormous advantages in the growth of food sensor

electronics and identification protocols of different target species and pollutants for food safety and quality evaluation. Various evaluation strategies based on chemical/biological sensors can be used online and are coordinated in the current assembly as quick, basic, and versatile sensors for food species that affect food quality and safety. Commercially available monitors or nano/microsensor devices provide real-time continuous measurement of food ingredients, nutrients, byproducts, pesticide residues, pathogenic microorganisms, chemical food additives, hazards, preservatives, food contaminants, packaging, and other wastes [5]. Current progresses in the design and manufacture of food-based sensors offer great advantages in sensing food contaminants. Moreover, great efforts have been devoted to developing food sensors that feature cost-effectiveness, short response time, and low complexity.

Surveying and estimating the level of definite target molecules in food significantly affect the analysis and prediction of risks to human health [4-6]. Disproportionate qualities and changes in the levels of targeted species, including organic agents, inorganic agents, and biomolecules or their byproducts, threaten human health [7]. Studies have also been performed to improve sensing tools and devices for screening and controlling various targets, including reactive species and additives, such as AA, H_2O_2, UA, and nitrite and sulfite anions. These targeted agents have been produced through transformation in human metabolism or through various nutritional and industrial processes of foods. Moreover, early and real-time monitoring of pathogenic hazardous species, including bacteria, viruses, and pesticide residues, in food have a considerable key factor in food safety assessments [8-10]. Furthermore, global restrictions on tracking and packaging food processes and eating or handling food (including frozen food) via surface touching from individuals have been implemented to avoid the spread of COVID-19 pandemic. Therefore, the development of food-based sensory and screening tools of these targeted agents, hazardous species, and SARS-CoV-2 antigens are vital in food analysis and environmental and health monitoring [8-11]. The early recognition, real-time assessment, and

detection protocols of SARS-CoV-2 antigens, pathogenic microorganisms, toxic species, food additives, and pesticides in food play an essential role to ensure human healthcare. To date, great developments have been achieved to manufacture effective and operative sensing devices for the assessment of food contaminations and risks.

In this context, this review highlights numerous designs of nanomaterial-based sensors associated with food safety concerns. Demands for smart compact nano/microsensor electronics have increased to overcome low temporal/locative settling and conventional techniques associated with analysis problems. Therefore, studies have developed several sensors design and mobile health monitoring technologies that enable the precise management of the levels of various species affecting the food quality. More specifically, this review provides insights into the current state of the COVID-19 pandemic and its relationship with food quality and various industries. In addition, this review enumerates effective strategies and recent progress in numerous analysis techniques, building blocks of sensor designs, and protocols that serve as a basis for improving the controlled management, risk assessment, and early warning detection of food contaminations associated with food hygiene, storage, chemical additives, enzymes, bacteria, and pesticides. Novel conductive materials used in portable sensor devices offer an extraordinary control of a new generation of developed sensing/detection protocols for food safety management.

2. Prospective assessments for food safety

Researchers and industrial partners have recognized the potential of nanotechnology in different food sectors, including agriculture and farming (e.g., pesticides, fertilizers, and vaccines), food processing, food packaging (preservation and protection), and nutrient supplements. The most dynamic assessment reports in food science are based on the advanced fabrication of nanoscale sensor devices that can be utilized in a diverse range of food safety applications. In this manner, assessment strategies

and apparatuses are utilized in food development, creation, handling, and packaging (Scheme 1A) [5, 12]. To date, the rapid increase in the widespread testing and risk assessment of COVID-19 infection is the major concern of worldwide interest. Thus far, the transmission of COVID-19 infection through food products is not yet confirmed. However, the urgent need for monitoring SARS-CoV-2 antigen associated with food products is unquestionable for inexorably global health protection and food safety.

2.1. Key elements for food assessment protocols

For genuine and favorable food safety management board tools, the development of a mature, reliable, and dependable innovation for next-generation nano-future food management devices is crucial. For food safety and management, sustenance examination should focus on the whole food cycle, which includes the final product, nourishment freshness, strengthening, or dangerous ingredients utilized in food or during food processing and microbiological quality. In any case, a device for the fast and accurate response discovery of targeted concentration levels remains to be developed.

For the progress in health integration and food safety, the well-controlled assessment protocol and large-scale manufacturing of food sensors that can be integrated with the exact transmitter into portable devices are required with the following key controls:

(I) To ensure that the duration of targeted and systematic analysis and improve real-time and continuous monitoring

(II) To reduce complications and serious adverse events of other associated problems

(III) To overcome the restrictions of self-revealing techniques

(IV) To offer logical estimations of food species by tracking physiological operations

(V) To improve methodologies for reading out and sorting tool performance and automatically track and distinguish each target

(VI) To determine the effectiveness of long-term food management practices in indoors and outdoors through continuous supply, along with wireless applications

With regard to the recently created contemporary nanotechnology outskirts and around future proof choices to precise, accurate, reliable, and low-cost individuals, a nanosensory system combined with patch, adaptable, flexible, and intelligent fabrics remains important for managing long-term food safety and healthcare. Such key creative endeavors not only provide a consistent and implantable screening process for target ranges but also permit the complete estimation of controlling food quality or doses and techniques of beneficial food additives.

Scheme 1

2.2. Sensing techniques for food quality and safety

For food quality and safety, chemical sensor techniques are widely used to measure or distinguish physical parameters and changes in reactive species, agents, and contaminant targets into read-out signals through observation or instrument use. Sensors can permit real-time investigation with high sensitivity and selectivity, thereby revolutionizing examination in the food safety field, including agriculture and farming, food processing, food packaging, and nutrient supplements under basic consideration. Progress on sensors can be identified on the basis of different keys, including (i) intrinsic property evaluation (selectivity, sensitivity, sensory detection range, limitation, and lifetime), (ii) economic manufacturability, (iii) new research methods with a fast response, (iv) simple sensing strategy, and (v) real applicability [13, 14]. For example, the construction and engineering of biosensors primarily depend on incorporations between two components, namely, a bioreceptor and a transducer. Bioreceptors immobilize sensitive biological elements (e.g., enzymes, proteins, antibodies, and whole cells) that act as an active interfacial surface, and transducers convert the physiochemical change resulting from the interaction between food reactive targets and biological

elements to a quantified signal, whose intensity is associated with target concentrations [15, 16]. Regarding transducing elements, chemical sensors and biosensors can be categorized into electrochemical (potentiometric, amperometric, and conductometric) sensors, optical (including reflectometry or absorptiometry, fluorescence, and surface plasmon resonance [SPR]) and surface-enhanced Raman spectroscopy (SERS) assay sensors, piezoelectric sensors, and thermal sensors, which can convert reactions or binding with target species into a digital signal (Scheme 1B) [13, 15, 17-19].

Studies should focus on the developmental engineering of powerful nanoscale sensor designs, devices, and protocols for a wide scope of food safety assessments. A considerable progress on sensor device manufacturing provides periodical transduction into easy-to-track output signals, fast response analysis, and dead-end-use examination, leading to the precise assessment of food contamination. Therefore, the integral optimization of nanoscale sensor chipsets into robotics, smartphones, and wearable, patches, and touchscreen devices is the key principle for the future steadfast advancement in sensing, analytical, and biotechnological applications. Portable sensor disciplines offer contamination monitoring and environmental food assessment with short time consumption and simple operation.

3. Nanoscale-developed food sensory platform models

Nanoscale sensor platforms have been developed with 0D–3D materials that have hierarchical engineering, well-controlled shape morphology, surface heterogeneity, molecular arrangement structures, and highly physical/optical/mechanical properties, enabling to improve food target diffusivity, electronic surface charge transfer, and sensitive signaling and absorptivity. These platforms serve as precise environments suitable for sensory designs and effective sensor protocols (Scheme 2) [8, 15, 20-27].

Nanoscale sensory techniques are of great interest because they provide basic solutions to many daily problems, especially in environmental, healthcare, and medical sectors. These techniques improve optical and electronic properties, expand the surface of the transducing range, and increase the surface-to-volume ratio for sensitive reading out signals [28-32]. Moreover, nanomaterials with a highly controlled anisotropic composition and surface functionality can be used to generate modern sensors with special features associated with electrical conductivity, power consumption, weight, and diffusion for the precise and highly sensitive real-time detection of targeted food species [33-39].

In general, nanomaterial-based platforms can provide the following advantages for food sensing protocols [11, 33-44]:

i) high surface-to-volume ratio, which stimulates massive and multidirectional target accessibility

ii) changes in the number of surface-active atoms in the correspondence to defects, such as vertices, which hamper unconventional surface reactivity in sensory signaling

iii) aligned geometries in different dimensions provide surface coordinates with electrical association during target detection

iv) surface modification with a highly reactive stationary platform facilitates the selective reaction of target species with active signaling sites

v) production of highly mechanical, conductive, and stretchable/flexible surface use

Scheme 2

To date, nanoscale materials are important for developing nano/microsensor devices and sensing protocols for target species in food. These nanoscalable monitoring designs provide effective assessment efficiency, signal output, amplification, rapid response, real-time analysis, and

analytical diffusivity [8, 11, 29, 30, 35, 38, 39, 41, 42, 45]. To date, nanoscale structure-based sensors show real evidence as alternative devices for the rigorous analysis of the final quality, sensitivity, and other complex features (Scheme 2). Given the great technological advances in material platforms, nanoscale sensory designs provide insights into the following key processing features [15]:

(i) hierarchical superstructures and three-dimensional (3D) architecture geometrics for outstanding electronic and conductive signaling devices

(ii) well-defined atomic-scale configurations and orientation structures, offering actively dense, high-index exposure facets, and versatile binding to ultra-traces of glucose

(iii) surface topographies, interfaces, and vicinities with entirely and diversely interior-space pores as transport gates for the multidiffusive accommodation of glucose targets and nonresistance movements of electrons/charges along surfaces

(iv) multidimensional arrangements and directional alignment around longitudinal and lateral axes for dense electron/charge transfer scales

Nanostructured material platform-based devices with multicomponent metal/nonmetal/metalloid hybrids and composites, interesting morphologies, electronic, optical, electrochemical, and conductive properties, high stabilities and surface activities, and flexible, stretchable, and compact size with low-power consumption can be used to develop diverse sensor devices for monitoring biomolecules, pesticides, pathogens, coronaviruses, chemical additives, and hazardous substances in food products. These nano/microscale sensor devices and protocols may have the following individual basic attributes in the improvement of food assessment:

(i) selective output signal analyses associated with noncomplex readout procedures

(ii) fast and multicultural sensing examination with an easy investigation for early detection purposes

(iii) sensitive operating conditions for the accurate evaluation and specific monitoring of food target dosage levels with >99% accuracy

(iv) real-time and self-interpretation of the examination of pesticides, pathogens, coronaviruses, chemical additives, and hazardous substances in food products to reduce food risks and contaminants

(v) indoor or outdoor online marking and identification, rapid, and convenient with long-range stability of analyses

In general, nanostructure materials are strong sensor candidates that meet the high requirements of the development of smart and compact food sensor electronics because of their optical, electronic, conductive, and magnetic features [20-22, 28, 29, 31, 33-35, 39]. The improvement of nano/microsensor devices and sensing protocols can be identified because of the following: (i) perennial electron transfer, (ii) proper accommodation of target species hosting, (iii) target-to-sensor surface interaction, and (iv) selective binding event and signaling [11, 38-42, 46]. Various nanostructured materials, including conductive polymers, metal hydroxides, oxides, carbon-based materials, quantum dots (QDs), and nanocomposite materials, have been utilized to create active platforms of nano/microsensor devices for food assessment (Scheme 2) [11, 20-22, 28, 40-42, 46-48].

4. COVID-19 pandemic and its relationship with food products

The COVID-19 pandemic is currently a global threat, causing massive loss of life, in addition to economic and commercial losses and disruption of daily activities in most countries. According to the data and last report of WHO on December 20, 2020, the total number of cases worldwide has reached 75 million and more than 1.6 million deaths have been recorded since the beginning of the pandemic [49-54]. Coronaviruses (CoVs) are infectious viruses that attack the human respiratory

system, causing pain, serious problems, and possibly death. Various kinds of CoVs include Middle East respiratory syndrome (MERS), severe acute respiratory syndrome (SARS), and SARS-CoV-2 (2019-nCoV and COVID-19) [55].

At the beginning of the COVID-19 pandemic, many reports related to the relationship between the COVID-19 pandemic and food have indicated that catching COVID-19 through food or its processing is unlikely. However, SARS-CoV-2 infection may be transmitted through direct exposure to respiratory droplets from the sneezing or coughing of an infected patient. Currently, considering the relatively small number of cases, people have some concerns and beliefs that food contamination contributes to the transmission of COVID-19 infection [56]. The first case of the food product infection appeared on June 12, 2020, at Xinfadi Agricultural Products Wholesale Market in Beijing, where SARS-CoV-2 was detected on a cutting board used for salmon. In this regard, frozen foods are considered a potential vector for COVID-19. Subsequent reports have confirmed that many infected cases may be due to food packaging materials. COVID-19 infections have been discovered in many foods, including salmon, shrimp, frozen chicken wings, and inside a shipping container [56, 57]. Therefore, the integrity of the global food safety monitoring system, international trade support, and food supply chain must be ensured. With the new generation of SARS-CoV-2, tracking the COVID-19 pandemic and its relationship with food should be prioritized to reduce the global risks that can threaten the food safety supply. A critical goal for food safety is growing fast to provide effective identification and on-time monitoring protocols of COVID-19 in food sources, ingredients, products, and infected food workers [58].

Prior to the outbreak of the COVID-19 epidemic, some speculations have indicated the possibility of the spread of the new coronavirus through food products or packaging as a potential risk factor [59]. Therefore, some precautionary measures have been taken, especially to employees who are working in the field of food retail, manufacturing, and distribution [60, 61]. SARS-CoV-2 can reach and

contaminate food products and then transmit COVID-19 infection in several ways: (i) touching of contaminated food package surfaces, (ii) contacting food products, fruits, and vegetables with an infected person, and (iii) consuming food products infected by animal viruses. However, several studies have confirmed that the real transmission of foodborne SARS-CoV-2 needs approval [62]. In a hypothesis, transmission may occur via frozen food or packaging, although its effective function may terminate within days after shipment [62, 63]. In general, although no logical explanation has confirmed the relationship between COVID-19 and food, the rapid evolution of the current situation regarding COVID-19 and the risks associated with its transmission and the detection of SARS-CoV-2 on frozen foods have contributed to the development of an updated strategy and provided insights into the assessment of the transmission risk through food and a review of the relationship between COVID-19 and food [59-65].

Several optical and electrochemical sensor techniques have been developed for COVID-19 detection through real-time polymerase chain reaction (PCR) to decrease direct contact among patients. However, the on-site, rapid, and accurate detection of COVID-19 by using wearable optical and electrochemical sensor devices remains challenging [66-68]. Currently, reverse transcription (RT) PCR examination is the most important laboratory technique for analyzing SARS-CoV-2. However, RT-PCR has several difficulties and limitations, such as (i) long processing times ranging from 2 h to 3 h to obtain the results, (ii) difficulty in operating, (iii) the necessity for well-trained technicians and qualified laboratories, (iv) expensive equipment, and (v) some false negative results obtained for infection [66-68]. In this regard, several studies on the development of COVID-19 screening have been performed to overcome these limitations [66-68]. Thus, the indoor/outdoor identification assay of SARS-CoV-2 antigen associated with food products and its industrial processing are urgently needed to control the infectious effect of the spread of COVID-19 pandemic.

5. Sensor protocols for the assessment of food ingredients, nutrients, additives, and byproducts

5.1 Scalable sensor devices of AA in the food industry

Vitamin C or AA is a vital nutrient of the monosaccharide family with wide functions. The biological activities of AA are conferred by its strong antioxidant property, and AA enhances the immune system's efficiency against various diseases, including scurvy and colds [69-71]. It is soluble in water and a distinct ingredient of the Mediterranean diet. In addition, AA and its derivatives are widely utilized in the food industry as an antioxidant material and stabilizer [72, 73]. The consumption of AA in foods such as fruits and vegetables is essential for various metabolic processes because of the absence of L-gulonolactone oxidase that produces vitamin C from glucose [74]. Upon intake, AA exerts low toxicity to the human body. The most common complaints are diarrhea, nausea, stomach issues, and other gastrointestinal disorders because of the lack of a decreased effect of vitamin C on gastrointestinal nutrients. In addition, high AA intake is related with an expanded danger of cardiovascular disease, increased kidney stones, and extensive iron expansion that affect people with a hereditary plaque. The chronic consumption of AA can damage tissues, chromosomes, and DNA; cause cancer development; reduce B12 nutrient and copper levels; accelerate digestion or AA secretion; and promote tooth enamel erosion [75-78]. The permissible and recommended dietary level of AA has been estimated to be 100–120 mg per day. Vitamin C can be obtained from various food products, including citrus fruits, hips, tomatoes, cabbage, strawberries, spinach, and others. Therefore, scalable sensor devices for the accurate detection of AA in the food industry are important to ensure food safety [79-83].

AA detection is critical for the food industry and diagnostic application. The absence or lack of AA concentration leads to scurvy, whereas an increase in AA has many health effects. In this regard, significant endeavors have been given to build up an accurate, portable, straightforward, convenient,

and cost-effective sensor for AA detection (Table 1). Therefore, progressed sensory devices have accomplished genuine headway in daily checking and early warning requirements in relevant fields, such as food safety, military, life security, environment control, and medicinal observation [3, 5, 8, 15, 84-86]. For instance, numerous optical sensor techniques are utilized to detect AA levels [87-89]. In this respect, advancements in nano/micromaterial-based optical sensor devices for quick, ultrasensitive, and specific AA species are remarkable challenges that meet the necessities of daily monitoring assays of AA in the food industry.

Noble metal nanoparticles (NPs), such as Ag NPs and Au NPs, are widely used to design good SERS-based sensors for the visual detection of AA samples in foods [87, 90-93]. Fluorescence-based sensors are generally utilized in numerous applications, such as pharmaceutical enterprises and food and clinical analyses. Basically, a fluorescence approach to construct noninvasive AA sensors has numerous favorable benefits, including high sensitivity, host system protection, low cost, simplified procedure, and analysis, can be completed with fluorescence decay times [94-97]. Diverse analysis techniques based on fluorometric estimations, including chemiluminescence (CL), electrochemical chemiluminescence (ECL), surface-enhanced fluorescence, and surface-enhanced infrared absorbance, are used for AA detection in food, fruit juice and pharmaceutical products, and human samples [94]. For example, Ferreira et al. [98] described the design of optical paper-based sensors for the quantitative analysis of AA by using AgNPs and Ag ions as a chromogenic substance. A clear change in the color of a paper sensor strip indicates the simple detection of AA concentrations in real samples. Rostami et al. [99] fabricated AgNPs through seed-mediated growth on a substrate for a wide range of detection (ROD) of AA (0.25–25 μM) and LOD of 0.054 μM in commercial lemonade and pharmaceutical tablets (Scheme 3A). An Eu (III) luminescent complex is prepared by conjugating two nitroxide radicals as a sensory probe for AA visual imaging in living cells with a LOD of 9.1 nM (Scheme 3B) [100].

Scheme 3

Variable carbon-based nanomaterials, including carbon dots (CDs), QDs, graphene QDs, N-, S-, and P-doped CDs, silicon QDs, and polyallylamine-AuNNCs@MnO_2, are used to fabricate the fluorescence sensors of AA in vitamin C tablets, human serum, fresh fruits, and commercial fruit juices [92-97] [95, 101-109]. Furthermore, a fluorescent switchable sensor is constructed by using carbon dots (CDs) doped with heteroatoms, such as sulfur and nitrogen (N, S-CDs), for AA detection in some fruits, including tomato, apple, grape, and kiwi (Scheme 3C) [110]. The designed sensor permits the detection of AA in the ROD of 10–200 μM and LOD of ~4.69 μM. An integrated sensing protocol based on the quenching mechanism of probe by Fe^{3+} is designed by using a dual fluorescent sensor to enhance a linear wide ROD of AA (Scheme 3D).

Along with optical sensors, CL-based sensors have lower emission background that avoids light scattering noise and shortens lifetime compared with fluorescence-based sensors. In general, the selection of substrates, reagents, and immobilization conditions is important for the development of efficient CL sensors. The advantage of CL sensor signal clearance is related to chemical reaction changes; consequently, it can provide an appropriate approach for the quantitative measurement of AA concentrations in the real samples of juice and food [111-118]. In this regard, AuNPs with different sizes are used to catalyze and improve the function of a luminol-$K_3Fe(CN)_6$ CL sensor, enabling the detection of AA in vitamin C tablets and fruit juice with ROD and LOD of 0.1 nM–1.0 μM and 0.2 nM, respectively [115]. CL analysis shows the improved properties of AA and amino acids on the same system. Cu^{2+} is used to enhance the CL efficiency of a luminescent probe, i.e., graphene QDs doped with nitrogen, during the detection of AA species in fruits [117]. This luminescent probe produces CL through oxidation with H_2O_2. In addition, the presence of Cu^{2+} expands the CL intensity by two orders of magnitude. This enhancement in CL intensity can be

attributed to the Fenton-like catalytic reaction of Cu^{2+}. This sensor determines the AA concentration with a LOD of 0.5 μM in fruits.

Scheme 4

Several fabrications of electrochemical sensor-based devices with carbon nanomaterials, metal nanoparticles, metal oxide nanostructures, polymers, and their composites have been reported for the promising detection of AA in food products, such as vitamin C tablets, orange juices, and other beverages [119, 120]. As such, an electrochemical sensor with a sulfur-doped microporous carbon microsphere (S-MCMS) electrode is used to detect AA in different resources, such as food and pharmaceutical products (Scheme 4) [11]. The annealing temperature under the N_2 flow is a key factor for producing a highly electroactive material with good characteristics of a porous surface, %S content, and microspherical orientation. The designed S-MCMS-modified electrode, which has a LOD of 1 μM and high stability and reproducibility, is utilized to detect AA in commercial juice products. A NiO/graphene nanocomposite film is employed for the detection of AA and folic acid in the real sample of vitamin C tablets with high sensitivity, selectivity, stability, and reliability [120]. Nanoporous carbon/cobalt oxide (NPC/Co_3O_4) nanocomposites for AA sensor electrodes in vitamin C tablets are synthesized through the dispersion of Co_3O_4 molecules (10 ± 2 nm) in the matrix of NPC through the direct thermal treatment of a ZIF-67 precursor (Scheme 5A) [121]. A reliable electrochemical sensor is obtained with high sensitivity (LOD = 20 nM), fast response, reproducibility, good stability, and capacity for the real-time monitoring of vitamin C tablets with 98%–102% recovery. In general, AA electrochemical biosensor electrodes constructed by using carbon materials alone and in combination with inorganic nanostructured materials have attracted great attention because of their promising properties [122, 123]. A glassy carbon electrode modified with Fe_3O_4/graphene oxide is fabricated using a green methodology for AA detection in vitamin C tablets [123]. Liu et al. [122] applied a plasma-assisted approach to prepare carbon fiber/ZnO core–

shell hybrids and fabricate microelectrodes that demonstrate a robust electrocatalytic biosensing performance to AA and DA with a linear ROD of 600–2000 and 20–200 μM, respectively (Scheme 5B). Metal nanoparticles, such as AgNPs, are employed for AA detection. In this manner, AgNPs are synthesized via microwave technique by utilizing *Psidium guajava* leaves as a source of capping and reducing agents [124]. The modified electrode with AgNPs exhibits a single electron reaction of AA in the control range of 150 μM ≤ AA ≤ 2000 μM.

Scheme 5

Scalable electrochemical organic transistors, such as poly(3,4-ethylenedioxythiophene) polystyrene sulfonate, are used to produce an electrochemical sensor electrode for AA detection in commercial juices, such as orange, and foods rich in vitamin C with a low LOD of 80 μM [125]. Li et al. [126] studied and constructed an electrochemical electrode for AA monitoring through the modification of a glassy carbon electrode (GCE) with AuNPs, MWNTs, and polyethyleneimine (PEI), producing AuNPs/MWNTs/PEI/GCE for stripping voltammetry detection. This electrode provides a high sensitivity toward a wide ROD of AA (0.5 pM–0.1 nM) and LOD of 15 fM. A highly sensitive copolymer of pyrrole and *o*-phenylenediamine layer is designed by modifying a pencil graphite electrode (PGE) through cyclic voltammetry copolymerization for the electrochemical detection of AA with a LOD of 0.263 μM [127]. Kong et al. [128] prepared poly(*o*-phenylenediamine-*co*-*o*-aminophenol) as a molecularly imprinted copolymer to detect AA electrochemically in orange juices and vitamin C tablets. During copolymerization, AA as a template molecule is incorporated, and electrochemical reduction is achieved by using an ammonium solution. Differential pulse voltammogram analysis reveals a ROD of 0.1–10 mM and a LOD of 36.4 μM.

Nanocomposite-based electrochemical sensors are used effectively to detect AA in food products. For example, nanometal/metal oxides and carbon materials, such as graphene, and MWCNTs have

been widely used as active nanosensors for the selective monitoring of AA. A sensitive, fast-response, and reproducible sensor for AA detection in a vitamin C supplement is constructed using TiO_2/rGO nanocomposites [129]. The designed sensor yields the fast response detection of AA (<5 s), a LOD of 1.19 μM, a ROD of 25–725 μM, and a sensitivity of 1.061 μA μM^{-1} cm^{-2}. Many researchers attempted to construct exceptionally delicate sensing platforms by using graphene-based compounds. Liu et al. [130] designed a nanocomposite of copolymerizing neutral red and RGO for AA detection in real samples, including vitamin C beverage. In addition, graphene–inorganic metal oxides and graphene–inorganic metal oxide/organic polymer nanocomposites have a wide range of applications in this field [131]. Das et al. [132] utilized graphene–iron oxide–polyvinyl alcohol (PIG) to modify a PGE for AA detection with a ROD of 0.04–4.1 mM and a LOD of 0.234 μM (Scheme 5C). Table 1 highlights AA sensory-based protocols fabricated by variable types of materials such as carbon, metal nanostructures, metal oxides, polymers, and composites. These novel sensory systems, sensing protocols, and analytical techniques enable the sensitive detection of AA in various food sources, dietary supplements, and human fluids.

Table 1

5.2. Sensing designs of reactive oxygen species for a safe food grade

Reactive oxygen has been used in food processing, industry, and medical applications to regulate physiological balance in living cells. H_2O_2 is the most recognized and stable oxygen reactive molecules. The presence of H_2O_2 accompanies the degradation and formation of free radicals, including O_2^- and OH^-. H_2O_2 can destroy the walls of bacterial and viral cells through the conversion of the harmful byproduct H_2O_2 to O_2 and H_2O. Therefore, it is used as an antibacterial agent in foods, such as wheat flour, egg white, and milk, and as a sterilizing agent in food packaging. Moreover, enough H_2O_2 dosage should be used for food-grade purposes. Unfortunately, undesired H_2O_2 levels are considered the main causes of (i) unsafe food grade and (ii) various pathological disorders,

including Parkinson's and Alzheimer's diseases [133-135]. Although the use of H_2O_2 in the food industry is important to avoid food spoilage and increase its shelf life, but H_2O_2 is harmful because of lipid oxidation, caustic spoilage, reactive oxygen species formation, corrosive properties, and tissue damage [136, 137]. Thus, sensory H_2O_2 designed with high economic values, sensitivity, fast response, and selective signals in food safety has been widely explored in industrial and nutrition fields (Table 2).

Optical H_2O_2 sensors based on optical fiber probes are a technological development in chemical and molecular biochemical detection for many sensor applications [138, 139]. A H_2O_2 sensor based on optical fibers is constructed by coating fiber optics with polyvinyl alcohol decorated with AgNPs connected to SPR (Schemes 6A and 6B) [140]. This sensing system can detect H_2O_2 in the ROD of 0.01 μM–0.1 M. Potassium ferricyanide has been used as a precursor for the chemical deposition of a PB-nanostructured film into a multimode fiber optical tip, which can serve as a sensitive probe for H_2O_2 molecules [141]. The sensing mechanism is based on the possibility of using AA to reduce Prussian blue (PB) and produce Prussian white (PW), followed by re-oxidation via H_2O_2 (Schemes 6C and 6D) [142]. In addition, fiber optics based on HRP immobilization on a bovine albumin/glutaraldehyde matrix is enzymatically modified to improve the selectivity of H_2O_2 detection with a LOD of 0.5 μM [143, 144].

Scheme 6

Fluorescence-based sensors have attracted considerable attention because association with a target species provides a great opportunity for mapping and differentiation [145-153]. Hu et al. [145] reported a selective fluorescence detector for H_2O_2 based on the aggregation-induced emission manners of tetraphenylethylene interacting with H_2O_2 (Scheme 7A). Two-photon dyes of 6-hydroxy-2,3,4,4a-tetrahydro-1H-xanthen-1-one fluorescent-based probes are synthesized to detect H_2O_2 with a fast response in 9 min and can be used in the optical imaging of H_2O_2 in living organisms and tissues

(Scheme 7B) [154]. Ratiometric fluorescent sensors based on mitochondrion-targetable HBTPB (fluorescent probes) for H_2O_2 detection with a near-infrared emission present a high selectivity toward H_2O_2 with a LOD of about 0.59 μM (Scheme 7C) [155]. The performance of these sensors depends on the presence of H_2O_2 oxidizing HBTPB and the generated free OH group from 1,6-elimination reactions. In addition, a mitochondrion-targeting sensor is developed using a benzothiazole-based radiometric fluorescent chelating agent (HKB) with a wide Stokes shift for H_2O_2 detection (Scheme 7D) [156]. Shen et al. [157] revealed that a colorimetric and radiometric fluorescence sensor for H_2O_2 can be developed by altering a mitochondrion target with a coumarin moiety (Scheme 7E). The sensing protocol is dependent on the intermolecular charge transfer (ICT) and has a wide ROD and LOD of 0.1 nM.

A ratiometric near-infrared fluorescent sensor for highly selective H_2O_2 recognition under alkaline conditions and in vivo imaging application is established using a boric acid derivative to develop a sensitive fluorescence signaling [158]. A water-soluble turn-on fluorescent dipyrromethene boron difluoride (BODIPY) is designed for selective in vivo H_2O_2 detection in HepG2/LO2 cells and angelfish (20 days old) (*Pterophyllum scalare*; Scheme 7F) [159]. As shown in fluorescent images, the probe can penetrate the fish body because of the obtained weak fluorescence; a clear fluorescence is detected after incubation with H_2O_2 because of the reaction between the probe and H_2O_2 inside the body.

Scheme 7

H_2O_2 should be identified and tracked, so simple sensing strategies, including CL and ECL techniques, have been used, and they have high sensing performance and selectivity depending on the control of sensor nanostructure designs. In this regard, various nanostructured materials, such as CuO NPs, $CoFe_2O_4$, bovine serum albumin-capped AgNCs, titania nanotubes, and platinum black-

functionalized indium tin oxide (ITO), significantly improve CL signals [160-163]. Other CL sensor designs based on nanostructured materials are potentially efficient candidates for the detection of H_2O_2 in the food sector [164, 165].

Electrochemical sensor designs based on nanostructural electrode surfaces have been widely explored as effective techniques for H_2O_2 species detection in food products [166-168]. In this regard, efforts have been devoted to developing enzymatic-/nonenzymatic-based electrochemical sensors and methods for H_2O_2 monitoring. Moreover, a prospective enzymatic sensor platform for H_2O_2 detection has been designed through enzyme immobilization, such as cytochrome C (Cyt c), into nanostructured materials to improve the electrocatalytic performance and redox efficiency of sensors toward H_2O_2 molecules in terms of sensitivity and selectivity [169-171]. An enzyme-based electrochemical sensor approach has many advantages, including high selectivity, high sensitivity, simplicity, and easy miniaturization (Schemes 8 and 9) [172-174]. Heme proteins, such as myoglobin, hemoglobin, and Cyt c, are used as H_2O_2 biosensors after the immobilization of the heme protein into an electrode surface for simple H_2O_2 detection (Scheme 8) [175]. Hemoglobin is actively immobilized at AgNPs encapsulated in a poly(amidoamine) dendrimer for H_2O_2 biosensing. The sensitivity of the sensor to H_2O_2 is in the ROD of 50–1150 μM with good reproducibility and stability [176]. However, a drawback of this approach is associated with its environmental sensitivity because of possible degenerate inactivation and aggregation of enzymes, co-enzymes, and proteins after immobilization into an electrode surface. Moreover, the immobilization of active signaling sites used for the electrode fabrication of an enzyme-based electrochemical sensor is more cost-effective than the nonenzymatic approach.

Scheme 8

Scheme 9

Numerous nanostructured materials, including NiO/graphene nanocomposites, cobalt oxide polyhedron-incorporated 3D graphene oxide (3D GO–Co_3O_4 PH), Co_3O_4 materials, cobalt(II) dicobalt(II) oxide nanoparticles, MW-CNT nanocomposite, (α-Fe_2O_3/rGO), (NP-Fe_2O_3/CoO) CoO nanocomposite, and Co_9S_8 hollow spheres are designed electrochemical electrode sensors for sensitive and selective H_2O_2 detection [166-168, 177-183]. Nanocomposites of Co_3O_4 NPs and mesoporous carbon nanofiber (Co_3O_4-MCNFs), AgNWs, and AgNP-embedded N-doped carbon nanofibers (Ag/NCNFs) are synthesized as a nonenzymatic H_2O_2 selective sensor in milk samples with high sensitivity, stability, ROD up to 20 mM, and LOD of 0.15 μM [179, 184]. The electrochemically dense and uninformed decoration of PtNPs on a reduced graphene (RGO)/GCE electrode surface is used as a nonenzymatic H_2O_2 sensor with a LOD of 0.2 μM; this sensor enables the in vitro detection of H_2O_2 in living cells (Scheme 10A) [31]. Furthermore, graphene-based electrode materials, including Pt NP-decorated nonporous graphene (PG) and graphene (G)/CNT-encapsulated AuNPs, provide a highly active nonenzymatic electrode for H_2O_2 detection [182-185]. The nanocomposite of MoS_2 nanosheets (NS)/N-doped carbon NWs (produced from the sintered polypyrrole NWs) is synthesized for the electrochemical detection of H_2O_2 with a LOD of 0.73 μM and the possible detection of H_2O_2 released from A549 cells (Scheme 10B) [186].

Metal organic frameworks, such as ZIF-67, have been used to design electrochemical H_2O_2 sensors [187, 188]. An encapsulated Au@ZIF-67 is utilized to synthesize a hierarchically porous dodecahedron (Au@C-Co_3O_4) electrode for the H_2O_2 detection with a LOD of 19 nM, the recognition of H_2O_2 released from living organisms, and the identification of cancer cells (Scheme 10C) [187]. The carbonization of cobalt with an MOF (ZIF-67) to produce mesoporous Co-NPs doped with C-N featuring a rhombic dodecahedral morphology for nonenzymatic electrochemical H_2O_2 detection with a fast response (6 s), a wide ROD (0.001–30 mM), and a LOD of 0.143 μM [188]. A hierarchized $Ni(OH)_2$/RGO/Cu_2O sandwich in situ fabricated on Cu foil hydrothermally for H_2O_2 and glucose

detection exhibits a high amperometric response as a nonenzymatic detector with a LOD of 0.20 μM and a ROD of 0.5–7.5 μM (Scheme 10D) [189].

Scheme 10

The modulation of MWCNTs deposited on a tantalum (Ta) sensor electrode by a Pd-doped α-MnO_2 film via a spray pyrolysis approach shows high efficiency and sensitivity to assess the catalytic activity of H_2O_2 in milk samples with a sensitivity of 116.1 $\mu AmM^{-1} cm^{-2}$, a ROD of 0.0032–22 mM, and a LOD of 0.02 mM [137]. In addition, a hybrid MnO_2/CNT/Ta nanocomposite sensor designed to detect H_2O_2 in milk in the ROD of 3–3025 μM with a LOD of 0.04 μM and a sensitivity of 83.3 $\mu AmM^{-1} cm^{-2}$ [190]. Easow et al. [191] modified a GC electrode with a bimetallic Ag@Cu nanowire to improve electrocatalytic performance toward H_2O_2 compared with that of the modified GC electrode with Ag seeds and a bare GC electrode. This bimetallic NW sensor shows the successful detection of H_2O_2 in a pasteurized milk sample with a LOD of 3 μM and a wide ROD of 1–10 mM. A nanocomposite of PtNPs (2 nm)–TiO_2 (8 nm)-coated RGO is fabricated via a microwave-assisted pathway to design flexible screen-printed sensors for the amperometric detection of H_2O_2 in milk [192]. The modified screen-printed electrodes by TiO_2/RGO, PtNP/RGO, and Pt–TiO_2/RGO can detect H_2O_2 in the ROD from 0 mM to 20 mM and a sensitivity of 40 $\mu AmM^{-1} cm^{-2}$ [187]. A hybrid magnetic Au/Fe_3O_4-based sensor exhibits an outstanding H_2O_2 detection performance in milk and juice samples with a LOD of 0.108 μM, a ROD of 0.001–1 mM, and a sensitivity of 266 $\mu AmM^{-1} cm^{-2}$ [193]. The hierarchical structures of N-doped carbon nanofibers comprising CoNPs and hollow mesoporous carbon particles with a good mechanical and electrical conductivity are characterized by excellent sensitivity and selectivity to H_2O_2 in food. A GCE electrode-modulated Co-NC/CNF leads to a high sensitivity to H_2O_2 detection of 300 $\mu Acm^{-2} mM^{-1}$ in milk. Moreover, the formation of a Co-NC/CNF film on screen-printed electrodes (SPEs) enables the portable sensing of H_2O_2 in juice and milk samples [194]. An amperometric sensor based on the immobilization of the nanocomposite of

MWNTs and [Fe(III)-5,10,15,20-tetrakis(α,α,α,α-2-piv-alamidophenyl)porphyrin] bromide [Fe(TpivPP)Br] on GCE (MWNTs/FeTpivPP/GCE) for H_2O_2 detection in commercial beverages with a highly sensitive performance and a LOD of 0.05 μmol L^{-1} [195]. Challenges in the orientation of nanoscale sensor materials into portable sensing devices for H_2O_2 monitoring in food and beverage samples remain sobering scenes.

Table 2

5.3. Detection protocols of high-purine foods for health risk assessment

High-purine foods, such as alcoholic beverages, some fish, and some kinds of meat are essential and daily food. The metabolism of these kinds of foods produces a uric acid (UA) and appears in different bodily human fluids, such as urine and serum. UA can affect various physiological functions of physical systems [196]. Given its chemical composition, UA serves as an antioxidant agent in physiological human processes. In addition, it acts as a reducing agent in bodily human fluids and accounts for half of the active antioxidants present in blood samples [197]. Protection from some neurological diseases, including Parkinson's disease, Alzheimer's disease, and multiple sclerosis, is related to a high UA level. This protection is conferred by the antioxidant activity or other obscure properties of UA [198, 199]. UA levels in bodily human fluids may also be associated with some clinical diseases, such as hypertension, metabolic syndrome, diabetes, gout, hyperuricemia and its related diseases, and erectile dysfunction [196, 197, 200, 201].

Fluorescence biosensors are noninvasive and simple tools for UA detection in human biological samples. Azmi et al. [202] constructed a fluorescence sensor for UA based on a CdS QD–enzyme system encapsulated in a 96-well microplate format. This sensor detects UA based on the quenching properties of H_2O_2 produced from the CdS QD–enzyme system toward the QD fluorescence intensity (Scheme 11A). The designed sensor has a UA ROD of 0.06–2 mM and a LOD of 50 μM. C dot-

engulfed Fe_3O_4 nanocomposites are used to design an electrochemical UA detection with a LOD of 6.0 nM in the linear ROD of 0.01–0.145 μM [203].

Tb^{III}-dtpa-bis(2,6-diaminopurine) is prepared as an UA fluorescent sensor with a LOD of about 5.80 μM [204]. The quenching feature of H_2O_2 is used as a base to determine UA concentrations. In this regard, the fluorescence quenching of CdTe NPs capped with various ligands is applied to enzymatically detect UA [205]. A fluorescent sensor containing Co^{2+}/H_2O_2–Amplex® UltraRed (Co^{2+}/H_2O_2–AUR) is designed for UA detection. The mechanism of detection depends on the oxidation of H_2O_2 and Co^{2+} to provide Co^{3+} and OH radicals that interact with an AUR fluorescence reagent (Scheme 11B) [206]. UA oxidation can produce different species, such as urea, which affects Co^{2+} catalysis and AUR oxidation, leading to a decreased fluorescence intensity. The change in fluorescence intensity is associated with UA concentration. The designed sensor can detect UA in a wide ROD range of (0.05–1.0 μM) and a LOD of 20 nM.

A Cu^{2+}-based TMB (3,3,5,5-tetramethylbenzidine) with Fenton-like properties was constructed as a colorimetric-based sensor for UA detection, where H_2O_2 is a product generated during the enzymatic catalysis of UA [207]. The designed sensing platform can detect UA with a LOD of 0.64 μM. Wang et al. [208] used $HAuCl_4$ to oxidize TMB while inducing a blue color as a function of UA concentration with a ROD of 0.001–80.0 μM and a LOD of 0.67 nM. Various reports have focused on UA detection by using the CL technique [209, 210]. *N*-hydroxyphthalimide (NHPI) is used as an efficient CL–luminol system to develop a luminol–*N*-hydroxyphthalimide system. The luminol–NHPI system provides high sensitivity with a LOD of 910 nM [211]. An ITO electrode modified with N-doped graphene is utilized to detect UA electrochemically [212]. Many approaches have been designed for selective UA monitoring in the existence of AA and dopamine (DA) depending on the fabrication of nanostructured metal oxides and carbon materials. For instance, sulfur-doped carbon, NiO, and Fe_2O_3 show a good selective performance for UA detection with a wide ROD and a low

LOD [41, 213, 22]. Various kinds of nanoscale materials of metal/metal oxides and carbon-based materials have been designed as extremely active materials for selective and sensitive UA detection and used for nanodevice fabrication.

Scheme 11

6. Nanoscale sensors for the assessment of food packing ingredients (nitrites and sulfites)

Nitrite anion is a well-known inorganic pollutant not only in the environment, water, and soil but also in the human body [214]. The various applications and usage of nitrites in food preservation, corrosion inhibitors, fertilizers and products, dye industries, and antimicrobial activities have led to their spread and harmful impact on public health [214-216]. The hazardous effect of nitrites on the human body is associated with the following reactions:

i) The reaction of nitrites with amines in food leads to the formation of carcinogenic N-nitrosamines (causing stomach cancer).

ii) The combination of nitrites with hemoglobin leads to the transformation of methemoglobin (Fe(II) to Hb-Fe(III)) (causes blue baby syndrome) [215].

Exposure to high nitrite levels may lead to some health risks, such as decreased blood pressure, increased heart rate, decreased ability of tissues to carry oxygen, headaches, abdominal cramps, vomiting, and even death [217]. Thus, developing nitrite sensors, such as optical and electrochemical sensors that feature a fast response, a low cost, high sensitivity and selectivity, stability, and reproducibility have attracted considerable interests (Table 3).

The development of visual detection protocols is one of the greatest approaches used in anion species assessment in foods [218]. Many designs of optical nitrite (NO_2^-) sensors based on colorimetric and fluorometric signaling for food analysis have been reported [224-231]. A colorimetric sensor for NO_2^- is designed through the modification and stabilization of AgNPs with *N*,*N*′-bis(2-

hydroxybenzyl)-1,2-diaminobenzene as a chelating agent [219]. Hu et al. [220] prepared a fluorescent and colorimetric sensor based on CDs through a rapid microwave technique for NO_2^- visual detection with low LODs of 196 and 0.518 nM (Scheme 12A). A design of NO^{2-} optosensor is fabricated by incorporating self-adhesive poly(n-butyl acrylate) microspheres with Safranine O reagent, leading to the creation of a visual detection protocol with a concentration ROD of 10–100 ppm in food samples [221]. NO^{2-} concentrations are detected in real samples by using strip-typed colorimetric sensors covered by a polyethylene glycol hydrogel to diminish the nonspecific connection of bio-samples and color immobilization-producing probes (Scheme 12B) [222]. The proposed strip sensor modified with a colorimetric sensor based on *N*-(1-naphthyl) ethylenediamine and sulfanilamide has a ROD of 10 – 5000 μM and a LOD of 10 μM.

Scheme 12

Cardoso et al. [223] designed μPADs (microfluidic paper-based analytical devices) for colorimetric NO^{2-} detection in environmental, food, and clinical samples with a LOD of 5.6 μM. The mechanistic detection of NO^{2-} is achieved through the modified Griess reaction by using a solution of sulfanilamide, hydrochloric acid, and N-(1-naphthyl) ethylenediamine. Zhan et al. [224] reported diazonium salts formed through the reaction of NO^{2-}, and aminated m-CDs can be used for visual NO^{2-} monitoring for food quality evaluation and control. The designed fluorescent sensor successfully detects a low level of NO^{2-} species in a ROD of 0.063– 2 μM and a LOD of 0.018 μM in food and environmental products. Moreover, an optical fluorescence sensor based on hyperbranched polyethylenimine-capped CdS quantum dots (5 nm diameters) is fabricated for the selective and sensitive monitoring of NO^{2-} species in vegetable and water sources in a wide ROD of 0.1–100 μM [225]. The mechanistic TMB oxidation reaction by nitrite species to form yellow ox-TMB leads to the formation a colorimetric sensor assay. NO^{2-} reading out signals are detected through digital image colorimetry (DIC) designed to detect nitrite in food samples via a smartphone [226].

The reading out strategy relies on the color contrast of the saturated images and analyzes color by using a red, green, and blue (RGB) model. In addition, this sensing strategy provides the quantitative detection of NO^{2-} in cabbage, pickle, and pork in the ROD of 10–440 μM and a LOQ of 2.34 μM. Studies related to the design of active electrode materials have been devoted to the effective detection of electrochemical NO^{2-} [227-229]. The air annealing treatment of carbon fiber paper (CFP) activates surface properties in terms of increased oxygen containment, higher roughness, enhanced wettability, and produced more defective edge/surface locations [230]. The electrochemical sensors designs have been developed based on nanoengineering of various metal nanoparticles, metal oxides nanostructure and their campsites for sensitive and selective monitoring of nitrites [231-238].

This treated CFP is used to detect NO^{2-} species in food samples in the ROD of 0.1–3838.5 μM, a LOD of 0.07 μM fast current response of 1 s, and a sensitivity of 930.4 $\mu A m M^{-1} cm^{-2}$. Selective NO^{2-} is detected in meat samples by using a portable Pt-Nafion-based electrochemical sensor [239]. Üzer et al. [240] fabricated an electrochemical sensor for NO^{2-} species by electrochemically modifying a working electrode (Au) by using polyaminothiophenol (PATP) and Au NPs. The designed Au/PATP-AuNP electrode sensor shows high stability and sensitivity for NO^{2-} identification in sausage samples with a LOD of 0.12 mg L^{-1} and a wide ROD of 0.5–50 mg L^{-1}. An electrochemical sensor electrode is designed through GCE modulation by using ZnO/PtNP/MWCNT nanocomposites to detect NO^{2-} in pickled food with high sensitivity [241]. This well-designed ZnO/PtNP/MWCNT/GCE sensor shows the detection of NO^{2-} in the ROD of 0.4–200 μM and a LOD of 0.082 μM. Rao et al. [242] designed sensing protocols by using a AuNP/chitosan @N,S co-doped MWCNTS electrode for the selective and sensitive monitoring of NO^{2-} detection in some food products (mustard tuber, ham sausage, and fermented bean curd) within the ROD of 1–7000 μM and a LOD of 0.2 μM. A rGO/MoS_2/poly (3,4-ethylene dioxythiophene) (PEDOT) nanocomposite is used to design a nonenzymatic NO^{2-} sensor electrode in water and milk samples [243]. rGO/MoS_2/PEDOT

nanocomposite-modified GCE enhances the electrocatalytic performance toward NO^{2-} oxidation, leading to a good NO^{2-} sensitivity of 874.19 $\mu A \mu M^{-1} cm^{-2}$, a LOD of 0.059 μM, and a wide ROD 0.001–1 mM. These reports have reflected the necessity of NO^{2-} detection to ensure food quality and healthcare. In addition, these sensor patterns and devices have been used for nanosensor designs and NO^{2-} detection in the food chain.

Inorganic anion species, such as sulfites (SO_3^{2-}), are important in food evaluation because of their wide use in food processing industries, including food storage and preservative additives for fruit juices, dried fruits, and wines. Sulfate anions are important in improving flavor manifestation through all food processing stages, including preparation, storage, distribution, and color stabilization [244, 245]. Furthermore, SO_3^{2-} is commonly used for antimicrobial growth, bleaching agents, enzyme inhibitors, oxygen scavengers, and antioxidants [246, 247]. In this regard, great endeavors have been made for designing sensitive and selective SO_3^{2-} sensors, especially in the food industry [248-250]. Several sensing methods, including colorimetry, electrochemistry, fluorimetry sensors, are designed on the basis of a nanosensor platform to detect SO_3^{2-} with satisfactory selectivity and sensitivity. For example, the capability of SO_3^{2-} to inhibit Ag_2O and Ag_2O nanoparticles enables the colorimetric detection of SO_3^{2-} in the ROD of 0–300 μM and a LOD of 1.74 μM [251, 252]. Ag_2O acts as an oxidase that catalyzes the oxidation of peroxidase substances. SO_3^{2-} is detected using colorimetric and near infrared fluorescent probes. Fluorescent organic nanoparticles (FONs) are designed via the self-assembly of tetraphenyl imidazole (TIBM) for ultrafast SO_3^{2-} detection (15 s) and a LOD of 7.4 nM [253]. A red-emitting ratiometric fluorescence probe of 6-(dimethylamino) quinoline-2-carbaldehyde) acetonitrile and 2-(1-H-benzo[d]imidazol-3-ethyl-2-yl (BIQ) is fabricated for the sensitive and selective detection of HSO_3^- in food chains of white wine and sugar [254]. A BIQ probe displays fast fluorescence and color response (<2 min) with a LOD of 0.29 μM. Fang et al. [255]

considered the quenching properties of fluorescent carbon quantum dots (C-dots) with SO_3^{2-} and Cr(VI) ions to design an effective fluorescence probe for SO_3^{2-} monitoring with a LOD of 0.35 μmol/L.

The modification of carbon paste electrode (CPE) with 3-n-propyl(4-methylpyridinium) silsesquioxane chloride ($Si4Pic^+Cl^-$)/AuNPs(45nm) is designed an electrochemical SO_3^{2-} sensor in coconut water and white wine samples [256]. The designed ($Si4Pic^+Cl^-$)/AuNPs/CPE sensor shows good performance in the ROD of 2.54–48.6 mg/L with a LOQ of 0.88 mg/L and a LOD of 2.68 mg/L. Devaramani and Malingappa [257] modified CPE by using cobalt nitroprusside (CoNP) NPs and showed high sensitivity to detect SO_3^{2-} in food samples, including sugar, dry grapes, and wine with a LOD of 0.04 μM and a LOQ of 0.229 μM in the ROD of 1–8 μM. Devadas et al. [258] used a praseodymium hexacyanoferrate electrode for the electrochemical detection of SO_3^{2-} in red wine samples with good high sensitivity of 0.036 mA mM^{-1} cm^{-2} and a LOD of 2.15 mM. The modification of graphitic carbon electrode by using cobalt hexacyanoferrate is designed for the amperometry detection of SO_3^{2-} in various food samples of tomato ketchup, wine, jam, sugar, and dry grapes with a LOD of 1.7 mM in the ROD of 4–128 mM [259]. The immobilization of synthesized phenothiazine imidazolium and hexafluorophosphate counter anion (PTZ-IL) into the modified GCE with MWCNTs to produce a PTZ-IL/MWCNT/GCE sensor utilized to detect SO_3^{2-} in the ROD of 30–1177 μM with a LOD of 9.3 μM and a sensitivity of 282.2 μA mM^{-1} cm^{-2} [260]. Moreover, the modification of CNTs with active organic materials, such as chitosan and graphene transistors, are used for sensitive sulfite anion detection in food chains [261, 262]. Currently, various sensing strategies and nanomaterial-based sensors are used to efficiently screen sulfites in food samples (Table 3). However, the development of portable nanosensor devices for the selective and sensitive assays of nitrite and sulfite species in food products and industry has attracted increasing interests.

Table 3

7. Nanosensor designs for the detection of organic and inorganic toxins in foods

7.1 Sensing protocols of toxic heavy metals in food products

Environmental pollution with heavy metals and their direct or indirect association with food processing threatens the quality of food and agricultural products and human health. In general, food can become contaminated with heavy metals from environmental/industrial tools, agricultural water, marine, and beverage chemicals and additives. Food delivery associated with labeling materials and package contents (text/ink patterns, and packaging bottles and papers) may lead to polluted food [263-265]. Adverse health effects are unquestionable with the consumption or intake of large/low amounts of contaminated food sources.

For instance, marine environmental pollutants by naturally occurring amounts of heavy metals pollute marine organisms, fish, and seafood products (fish and shellfish). The accumulation of nondegradable and harmful heavy metal contaminants in marine food chains above the legal limits potentially threaten human health. Several studies have been conducted in Bangladesh (Saint Martin Island) and showed evidence on the presence of high level of toxic heavy metals such as Pb^{2+}, Hg^{2+}, As^{III}, Cr^{6+}, Cd^{2+}, Fe^{3+}, Cu^{2+}, Zn^{2+}, and Mn^{2+} in the muscles/armor/exoskeleton of shrimp, lobsters, and crabs [266]. Several sensing techniques, such as atomic absorption/emission spectroscopy (AAS/AES) and inductively interconnected plasma mass spectroscopy (ICPMS), are used to detect the traces of heavy metal contents in food and environmental samples [263, 266, 267]. These sensing techniques are used to detect sensitively toxicant metals, but some challenges are associated with the high cost, sample preparation, and complexity of analysis and users' technical expertise. In this regard, great efforts have been devoted to developing a simple, accurate, and cost-effective approach for the fast tracking and indoor/outdoor field trials of heavy metals to ensure food quality (Table 4) [33, 84, 85, 268-275].

Optical and electrochemical sensors have been widely used for metal ion monitoring and the efficiency of remediation/treatment with good selectivity and sensitivity without requiring further treatment [271, 276-291]. In this context, different chelating agents, such as N,N′-disalicylidene-4,5-diamino-6-hydroxy-2-mercaptopyrimidine (DSAHMP), (4,5-diamino-6-hydroxy-2-mercaptopyrimidine and diphenylthiocarbazone), and dicarboxylate 1,5-diphenyl-3-thiocarbazone (III) are used as colorimetric probes for the visual detection and extraction of Zn^{2+}, Pd^{2+}, Cd^{2+}, Cu^{2+}, Co^{2+}, and Hg^{2+} [85, 279, 280, 292]. These visual sensors provide fast and easy-to-use on-site detection of target metal ions in water, food products, marine organisms, and other environments. Fluorometric sensors have been widely used to monitor heavy metals in various samples, including water, food, and pharmaceuticals [293-296]. A sensitive and selective fluorescent probe, namely, 2,2′-((1Z,12Z)-5,9-dithia-2,12-diazatrideca-1,12-diene-1,13 diyl) diphenol, is synthesized and loaded on Zr-MOFs for the detection of Zn^{2+} and Bi^{3+} [294, 297]. Tumay et al. [298] fabricated an optical sensor based on pyrene-modified nanocrystalline cellulose to detect Cd(II) ions in food plant samples in a linear ROD of 0.1–60 μM with a LOD of 0.09 μM.

Nanostructure-based materials for electrochemical sensor designs are widely used to improve the performance of detection sensitivity [299, 300]. For the electrochemical monitoring of heavy metals, a number of identified compounds, such as aptamers [301] and anticell and enzymes [302, 303], are used with nanostructured carbon-based materials. An imprinted chitosan/GR/GCE electrode is designed for Cd^{2+} detection in milk and drinking water in the ROD of 0.1–0.9 μM and a LOD of 0.162 nM [304]. Wang et al. [305] designed an electrochemical aptasensor-based sensor. This sensor can detect Hg^{2+}, Pb^{2+}, Cd^{2+}, and arsenic in food samples. A double-sided conductive carbon tape modified by a thin Au layer enhances the electrochemical detection of Cd^{2+} in rice based on a paper-based electrode with a LOD of 0.1 μg/L and a linear ROD of 2–50 μg/L [306]. Wu et al. [307] fabricated Fe_3O_4/F-MWCNT nanocomposites to detect heavy metals in food chains. The designed

Fe_3O_4/F-MWCNT platform is effectively used for Cd^{2+}, Pb^{2+}, Cu^{2+}, and Hg^{2+} detection in food with good sensitivity of 108.79, 125.91, 160.85, and 312.65 μA mM^{-1} cm^{-2}; a LOD of 0.05, 0.08, 0.02, and 0.05 nM; and a wide ROD of 0.5–30, 0.5–30, 0.5–30, and 0.5–20 μM, respectively. Moreover, a modification of working electrode by MOF materials has been effectively used to detect multiple heavy metal actions, such as Pb^{2+}, Cd^{2+}, Cu^{2+}, and Fe^{3+} with high sensitivity and selectivity [308-310]. Indeed, current reports indicate the key roles of nanostructured materials in designing extremely selective and sensitive sensors for the critical assessment of heavy metals in food samples. The development of smart and compact nanosensor devices for toxic metal detections in food remains a practical challenge. Nanosensors integrated in portable devices enable on-time usage in the basic laboratory assessment and evaluation of food quality in-home and commercial markets.

7.2 Sensing protocols and designs of bisphenol A toxicants

Bisphenols, such as bisphenol A (BPA), are a group of organic compounds that containing two hydroxyphenyl bridged by one carbon atom. From the 1960s, BPA has been widely used in the production of polycarbonate plastics and resin industries [311]. It has been magnified as a serious toxicity to food and human health. It can be released to food through the packaging and contact process (food packaging, tableware, and cooking utensils), which poses a health threat associated with an endocrine disrupter with a reduced estrogenic behavior [312-314]. Recently, the European commission decreased the permissible contents of BPA in plastic materials from 0.6 mg/kg to 0.05 mg/kg [315]. In Catalonia, Spain, traces of PBs corresponding to 93% and 36% are present in canned and noncanned foods, respectively [316]. Many techniques, including optical, liquid chromatography-tandem mass spectrometry, electrochemical, and other methods, have been used to evaluate the risk and detect BPA with good sensitive and selective screening in various samples (Table 4) [311, 317-320].

This critical report aims to assess and recognize the BPA in fish and water samples. For example, a colorimetric sensor is designed using Fe^{3+} nanocomposite and fabricated BTSIXO (3′,6′-bis(diethylamino)-2-((3,4,5-trimethyl benzylidene) amino) spiro[isoindoline-1,9′-xanthen]-3-one) [321]. This optical sensor performs a high sensitivity with a LOD of 0.02 ppm and a wide ROD (0.1–150 ppm). Several studies have revealed the importance of AuNPs for the potential design of aptasensors in the colorimetric detection of BPA [322-324]. Jia et al. [322] reported a label-free aptasensor with the truncated 38- and 12-mer aptamers conjugated to AuNPs, providing a LOD of 7.60 and 14.41 pM, respectively. Color changes from red to blue associated with AuNP aggregation in the presence of low concentration BPA levels. This colorimetric sensor is used for BPA detection in grain rice with a LOD of 0.004 nM [323]. In addition, AuNP aggregation induced by the BPA–aptamer and cationic polymer is used to detect BPA with a LOD of 1.5 nM [324].

A visual microfluidic paper detector is designed through the integration of $ZnFe_2O_4$, molecularly imprinted polymer (MIP) and cellulose fibers to detect BPA with a LOD of 6.18 nM in a wide concentration ROD of 10–1000 nM [325]. BPA concentrations can be detected as a function of the change in gray color intensity because of the catalytic activity of the 3,3′,5,5′-tetramethylbenzidine and $ZnFe_2O_4$ peroxidase mimetics. Lee et al. [326] reported the conjugation of aptamer/AuNPs and fluorescing single-strand DNA (ssDNA) aptamer as a fluorescent probe for BPA detection with a LOD of 9 pg/mL. Moreover, the conjugation of DNA-QD_{655} with magnetic beads-QD_{565} and the aptamer is used to design a selective fluorescence sensor for BPA with a LOD of 1.0 ng/mL in the presence of bisphenol B and C [327]. A fluorescent sensor based on a field-effect transistor (FET) through aptamer-modified multichannel carbon nanofibers (MCNFs) is used for selective BPA detection with a LOD of 1 fM [328]. The integration of GO and anti-BPA aptamer (FAM-ssDNA) is applied to design a selective and sensitive BPA fluorescent sensor with a LOD of 0.05 ng/L in the ROD of 0.1–10 ng/mL [329]. Li et al. [330] developed a fluorescent sensor by using a specific BPA

aptamer, AuNPs, and CdTe QDs for the detection of BPA with a LOD of 1.86 ng/mL and a linear ROD of 10–80 ng/mL.

Most of the reported optical sensing methods have shown evidence supporting the sensitive and selective detection of BPA, but they suffer from some limitations, such as multiple step sensor design, time consuming, and short lifetime. The electrochemical sensing approach of BPA is widely available compared with optical detection strategies. Electrochemical BPA sensors have intense features, including the cost-effectiveness, short sensing time, on-site detection, high stability and reproducibility, and good sensitivity and selectivity [331-336]. The modified electrode of B-doped diamond and nanocarbon can serve as a potential sensor for BPA detection with good selectivity and sensitivity and LOD of 13 nM [331]. A carbon-based electrode of GO and MWCNTs functionalized by β-cyclodextrin is used for the selective monitoring of BPA in the ROD of 0.05−30 μM and a low LOD of 6 nM [332]. Moreover, a functionalization/immobilization of CNT materials with biomolecules (i.e., tyrosinase), carbon black, aptamers, and molecularly imprinting polymers offers simple and smart detection methods of BPA with good sensitivity and selectivity [333-336].

GCE modification with a Cu–Zn/GO nanocomposite shows high sensitivity and selectivity for BPA detection at pH 7.1 by using square wave voltammetry (SWV) with a LOD of 0.88 nmol/L and a linear ROD of 0.003–20 μM [337]. The modification of a single crystal TiO_2 electrode via inorganic framework molecular recognition is applied to monitor BPA with high accuracy, good stability, low interfering response, and rapid response time. This electrode sensor displays a ROD of 0.01–20 μM and a LOD of 3 nM [335]. AuNP-decorated TiO_2 NT nanosensors are designed for photoenhancing the electrochemical detection of BPA with a LOD of 6.2 nM and electrode sensitivity of 2.8 $\mu A \mu M^{-1}$ cm^{-2} [338]. The coupling of Cu-MOFs with ball mill-exfoliated graphene is used to design an electrochemical sensor electrode for BPA detection [339]. Electropolymerized poly(pyrrole-nitrilotriacetic) acid and DNA aptamer with a pentahistidine peptide are functionalized and used for

BPA detection with high signaling stability, high signal affinity, wide linearity of 0.01–1000 nM, and high sensitivity of 372 Ω/unit [334].

Nanoscale materials are used in the development of various analytical approaches to meet the selective and sensitive sensor/biosensor designs of BPA. Progress in the field screening of BPA-based nanomaterial-sensors provides signaling enhancement, simple recognition, long-run durability and stability, fast response, and low cost. Significantly, the fabrication of portable sensor devices can save cost and time spent on analyses and minimize the risk of BPA contamination in food.

Table 4

8. Nanosensor-based devices for pesticide detection

One of the hot issues and global concerns in drinking and food safety are not only the treatment of chemicals, including pesticides, but also the detection of pesticide residues. Pesticides have a serious impact on the surface of water and food, thereby providing a driving force for major research efforts on effective ways to recover and manage these chemicals (Scheme 13A) [340-343]. Several pesticides are applied to agricultural fields each year to protect crops from damage and diseases, promote plant growth, and increase yield.

Lower than 0.1% of pesticides can prevent target pests from infesting crops. The remaining amount unnecessarily penetrates the environment, specifically contaminates the environment and enters the food system. Pesticides can be found in food or animal feed, and they may be indirectly or directly consumed by people. Eating pesticide-based nourishment is a principal method for pesticide pollution. As highly toxic species, some pesticide residues cause serious problems in aquatic life and food systems [340-343]. Because of the increased public awareness of the health and environmental risks of pesticides, detection, and monitoring of pesticide residue levels in the drinking and food chain has attracted great concern worldwide. Several techniques, including SERS, SPR, EISA, and electrochemical approaches, are used to determine the level of

pesticide residues [344-346]. Tracking and sensing of pesticide residues are essentially associated with food categories and pesticide species. Pesticide species can be classified as organic or inorganic substances and based on their physiological effects.

Given its ultrasensitive sensing, simple protocol, and cost-effectiveness, surface-enhanced Raman scattering is an effective strategy to detect pesticide residues in food chains. Nanomaterials based on noble metals, such as Ag and Au, have been used as a prevailing platform to detect pesticide residues with fast response and high sensitivity and selectivity [347, 348]. In addition, semiconductor–metal hybrid platforms have been utilized to improve the pesticide detection performance of SERS with good reproducibility, acceptable stability, and reusability. SERS may provide a promising approach for the direct pesticide detection in liquid samples, surface, and solid samples, but using it in complex solid food matrices is difficult.

Scheme 13

A great effort has been devoted to the engineering of flexible SERS frameworks based on the integration of active materials, such as carbon, and noble metals with flexible materials, including cellulose paper and polymer membranes that can be applied as a batch combined with food surfaces for SERS analysis [349-353]. Ma et al. [354] fabricated an integrated hybrid paper-based SERS for pesticide residue detection in vegetables and fruits by using Ag NPs and GO on cellulose paper through a screen-printing technique (Scheme 13B). The designed SERS paper offers a high sensing performance toward different pesticides in complex surfaces and LODs lower than permissible levels based on pesticide types, such as about 0.26 ng cm^{-2} for thiram.

A SERS sensor is modified with Ag nanowires with M13 bacteriophages through a mixing and filtration process involving glass-fiber filter paper [355]. In this process, the glass-fiber paper is stacked with Ag nanowires, and the surface is decorated with a tryptophan–histidine–tryptophan

peptide sequence (BPWHW) as a bioreceptor to produce a selective sensor for paraquat pesticide (Scheme 13C). Cellulose filter paper-based sensors are modified with an alkyl ketene dimer to improve the hydrophilic nature of the filter with increasing density and dispersion of AgNPs in the filter paper for pesticide-based SERS [356]. The modified SERS sensor has LOD of 0.46 and 0.49 nM for thiram and ferbam, respectively.

Yao et al. [357] designed a magnetic molecular imprinting sensor based on polydopamine and Fe_3O_4 NP nanocomposites to improve the sensitivity and specificity of SPR to pesticide detection with a LOD of around 0.76 nM in the ROD of 0.001–10 μM. Multiple classes of pesticides are detected through the immobilization of glutathione-*S*-transferase amperometry biosensors [358]. Pesticides such as carbamate and OPs working as inhibitors for acetylcholinesterase (AChE) cause neurological diseases; AChE has the responsibility to terminate nerve impulse transmission at the synapse [359, 360]. da Silva et al. [361] constructed glassy carbon/rGO/AChE as a biosensor electrode for carbaryl monitoring in tomato. AChE is immobilized into Pd–Cu nanowires to construct a modified electrode for the quantitative monitoring of organophosphate pesticides (OP) in fruits and vegetables [362]. The proposed biosensor electrode displays a high sensitivity toward malathion in the ROD of 0.005–1 and 500–3000 ppb with a LOD of 1.5 ppt. Moreover, malathion is detected using an electrochemical sensor electrode based on AChE-modified transition metal carbide ($Ti_3C_2T_x$-based) nanosheets and chitosan [363]. The designed AChE/CS-$Ti_3C_2T_x$/GCE electrode displays a high electrochemical performance for malathion monitoring with a LOD of 0.003 pM. Lu et al. [364] immobilized AChE into 1D Pd@Au core–shell nanorods to prepare a highly sensitive biosensor electrode for detecting OP pesticides, such as paraoxon, with a LOD of 3.6 pM in a wide ROD of 3.6 pM–100 nM.

The photoelectrochemical (PEC) detection of targeted species provides many advantages, including high sensitivity with a completed separation between the photocurrent signal of the

detector and the excitation light source, low background noise, simple device, convenience, and low cost. Cheng et al. [365] designed a PEC biosensor to detect highly toxic OP pesticides widely used in agriculture. This electrode is constructed by immobilizing an AChE "bioreceptor" with glutaraldehyde as a cross-linking agent into a TiO_2NP "photoactive material" and a nitrogen-doped carbon QD "photosensitizer"-modified ITO electrode to produce a biosensing platform. Nitrogen-doped carbon QDs with a brilliant optical performance and a high electrical conductivity can improve the visible light of the TiO_2NP-ITO platform by 42 times. The designed PEC biosensor is used to detect chlorpyrifos in the ROD of 0.001–1.5 μg/mL and a LOD of 0.07 ng/mL. In this context, graphene QDs, AChE, and choline oxidase (CHOx) are designed as an active GQD/AChE/CHOx platform for the direct PEC detection of OPs (Scheme 14A) [366]. The mechanism of the sensor is based on the generation of H_2O_2 from the AChE–CHOx reaction. The reaction of H_2O_2 with GODs generates turn-off photoluminescence properties at 467 nm, and turn-on photoluminescence can be recovered in the presence of OP pesticides. The LOD of the designed electrode toward dichlorvos is 0.172 ppm. A Au nanostructure is commonly used as a sensitive substrate to detect amperometric dimethoate pesticides with LODs of about 3.9 nM and 16.4 μM [367-369]. Chen et al. [369] reported a fast colorimetric probe to detect pesticides, including dimethoate and terbuthylazine, with LODs of 20 nM and 0.3 μM, respectively, and necked eye visualization based on AuNPs (Scheme 14B). Various novel nanoscale materials are fabricated to develop the potential detection protocols of pesticides and to optimize and screen food safety and environmental quality.

Scheme 14

9. Monitoring protocols of foodborne pathogens

Pathogenic microorganisms are common forms of environmental pollution because of population growth, human consumption, and poor waste management. A safe drinking water

supply is a basic requirement for human health. In consideration of many types of microorganisms can contaminate drinking water and beverages, the total number of bacteria is the main feature of quality assessment. Waterborne microbial agents, such as bacteria, pose a major risk and cause many serious diseases; consequently, they have become a major burden on public health over time. Therefore, a rapid, sensitive, and selective approach of detecting pathogenic microorganisms should be developed. Several studies have focused on developing a method for the fast and good selective monitoring of bacterial pathogens [370-375]. Current detection methods require a significant amount of time. Samples should be concentrated by reducing the sample size for rapid contamination and by adopting pathogenic bacteria. Various types of nanomaterials have been manufactured for the rapid detection and elimination of pathogens [370, 372, 376, 377]. However, the selectivity of these protocols poses challenges because target bacterial pathogens are usually present in complex samples at very low concentrations.

Scheme 15

Various techniques used for bacterial detection include RT-PCR, SPR, bulk acoustic wave impedance biosensing, microscopic examination and ATP measurements, ELISA, fluorescence and bioluminescence assays, and fluorescent in situ hybridization [378-383]. Extensive reports have focused on the importance of the nanostructured features of metal oxides. Mesoporous hexagonal MgO nanosheets with a highly active surface are designed as a powerful antibacterial agent for *Staphylococcus aureus*, *Pseudomonas aeruginosa*, and *Escherichia coli* in water (Scheme 15A) [384]. The underlying mechanism is based on the interaction with the cell wall proteins that affect its permeability, and ROS released from the designed material reacts with cell components, causing death (Schemes 15A–15C) [384, 385].

Tokel et al. [386] developed a portable label-free pathogen platform based on the integration between microfluidic and SPR technologies to detect and quantify *E. coli* and *S. aureus* (Scheme 16). A microchannel chip design consisting of a single microchannel with an outlet is created as a cartridge. This microchannel is located at the center of a slice consisting of two methyl methacrylate layers (PMMA) joined by a layer of a double-sided adhesive (DSA). A microchannel shaped from a second DSA layer and Au-plated platform, and a PMMA-DSA-PMMA-DSA-Au chip are obtained. The designed sensor displays a reliable ROD of *E. coli* at ~10^5–3.2×10^7 CFU/mL in PBS. A simple DC process is used to manufacture a flexible SERS platform through AuNP deposition on dragonfly wings, thereby creating a promising bioplatform to detect pesticide residues [387]. The designed platform is utilized to detect cypermethrin (pesticide residue) in tomato husks through a pressure and peeling method. The platform can rapidly and reliably detect cypermethrin with a LOD of 10^{-3} ng cm^{-2}.

Scheme 16

Sedki et al. [370] fabricated an RGO-hyperbranched chitosan nanocomposite as an active electrode for the sensitive and real-time detection of bacterial cell viability based on microbial electrochemical systems (Scheme 17A). *E. coli* and *P. aeruginosa* are used as targeted pathogens to evaluate electrode performance. The results show that the designated nanocomposite electrode exhibits the fast response/detection of cell viability and enhances the bioelectrochemical detection limit. Optical scanning microscopy is used as a digital, rapid, accurate, and label-free strategy to evaluate the microorganism's viability through the development of bacteria on a glass-slide cell culture device (Scheme 17B) [371]. Using *E. coli* as a model bacterium confirms the fast response of the device with a decreasing experimental duration from 13 h to 5 h with the accurate quantitative determination of bacteria and the automatic accurate counts of microcolonies. In addition, the designed system allows the use of small pieces of agar plates

instead of whole agar, thereby shortening bacterial counting. Højris et al. [388] provided an optical on-line bacterial sensor through the algorithmic analysis of 3D image recognition by considering 59 quantitative parameters of the obtained image. The designed sensor allows the individual quantification, counting, and classification of outstanding targets, such as bacteria or abiotics, in single and mixture suspension solutions. This study is presented for the rapid detection of bacteria that may contaminate a type of water sources used for food productions. Yu et al. [389] reported an accurate strategy for the total quantification of *E. coli* ER2738 in contaminated water through flow cytometry and PicoGreen nucleic acid fluorescence staining (Scheme 17C). Detection is based on the scattering and fluorescence signals of the targeted bacterial cells. On the basis of this background, the presence of a bacterial cell can be confirmed as a function of equivalent detection of signals.

Scheme 17

Phillips et al. [390] developed a sensing assay by using hydrophobically functionalized AuNPs for discriminating three *E. coli* strains. The mechanism of the sensing protocol involves the replacement of negatively charged conjugated polymers with pathogenic cells in the sensing protocol; as a result, polymer fluorescence changes. In addition, ultralow concentrations of volatile organic compounds can be detected easily by the human's nose. Duncan et al. [391] reported a selective bacterial cell sensor composed of hybrid and functionalized NPs. The platform is constructed on the basis of three components, namely, functionalized AuNPs, pro-fragrance molecules that offer a "turn-on" response and produce distinctive odiferous, and anti-pro-fragrance enzymes that create an olfactory output (Scheme 17D). The displacement of lipase in the lipase–NP complex enhances the detection performance as the signal response increases, achieving high sensitivity within 15 min. Three types of quaternized magnetic nanoparticle–urease are fabricated and designed for the sensitive detection of Gram-positive or Gram-negative

bacteria (Scheme 17E) [392]. Detection can be achieved through the displacement of urease to hydrolyzed urea. The designed sensor has a high sensitivity of 10^2 CFU mL^{-1} with an accuracy of 90.7% within 30 min. In addition, Wan et al. [393] designed a nanocomposite platform for the quantitative recognition of bacteria by using three quaternized magnetic nanoparticle–fluorescent polymers. The designed sensor displays a high sensitivity of 10^7 CFU mL^{-1} and an accuracy of 87.5% within 20 min.

On the other hand, reports have confirmed that distinguishing and evaluating food-related viruses, which pose a serious threat to the food industry, is a priority task for food safety. Therefore, food safety experts have provided appropriate techniques and measures to detect and control viruses at all stages of the food chain and their control in the food industry [394-400]. Viruses obligate intracellular parasites and sensitive host cells for reproduction and the infection of their host. Incidentally, the design of the gastric extracellular matrix is simple; it consists of the nucleic acid, either single-stranded (ss) or double-stranded (ds) DNA or RNA, surrounded by a protein envelope. Viruses are classified as enveloped or non-enveloped types based on the presence or absence of an envelope of lipid bilayer derived from host cell membranes and viral proteins. In general, many different viruses, such as rotaviruses, astroviruses, saboviruses, enteroviruses, adenoviruses, and hepatitis E, are associated with the human digestive system. Subsequently, viruses cause a variety of diseases, such as gastrointestinal (stomach and intestinal) inflammation or hepatitis, which are transmitted through food or drink. Furthermore, the transmission of these gastrointestinal and liver diseases through food is associated with human norovirus (HNoVs) and HAV, respectively.

In 2012, approximately 21 million cases of acute gastroenteritis were detected in the United States, and 800 deaths were reported; moreover, the economic cost of infection with HNoVs is $5.8 billion annually in the United States [394]. Viral HNoV particles can survive for a long time

in various environments, including food products, and they are transmitted from the host via the fecal oral route, contaminated surface contact, and water resources [395, 396]. Electron microscopy, enzyme-linked immunosorbent assay (ELISA), immunochromatography, and biosensors have since been developed to detect the HNoVs in their resources [396]. Moreover, the development of fast, sensitive, and portable sensors for HNoV detection is in great demand [395]. The reverse transcription-polymerase chain reaction (RT-PCR) provides a good analytical technique for quantifying HNoVs. Despite the importance of the RT-PCR strategy, it has many drawbacks, including high cost, high time consumption, complicated sample preparation, and the need for experienced technicians. Well-designed biosensors, such as optical biosensors (i.e., Raman, IR, fluorescence, chemiluminescence, SERS, and SPR), can help to overcome most of the existing disadvantages related to sensitivity, selectivity, temporal response, and portability [397, 398]. Guo et al. [399] successfully designed an immunosensor by immobilizing the monoclonal antibody of HNoVs on electrode surface and performed photoelectrochemical assays for HNoV detection with LOD of 2×10^{-10} g mL^{-1} (4.9 pM) with a fast response time of 30 minutes. Another study [400] modified the microfluidic chip with monoclonal anti-HNoV. In the design, HNoV fluorescence intensity tracking was detected using a smartphone image after the background noise was filtered. A rapid, fast-response, low-cost, and easy-to-use technique was developed by using colorimetric HNoVs sandwich immunosensor and cotton swabs. The cotton swabs were functionalized by anti-HNoVs and then immersed on labeled anti-HNoVs with Au NPs for detecting HNoVs in a variety of food samples, including cucumber, lettuce, and chicken, with LOD of 10 and 53 pfu/mL [401].

A Au/Ag core/shell NP-based colorimetric biosensor was designed to detect HNoVs based on the improving of peroxidase-like performance of Au/Ag NPs. The HNoVs were captured by the antibodies immobilized on the 96-well microtiter plate surface; moreover, the oxidation reaction

between Au/Ag core/shell NPs and H_2O_2/3,3′,5,5′-tetramethylbenzidine (TMB) presented an intense blue color with LOD of 10.8 pg/mL, which could be attributed to the liberation of Ag from the Au/Ag NP surface [402].

Aimed at the selective DNA detection of norovirus and influenza A, Lee et al. [403] designed an electrochemical sensor based on the Pt-interdigitated electrode modified by CNTs decorated by Au/ magnetic iron oxide nanoparticles (Au-MNP-CNT). The designed sensor was highly sensitive, with the selective assay presenting a wide DNA linear range of 1 pM to 10 nM and LOD of 8.8 pM for both viruses. Label-free electrochemical sensors have been designed for the fast-response, sensitive, selective, and onsite detection of HNoVs. Peptides of HNoVs were used for the selective binding of HNoV particles. The peptides were immobilized at the electrode surface of Au to design a sensitive selective HNoV electrochemical sensor. The LOD was 1.7 copies/mL and could be used in care bioassay to detect HNoVs in food samples [404]. Hong et al. [405] designed electrochemical biosensors based on the Au electrode modified by concanavalin A (ConA) for the sensitive and selective detection of HNoVs in food samples. The sensor offered a wide linear range of operation at 10^2–10^6 copies/mL and low LOD of 35. Hirano et al. [406] selected certain immobilization parameters, including immobilization time, concentration of aptamer, concentration of supporting electrolyte containing 4 mM $K_3[Fe(CN)_6]$, and investigated their effects on an electrochemical aptasensor designed for the selective detection of HNoVs by using the SWV technique. Giamberardino et al. [407] performed an onsite monitoring of HNoVs with LOD of 180 virus particles and developed an HNoV aptasensor after immobilizing ssDNA at the Au electrode via the SELEX process. To date, the effective monitoring protocols of foodborne pathogens and the novel progress of materials that can enhance sensing analysis are still required to improve the risk assessment of bacteria in food contaminations.

10. Food adulteration screening

Food adulteration, which is mainly related to the failure of a food product to meet legal standards, is the result of the change in nature and quality of food with the addition or substitution of a food ingredient with another unspecified ingredient; this scenario poses a serious threat to healthcare, especially in developing countries [408]. An example of food adulteration is the contamination of Chinese infant's milk with the addition of melamine in 2008, and global attention has since been drawn to the continuous analysis of all basic food products, such as milk, dairy products, and meat [409- 414]. Milk and dairy products, which can easily adulterate, are important for adults and infants as they include key complementary ingredients, such as fats, proteins, carbohydrates, vitamins, and minerals. Therefore, different techniques have been sought to verify food adulteration according to the nature of the foreign components or sources of food. Milk-like products are widely replaced by various plant protein sources, such as soya, rice, and almond proteins, and sold as natural milk products [411]. However, some proteins (e.g., such as soya, wheat, almond pea, rice, lupin, and maize) are labeled or/and clinically recognized as allergens by the Food Allergen Labelling and Consumer Protection (FALCPA) [412, 413]. In addition, the production cost of plant proteins, such as soya milk, is cheaper by 70% than natural milk protein, suggesting the prevalence of milk adulteration [414].

Consequently, many approaches and techniques, such as RT-PCR, high-performance liquid chromatography (HPLC), near-infrared (NIR), ELIZA, spectroscopy, and electrochemical methods, have been designed to investigate food adulteration [410]. ELISA can detect various proteins other than milk protein by labeling the monoclonal/polyclonal antibodies in these products [415]. The purity and originality of pasteurized milk powder protein was studied to determine the foreign mix of proteins (e.g., soya, pea, and wheat) by using the polyclonal

antibodies of these proteins [415]. This method can help to match the polyclonal data with the theoretical value by using relative standard deviations (RSDs) in the range of 5% to 22%. Moreover, skimmed milk adulteration by other proteins was evaluated via the UHPLC technique with high efficiency [416]. In addition, the turbidity measurements of selective tetraborate-EDTA buffer approach was used to detect insoluble plant proteins mixed with milk proteins by means of their separation and identification via mass spectroscopy [417].

Milk source and animal species difference quantification is challenging because of their genetic and nongenetic dependency. Milk source originality (genetic variant) was detected using the capillary electrophoretic (CE) technique [418, 419]. Bovine, ovine, and caprine milk proteins were used as the basis for identifying their respective genetic variant sources [418]. Currently, the ELISA and PCR techniques are widely used to detect the genetic adulteration of other milk sources (e.g., goat, sheep, and buffalo milk) in addition to cow milk [420]. The PCR test was successfully used to detect cow milk adulteration with respect to caprine milk. Cow milk in goat cheese, ewe milk cheese, and buffalo mozzarella cheese was also detected using the PCR test [421-424]. Moreover, the geographical source of milk can be identified by analyzing the isotopes and metal contents of the milk via inductively coupled plasma emission spectroscopy (ICP-OES), HPLC, and other elemental analytic techniques [425]. Elemental analysis provides information about milk geographical originality and contamination by hazardous inorganic materials [426, 427]. Milk additive ingredients, such melamine, urea, and other products, were detected using various techniques, such as spectroscopy NIR, GC-MS, HPLC, and SERS [428-433]. All of the abovementioned techniques can provide a sensitive and selective assay for detecting melamine and urea in the milk ingredients. In summary, many approaches have been developed to ensure milk quality assurance.

Meat adulteration, a major consideration in distinguishing meat sources, is a relevant topic because of cost and religious reasons. Meat adulteration attributable to other sources, such as mixing beef with donkey, pig, and horse meat, and labeling these meats as beef have been discovered globally. In 2013, horse meat was labeled as beef meat in European markets [434]. Various methods, such as ELISA, spectroscopy, and PCR, have since been used for food quality and content authentication [435]. Ha et al. [436] developed a PCR method to detect pork adulteration in meat products. The 294-bp mitochondrial DNA of pork was used for pig target-DNA sequencing to identify pig adulteration in various kinds of meats (i.e., sheep, cattle, and chicken meat). The developed technique could detect 1% pork in beef, chicken, and beef–chicken mixtures. Successive developments of the PCR test, including the multiplexed PCR, to detect different specific primers in a single run from various sources have since been reported [437]. Five meat specific-species primers (mitochondrial ND5, ATPase 6, and cytochrome b genes) were detected using the multiplexed PCR. The genes from pig, cat, rat, dog, and monkey meats were amplified as 141,172, 108, 163, and 129 bp DNA fragments, respectively. The method provided a highly sensitive assay for DNA detection in the range of 0.01–0.02 ng with a low suspected meat rate of 1%. The method, which was intended for commercial use, helped to observe Halal food quality of Muslim food. The multiplexed PCR was also used to identify various meat species (i.e., buffalo, chicken, ostrich, lamb, horse, rat, and fox species) with high efficiency, low time consumption, and high selectivity [438-441]. In general, PCR tests can selectively detect meat adulteration, but they suffer from various drawbacks, such as sample contamination, high time consumption, expensive technique, and low quantity [442].

Various techniques (i.e., ELISA, HPLC, lateral flow immunoassay, electrochemical immunoassay, etc.) are used to detect proteins and identify meat adulteration. The different types of ELISA (direct, sandwich, and indirect competitive techniques) are widely used to detect food

proteins and distinguish the food sources [443-445]. Sensitive and selective ELISA assays have been developed to identify pork adulteration in meat products. The IgG was immobilized in a microplate and competed with the extracted IgG to decrease the testing time; the assay showed a fast response time of 45 minutes with low susception (0.1%) of pork content [445]. The sandwich ELISA assay was developed to detect pork adulteration in cooked meats of lamb, beef, horse, chicken, and goat; this assay provided a highly sensitive technique of 0.00014% w/v and 0.0004% w/v for cooked and autoclaved pork, respectively [444]. Electrochemical sensors have various advantages, including rapid, sensitive, simple, and portable assays [446-448]. Label-free electrochemical immunosensors have been developed for the selective detection of porcine serum albumin (PSA). A study [449] functionalized the carbon nanofiber-modified SPE by 4-carboxyphenyl, and the PSA antibodies were immobilized at the modified electrode. The specific binding between the amino group of the antibodies and the carboxylic group at the 4-carboxyphenyl was determined. The LOD was 0.5 pg/mL, with a wide linear range of 0.5–500 pg/mL of PSA. Mansouri et al. [450] designed an electrochemical biosensor for meat adulteration detection and subsequent cooked sausage evaluation. The electrochemical biosensor was designed on the basis of a specific-species DNA probe. The electrochemical DNA probe could selectively detect donkey meat adulteration in sausage food. This technique provided a sensitive and selective assay with a fast response time, low LOQ of 148 pM, and RSD of 0.16%. Many other approaches of food quality and adulteration detection have since been developed, including the design of a portable chipset biosensor for onsite monitoring. These portable biosensors can detect multiple targets in a single run and obtain a fast response, hence their high economical value.

11. Portable sensor devices for daily food safety analyses

In principle, food assessment based on portable devices can be performed by self- and in-home or in-market and other places where a food sample is served. To date, many portable devices for food control are available, but the design of commercially available portable sensors should be further improved. Wireless electronic devices and portable sensor technologies for food and beverage products should be enhanced to improve the reliability of screen displays for visual monitoring and online acquisition, to address significant food safety and health management concerns.

Mixing alcoholic beverages with foods during eating is a passive way to suppress the direct adsorption of alcohol to blood stream. Alcohol is frequently used as a food ingredient. In addition, a large amount of alcohol intake is a health risk that leads to various diseases and about 2.5 million deaths annually worldwide. For example, alcoholism may cause significant health risks that may lead to deaths from possible traffic accidents. Therefore, an alcohol level detector is essential for human life and safety. Reliable microdetectors that can continuously detect the consumption and misuse of alcohol in liquids have attracted considerable attention [451, 452]. Blood alcohol concentration is an accurate measure that can be used for alcohol detection in the blood, but it is difficult to use because pain associated with blood sampling restrains alcohol level monitoring in the blood. Therefore, alcohol concentration is usually used to detect alcohol, but it needs a special case and requires frequent analysis because it can be affected by environmental changes. In addition, alcohol detection has been investigated through transdermal-based sensors in humans [453, 454]. Electrochemical-based alcohol sensors are used as a good non-invasive analysis tool because of the association between the interstitial fluid (ISF) and alcohol concentration in the blood to detect alcohol in sweat and estimate the corneal layer through vacuum pressure [455].

Scheme 18

In this context, a microneedle-based sensor has been reported as an attractive skin sensor for the continuous evaluation of alcohol in ISF based on electrochemical analysis (Scheme 18) [456-459]. This sensor is constructed through alcohol oxidase (AOx) immobilization on the integrated structure of a pyramidal microneedle design containing microcavity opening wires of Pt and Ag that have been modified with *o*-phenylene diamine through electropolymerization. Immobilization has been implemented in a medium chitosan layer with Nafion as an outer layer. Using AOx in a functionalizing working electrode enhances selectivity, stability, and continuous alcohol recognition from artificial ISF. Experimental results in an ex vivo skin mouse model show that the designed sensor is effective in subcutaneous alcohol detection. In addition, this design has potential for application in real-time noninvasive alcohol detection. A wearable sensor based on gold and zinc oxide as sensor electrodes can detect alcohol consumption by determining the amount of ethanol metabolite ethyl glucuronide (EtG) and by designing a LED-based device to detect EtG in human sweat (Scheme 19). This strategy is built on the basis of electrochemical EtG detection through the immobilization of monoclonal antibodies to EtG on the electrode in the ROD of 0.001–100 μg/L and a LOD of 0.001 μg/L [460].

Scheme 19

The real-time detection of ethanol levels in the blood is developed through a prototype device as a noninvasive strategy for ethanol detection in the blood through the transdermal alcohol concentration strategy (Scheme 20A) [455]. Ethanol concentration is detected through the amperometry measurement of ethanol in sweat. The sensitivity of this device is higher than that of breathalyzers, and the device can work in a wide ROD of 0.0005–0.6 g/L. Droplet microdroplet screening is utilized to determine ethanol levels in cell cultures (Scheme 20 B) [461]. The prototype is based on an electrochemical alcohol oxidase/HRP sensor, and it provides a useful device for detecting the alcohol consumption of drivers. Kim et al. [462] used a wearable

tattoo-based sensor as a noninvasive strategy to detect alcohol in sweat (Scheme 20C). A flexible wireless electronic device based on an integrated biosensor iontophoretic tattoo can transgenically deliver a pilocarpine drug that prompts perspiration to detect ethanol through amperometry by utilizing Prussian Blue and Aox. The proposed design as a wireless skin strategy shows potential for the real-time monitoring of alcohol consumption and can be easily expanded for further detection analysis.

Scheme 20

With the increasing attention of the self-monitoring of food quality and safety, portable senor devices contribute effectively in visual reading out and on-time and in-place analyses of bacterial contamination levels in food products with minimal restrictions. Portable electronic devices for the indoor and outdoor screening of pathogenic targets in food are important because of their distinct characteristics, including cost effective, providing fast and quantitative results on site. Based on visual detection through the fluorescence imaging of chemicals and biomolecules, an integrated system of a UV LED and a smartphone camera is used as a detector. In this context, the fluorescence imaging platform of a smartphone camera is utilized to detect *E. coli* concentrations at which excitation antibodies immobilized on quantum dots through UV LEDs are applied to detect bacterial concentrations based on fluorescence signals [463]. The results reveal a LOD of around 5–10 CFU mL^{-1}. In addition, Ludwig et al. [464] monitored milk antibodies, such as antirecombinant bovine somatotropin, by using an integrated system between a white LED and a cellphone-based diagnostic platform (Scheme 21A).

Peanut allergen in food is tested and detected through colorimetric assays based on a cellphone-based system (Scheme 21B) [465]. This strategy is based on the development of a two-tube mobile phone facility for test and control detection processes. Light intensity is detected using a smartphone applicationdeveloped to measure the concentration of allergens relative to reference

concentrations. Color tests are conducted using an ELISA test kit for peanuts. This method provides a digital tool to detect and measure peanut levels in food samples with a LOD of approximately 1 ppm. Clenbuterol (CLB) can be used to increase the growth rate in livestock, but this procedure is illegal. Therefore, a CLB detection system is developed on the basis of a mobile electromechanical device with a LOD of 0.076 ng mL^{-1} in 6 min [55]. CLB is prohibited as a feed additive because its aggregation in animal tissues has several health risks. Giordano et al. [466] reported an integrated data processing on a smartphone system for the successful reorganization of Brazilian honey (Scheme 21C). The designed sensor substrate is equipped with a USB connector and an integrated Bluetooth module in potentiostat devices to share data via various net applications.

Scheme 21

Portable sensor devices for the detection of pesticides have posed a great concern because of health risks associated with these compounds. For instance, OP nerve agents, such as VX and sarin, are highly toxic substances that affect the nervous system. Therefore, the presence of OP pesticides should be controlled to prevent illnesses caused by exposure to these compounds. In this context, a wearable glove sensor is developed for the electrochemical sensing of collected residues when the thumb touches the printed enzyme-based OP sensor (Scheme 22A). Xu et al. [467] monitored OP pesticides by using a wearable glove-based sensor of an integrated "lab-on-a-glove" system containing two fluorescent centers with an aerogel flexible host material (Scheme 22 B). The designed sensor provides a fast real-time response (30 s) with a LOD of 89 Nm and allows detection with the naked eye. Chen et al. [351] proposed AuNPs as an easy sampling of complex surfaces of a proof-of-concept SERS platform for the direct and fast sensing and extraction of 4-mercaptopyridine and pesticides (Scheme 22C). In this report, numerous pesticide residues, including chlorpyrifos, thiram, and parathion–methyl, are qualitatively

measured in vegetable, cucumber, orange, and apple. Wang et al. [468] reported a gecko-inspired nano tentacle SERS as a fast-sampling technique that can be used for pesticide detection based on the "press and peeled-off" strategy (Scheme 22D). A flexible and free-standing platform is constructed on the basis of 3D poly(dimethylsiloxane) nano tentacles and AgNPs for the recognition of three types of pesticides. In addition, Au nano islands on dragonfly wings are used as a SERS platform through a DC magnetron sputtering system for detecting pesticide residues from tomato peels with a LOD of 10^{-3} ng cm^{-2} (Scheme 22 E) [387].

Scheme 22

Scheme 23

The increased accumulation of UA and low secretion in human bodies are closely related to the onset of gout and excessive UA. They are strongly influenced by the intake of large quantities of food rich in purine. UA is found in higher plants and microorganisms (Scheme 23A). A real-time sensor for UA detection is designed on the basis of the integration system of a low-energy Bluetooth communication system-on-chip and a novel salivary metabolite mouthguard biosensor (Scheme 23B) [469]. Kassal et al. [470] designed a wireless smart bandage biosensor for UA detection (Schemes 23C and 23D) and constructed it based on the immobilization of urease with Prussian blue as a printed catalytic transducer to enable the detection of UA at low concentrations. The sensor bandage is integrated with a wearable potentiostat that provides reading out of the UA status on a smartphone, a tablet, or a computer.

New technology-based food analysis techniques, device-integrated smartphones, and on-time data acquisition tools are needed for the precise and rapid assessment of food quality. The development of portable food assessment devices represents a promising area with a significant scientific and commercial impact. The emerging effects of active nanomaterials in a portable sensor provide promising prospects for direct sensing, on-demand scanning, and self-analysis systems for home

testing. So far, wireless smart devices should respond to direct food assessment for applicable, accurate, and precise point-of-care analysis. Therefore, the incorporation of smart nanomaterials into sensor array devices may provide sensor designs with precise and customized properties. When integrated with smartphones, these portable sensor devices may be used for on-site testing. With effective advances in nano- and micro-metric devices, real assessment protocols should be developed for the enhancement of the quality of food and agricultural products with high sensitivity and accuracy.

12. Commercial/industrial market deployments of portable sensor devices for food assessment

To ensure the quality of food, the design of materials-based sensor devices (Table 5) in terms of readability (easy-to-read) and practicability needs special standards. In this regard, high-sensitivity wearable and implantable biosensors are needed to help improve real-time monitoring and food-sensitive detection. To date, the primary drawbacks of the traditional traceability approach in food quality assessment are as follows: (i) it requires multi-step inspections; (ii) it involves a time-consuming process; (iii) the method is labor-intensive, and well-trained personnel are needed; (iv) the method is unsuitable for onsite product analysis; (v) the results have low sensitivity; and (vi) risk of microbial contamination is common. Although non-invasive nanoscale/microscale designs with high efficiency and reliability and cyclic analyses are areas of interest in the field of disposable sensing platforms, the fully printable and wearable biosensing system is still in the research and development stage. Portable biosensors offer promising prospects for direct biosensing systems, on-demand screening, and home analysis for self-testing. However, a number of disadvantages need to be resolved, including the following: (i) high cost of sensor manufacturing devices, (ii) losing of its accuracy, sensitivity and selectivity in the presence of the interference species, (iii) short home and personal self-testing and on-time analysis, and (iv) special precautions for sterilization. Therefore, the recent developments in food sensor designs are required to improve the provision of (i) personal

monitoring use with compact device size, (ii) direct inspection, and (iii) accurate on-target screening as a means of preventing adulteration and improving food quality.

Personalized monitoring and checking of the quality of agricultural products, foodstuffs, and food beverage industry and their processing have received much attention to develop approaches for personal consumption and market determination. Therefore, the development and provision of analysis methods and electronic devices for testing the quality of food products are particularly interesting. Self-tester and portable readout sensor devices are on-demand, inexpensive, and convenient to attract consumers, researchers, and food manufacturers. To date, effective monitoring systems remain vital concerns to conduct regular checks for hazards and food quality, ensure food ingredient safety, and maintain public health. According to the increase in the global market growth rate and the requirements of the food control market, a number of companies introduced various devices and analytical methods that contribute effectively to food quality control (Table 5). Challenges remain for the commercial development of electronic sensor devices with miniature reading out, digital easy-to-read without supplying power, and wireless signal transmission into smartphones. Furthermore, the scalable manufacturing of electronic food sensor devices with actual and cheap cost in commercial/industrial market deployments has substantial issues.

Table 5

Conclusion and future outlook

With the need for today's food safety and management, assessment should be centered on the whole food cycle to determine and confirm food and microbiological quality. Providing safe food and water is an essential prerequisite for human wellbeing. A wide range of pesticides, microbial bacteria, hazardous contaminants, and essential food additives may exist in drinking and food chains. Thus, overall quality assessment is a key milestone of human health from the point of view of care. Given the prevalence of food safety and its impact on health, economic,

and social sectors, advancements in an ultrasensing, early detection, and real- and on-time monitoring strategy of vital reactive species, biomolecules, chemicals, and even hazardous agents for the food quality sector are urgently needed.

This review provides real evidence on the key impact of the recent building block design of the engineering of nanodynamic early sensory detectors in the improvement of standard food quality through the full control of (i) an extraordinary food safety test in terms of developed sensing protocols and tools; (ii) numerous and extensive scale auto-examining evaluations of reactive food species, including H_2O_2, UA, AA, sulfites, and nitrite anions; (iii) extensive monitoring and assessment of targeted hazardous species, including bacteria and pesticides; and (iv) conceivable, portable, and compact nanosensors for real-time analysis via a small sample size.

With significant advances in the diverse and competitive food and beverage market, consumer concerns about food safety, ingredients, contaminations, and processed foods have emerged. Food contamination has caused prevalent diseases and impacts on social, financial, and health sectors. Thus, sensory gadgets for accurate quantity screening, early explicit monitoring, assessment, and real-time detection should be developed. This review highlights new development monitoring technologies for a comprehensive treatment strategy, outstanding screen monitoring pattern, and restorative conditions for potential food safety. For the proximity control of food safety and management, special attention and efforts are still needed to provide appropriate sensing protocols and strategies that can be configured in sensitive and smart gadgets linked to basic, quick, convenient, and continuous target recognition devices.

In this context, we focus on engineering a powerful nanoscale sensor design and protocol that investigates the explicit restricting partiality to a wide scope of the food safety, periodical transduction into readable output signals, high-precision assessment of food contamination, dead-end-use examination, and fast response analysis. AA, H_2O_2, UA, nitrite, and sulfite anions, pathogenic

bacteria and viruses (i.e., *E. coli*, H1N1, HuNoN, and SARS-CoV-2), food adulteration, and pesticides have been covered as targeted species for food safety assessment. Thus, we provide details on advanced sensor development in monitoring, analysis, and evaluation sectors for food safety applications. Moreover, this review highlights the key principle for the future steady progress required in food safety and quality, biotechnological, analytical, and sensing applications.

Reducing the spread of COVID-19 is the first priority worldwide. Although more than a year has passed since the COVID-19 pandemic began, information and explanations about the nature of the infection remain scarce and unclear. Currently available information indicates that COVID-19 does not directly infect humans through food, but the hypothesis indicates the emergence of the virus in bats and its transmission to this organism used in food. With the emergence of new evidence, measures should be taken to follow up on even frozen foodstuffs and their preparation stages. In addition, as of writing this review, the design of any sensitive device for detecting COVID-19 in foods has not been disclosed, but efforts should be devoted to providing a sensor to assess food with high selectivity and sensitivity and prevent the spread of COVID-19 through the food production process and its manufacturing stages.

Nanodynamic portable sensors can be used to monitor contamination and assess environmental food with short-time consumption and simple operation. The precision control of present propels in the tangible transformation of nanomanufactured sensor innovation into a food test home-use facility can be assessed via the following capacities:

(i) Advanced detecting appraisal and precise assessment of natural examination parameters (e.g., sensitivity, real-time monitoring, calibration line, stability, quality, and reproducibility)

(ii) Timely and real-time investigation protocol, early checking and precaution treatment, and board analysis tests that can be connected to shorten treatment duration (e.g., quick reaction, early visualization and finding, brief span treatment, and precise detecting examination)

(iii) Simple design of a compact nanobiosensor in daily use (e.g., chipset sensor, well-planned reconciliation, wearable, adaptable, and brilliant material-based gadget stages) with proficient examination precision, security, and viability of self-customized observation of targeted levels in the food chain

(iv) Well-controlled, scalable configuration, and low-cost manufacturability of sensory gadgets

This review gives proof-of-evidence that the engineering and design of a powerful nanosensor are ongoing acquisitions, offering considerable future avenues for wide-range opportunities to control healthcare initiatives. With the headway of human advancement and progress in nanoscience and nano-engineering, the manufacture of effective and operative detecting devices for the early recognition and inhibition of food contaminations will be vital in food analysis and environmental monitoring. Up to date, one of the urgent nanodevelopment of the future is the building blocks of nanoscale sensor devices in sensitive portable, touchscreen, and wearable end-user products to enable the direct assessment of food quality. Continuous acquisitions and significant future orientations provide broad opportunities for food assessment and control. Next-generation nanoscale wearable sensors are urgently needed for rapid, simple, and on-time biosignature monitoring assays to ensure food safety. However, the controlled construction of the sensing, surface functionality, and on-site monitoring of target molecules are a challenge for the driven noninvasive sensor promotion of organic and nonorganic agents, targeted biomolecules, bacteria, pesticides, and pollutants that are naturally associated with food safety. This review gives evidence that the powerful engineering of nanosensor in handy IoT devices is an ongoing acquisition, offering considerable future avenues for wide-range contributions to perspective healthcare initiatives in Society 5.0.

List of Schemes:

Scheme 1: (A) Essential applications of nanotechnology in the food sector, and the key elements for food assessments. (B) Schematic representation of sensor workability and design in terms of fabrication and sensing assay through various transducers that converted this reaction or binding into digital signal.

Scheme 2: Nanomaterials-based sensor platforms with a wide range of domains of hierarchical control of the virtual and anisotropic orientations including the dendritic nanoarchitecture nanostrands inorganic metal oxide, nanoscale sheet orientation building blocks, metal organic frameworks (MOFs) materials, nanocomposite and hybrid nanocomposite materials, and uniform, multi-directional mesoporous accessibility of the nanoarchitecture was doped microporous carbon microspheres. The sensory design, clear orientation and formation such as cavities, geodes, tubes, spherical bodies, cubes, and multi-surface structures profoundly affect the sensitivity and selectivity of target species among competitive species.

Scheme 3. (A) Colorimetric sensor design based on AgNPs for quantitative AA detection in commercial and pharmaceutical samples, reproduced with permission [99]. (B) A "turn-on" Eu (III) luminescent complex sensory probe for AA visual imaging in the living cell using time-gated luminescence microscopy (TGLM) system, reproduced with permission [100]. Fabrication of a fluorescent switchable N, S-CDs sensor for AA detection in fruits based on the mechanism of N-,S-CDs/Fe^{3+} system (C,D), reproduced with permission [110].

Scheme 4. Electrochemical electrode design with a sulfur-doped microporous carbon microsphere (S-MCMS) for AA detection in in its real samples. (A-C) Analysis of the morphological surface structure of using FE-SEM images, (D) the electrooxidation design of AA on the S-MCMS electrode

surface, (E, F) representing the real amperometric detection of AA in Lemon juice and pharmaceutical products (Vitamin C tablets), Reproduced with permission [11].

Scheme 5. (A) Synthesis of NPC/Co_3O_4 nanocomposites through direct thermal treatment of ZIF-67 precursor as a sensitive electrode material for voltammetric detection of AA in vitamin C tablets, Reproduced with permission [121]. (B) Electrochemical detection of AA and DA with high sensitivity using a fabricated microelectrodes of carbon fiber/ZnO core–shell hybrids material, Reproduced with permission [122]. (C) Modification of pencil graphite electrode (PGE) by raphene-iron oxide-polyvinyl alcohol (PIG) for AA detection (C) [132].

Scheme 6: (A) Design of fiber optic sensor through the modification of plastic clad silica fiber core (FC, 0.6 nm in diameter) with Ag layer and nanocomposite of AgNPs-PVA. (B) Fixing of the designed fiber optic probe, FC/Ag film/Ag NPs-PVA nanocomposite, into a flow cell for H_2O_2 detection, Reproduced with permission [140]. (C, D) Schematic design for the detection of H_2O_2 using a fiber-optic probe based on the PB/PW response during the oxidation and reduction of sample, Reproduced with permission [142]. (D) The designed illustrated the detection mechanism of H_2O_2 using a fiber-optic PB/PW probe, the generated white light traveling through arm1 arriving at the sensor film of PB/PW, then the collected light directed back through the arm2 to measure the intensity of the reflected spectrum to confirm the PB/PW response during the oxidation and reduction process.

Scheme 7: (A) Selective detection of H_2O_2 species based on the turn-on fluorescence aggregation/deaggregation behavior of tetraphenylethylene based on the aggregation induced-emission during the reaction with H_2O_2 species, Reproduced with permission [145]. (B) Two-photon fluorescent probes mechanism for detect H_2O_2 detection in living cells and its successful use in imaging, Reproduced with permission [154]. (C) A turn-on fluorescence for selective H_2O_2 in living cells based on oxidizing the mitochondria-targetable ratiometric fluorescent probe, HBTPB (as a NIR-

emitting fluorescent probe), Reproduced with permission [155]. (D) The design of mitochondria-targetable modified with a HKB ratiometric fluorescent chelating agent for detecting H_2O_2, with the fluorescence analysis using 0–500 μM of H_2O_2, Reproduced with permission [156]. Schematic designed of the proposed fluorescence sensing process of H_2O_2 molecules via the mitochondria-targeted modification using coumarin moiety (E), Reproduced with permission [157]. Design of the real in vivo H_2O_2 detection using young angelfish (age 20 days) as a real example of living organisms (F), Reproduced with permission [159].

Scheme 8 (A) Schematic design of the enzymatic sensor design by controlling the immobilization of targeted enzymes into the electrode surface platform such as nickel foam, and (B) the full steps of Heme proteins modified Ni foam electrode for enzymatic electrochemical detection of H_2O_2, Reproduced with permission [172-174] .

Scheme 9. Schematic sensor design through hem-proteins immobilized of on the NiO nanostructures surface. The proposed mechanism of non-enzymatic H_2O_2 sensor based on the modification of Ni foam electrode through the immobilization of Cyt.C, Reproduced with permission [175].

Scheme 10. Design of a non-enzymatic H_2O_2 selective electrochemical sensor by the electrodeposition of PtNPs into modified RGO/GCE electrode for real and in-vitro cell application (A), Reproduced with permission [31]. The electrochemical real monitoring of H_2O_2 released from live cells (A549) using a GCE modified by MoS_2 NS/N-doped carbon NWs nanocomposite (B), Reproduced with permission [186]. Engineering of an encapsulated Au@ZIF-67 electrode sensor for electrochemical detection H_2O_2 released from stimulated living organisms to screen cancer cells (C), Reproduced with permission [187] [163]. The fabrication and proposed mechanism of $Ni(OH)_2$/RGO/Cu_2O@Cu electrode for glucose and H_2O_2 detection, (D), Reproduced with permission [189].

Scheme 11. (A) Schematic diagram of the main steps of the an encapsulated CdS-QDs-Uricase/HRP fluorescence biosensor engineering for UA detection, in addition to the mechanism of detection based on the quenching properties of H_2O_2 produced from the biosensor system, Reproduced with permission [202]. The turn-off design of Co^{2+}/H_2O_2–AUR fluorescence sensor for UA detection, and effect of different UA concentrations on the Co^{2+}/H_2O_2–AUR sensor (B), Reproduced with permission [206].

Scheme 12 (A) Mechanistic signaling of fluorescent and colorimetric sensor based on CDs during the the visual detection of nitrite anions, Reproduced with permission [220]. The glass fiber strip modified with the synthesized *N*-(1-naphthyl) ethylenediamine (1-Nap) preloaded PEG-hydrogel colorimetric detection of different concentrations of $NaNO_2$ (B), Reproduced with permission [222].

Scheme 13: (A) Schematic design showing the adsorption of different types of pesticides using the mesocage collector cavities (MCC) nanopocket materials with high efficiency (left side), and the complete process of carbofurane pesticides uptake into MCC nanopocket (right side), Reproduced with permission [341]. (B) Screen printing sensor design for detection of pesticide residues in vegetables and fruits by integrating cellulose paper with hybrid AgNPs and GO based on SERS-based approach, Reproduced with permission [354]. (C) A flexible glass-fiber paper patch of BPWHW/AgNWs for selective detection of paraquat pesticide in the apple, Reproduced with permission [355].

Scheme 14: (A) Design of active GQDs/AChE/CHO_x platform for direct detection of OPs based on photoluminescence properties at 467 nm, Reproduced with permission [366]. (B) A Colorimetric detection of pesticide residue of terbuthylazine (TBA) and dimethoate (DMT) in different real samples (apple juice, green tea and tap water) using AuNPs-based colorimetric sensor, Reproduced with permission [369].

Scheme 15. Schematic design of the bactericidal activity in the presence of hexagon MgO nanosheets (A), and the TEM images of *E. coli* growth in free Lysogeny broth (LB) environment (a) and after treatment with hexagon MgO nanosheets (b, c) (B), Reproduced with permission [370, 372, 376, 377]. The mechanistic reaction of hexagonal micro/macroporous MgO nanosheets and their potential with cellular components and the membrane of pathogenic bacteria (C), Reproduced with permission [370, 372, 376, 377].

Scheme 16. Design of a portable plasmonic label-free platform for pathogen detection using a modified microchannel chip SPR platform with layer of Au (50nm) along the disposable microchip surface, EDC (N-(3- Dimethylaminopropyl)–N′-ethylcarbodiimide Hydrochloride), MUA (11-Mercaptoundeconoic Acid), NHS (N-Hydroxysuccinimide) and with LPS (anti- Lipopolysaccharide) antibody for the for quantify detection of E. coli, Reproduced with permission [386].

Scheme 17. (A) A schematic diagram of the electrode construction for microbial electrochemical detection based on RGO-hyperbranched chitosan nanocomposite for the sensitive and real-time detection of bacterial cell viability, Reproduced with permission [370]. (B) Construction of a microbial culture device on a glass slide in a Petri dish with details of device integration, Reproduced with permission [371]. (C) The scattering and fluorescence of total bacteria detection in real tea beverages and drinking water using a HSFCM technique, Reproduced with permission [389]. (D) Design of bacterial sensor based on the AuNPs/anionic enzyme catalytic system of pro-fragrance molecules to produce “turn-on” response with odiferous fragrance, Reproduced with permission [391]. (E) Detection of the bacterial as a relation of pH changes due to the displacement of urease to hydrolyzed urea and increase the pH value using a litmus dye, Reproduced with permission [392].

Scheme 18. Schematic representation of different steps for the construction of integrated microneedle array for alcohol sensor based on the biocatalytic reaction (A, B). Photos of the microneedle array on the fingertip (C), and integrated design of Pt & Ag wires with the microneedle array (D). The design of alcohol sensing assay in artificial ISF through the mice skin by the microneedle (E), the images of the sensor, the mice skin and the penetrated sensor over the tested sample to detect alcohol (F), and the real-time alcohol detection through the mice skin, Reproduced with permission [451].

Scheme 19. Schematic representation of the integrated platform sensor for alcohol: general design of sweat evaluation test, and platform design (A), the immobilization strategy of the Dithiobis [Succinimidyl Propionate] (DSP) and EtG antibody into the electrode surface (B). Photos of the Au and ZnO sensors fixed on glass and polyimide substrates (C). Optical LED display for classification of measured EtG concentration and different alcohol consumption performance (D, E), Reproduced with permission [460].

Scheme 20: Wearable non-invasive sweat-based sensors for alcohol detection electrochemically using a bi-enzymatic monitoring cell (A), Reproduced with permission [455], Droplet microdroplet screening strategy, Reproduced with permission [461], the microfluidic chips for alcohol detection in sweat, and the noninvasive strategy for alcohol detection based on a wearable Tattoo-Based sensing system (C), Reproduced with permission [462].

Scheme 21: A schematic outline of the cellphone attachment for advanced fluorescence diagnosis (A), Reproduced with permission [464], iTube platform based on smartphone for colorimetric digital detection (B), Reproduced with permission [465], and Portable platform deployed for point-of-use analyses (C), Reproduced with permission [466].

Scheme 22: (A) Schematic overview of the printable, stretchable glove biosensor for direct and Bluetooth OP agent detection. (B) A non-invasive wearable glove-based sensor strategy for on-site

Op's detection on the surfaces of agricultural crops including tomato, green pepper, pear and apple based on porous CMC aerogel and EuMOFs, Reproduced with permission [467]. (C) SERS-tape strategy for tracking the surface quality of fruit and agricultural crops, Reproduced with permission [351]. Schematic preparation of G-SERS substrate for SERS analysis (D), Reproduced with permission [468]. The DC magnetron sputtering method for Au sputtering on dragonfly wing as SERS platform (E), Reproduced with permission [387].

Scheme 23: A collage image showing some foods that contain uric acid (A). Design of an integrated amperometry Bluetooth wireless mouthguard sensor for real time detection of UA in saliva samples (B), Reproduced with permission [469]. Engineering of a wireless wearable bandage for UA detection according to: (i) Integrated smart bandage design for screen printing by fixing uricase to PB modified carbon electrodes which are placed on commercial bandage; (ii) a wireless wearable potentiostat determines connected with a computer or Smartphone for UA detection; and (iii) show the amperometry detection mechanism of UA detection using wireless wearable bandage. Image pf a wireless wearable smart bandage used in the UA detection (D). Reproduced with permission [470].

References

[1] I. Apruzzese, E. Song, E. Bonah, V.S. Sanidad, P. Leekitcharoenphon, J.J. Medardus, N. Abdalla, H. Hosseini, M. Takeuchi, Investing in Food Safety for Developing Countries: Opportunities and Challenges in Applying Whole-Genome Sequencing for Food Safety Management, Foodborne pathogens and disease, 16 (2019) 463-473.

[2] S. Hoffman, B. Maculloch, M. Batz, Economic burden of major foodborne illnesses acquired in the United States, 2015.

[3] G. Bülbül, A. Hayat, S. Andreescu, Portable nanoparticle-based sensors for food safety assessment, Sensors, 15 (2015) 30736-30758.

[4] A. Panghal, N. Chhikara, N. Sindhu, S. Jaglan, Role of food safety management systems in safe food production: A review, J. Food safety, 38 (2018) e12464.

[5] F. Mustafa, S. Andreescu, Nanotechnology-based approaches for food sensing and packaging applications, RSC Adv. 10 (2020) 19309-19336.
[6] L. Li, Y. Wang, L. Pan, Y. Shi, W. Cheng, Y. Shi, G. Yu, A nanostructured conductive hydrogels-based biosensor platform for human metabolite detection, Nano letters, 15 (2015) 1146-1151.
[7] D. Li, S. Suh, Health risks of chemicals in consumer products: A review, Env. Int.123 (2019) 580-587.
[8] S. El-Safty, M. Shenashen, Nanoscale dynamic chemical, biological sensor material designs for control monitoring and early detection of advanced diseases, Mater. Today Bio, 5 (2020) 100044.
[9] N. Shoaie, M. Daneshpour, M. Azimzadeh, S. Mahshid, S.M. Khoshfetrat, F. Jahanpeyma, A. Gholaminejad, K. Omidfar, M. Foruzandeh, Electrochemical sensors and biosensors based on the use of polyaniline and its nanocomposites: a review on recent advances, Microchim. Acta, 186 (2019) 465.
[10] C.-F. Wang, X.-Y. Sun, M. Su, Y.-P. Wang, Y.-K. Lv, Electrochemical biosensors based on antibody, nucleic acid and enzyme functionalized graphene for the detection of disease-related biomolecules, Analyst, 145 (2020) 1550-1562.
[11] M.Y. Emran, M.A. Shenashen, A.A. Abdelwahab, M. Abdelmottaleb, S.A. El-Safty, Facile synthesis of microporous sulfur-doped carbon spheres as electrodes for ultrasensitive detection of ascorbic acid in food and pharmaceutical products, New J. Chem. 42 (2018) 5037-5044.
[12] B.S. Sekhon, Nanotechnology in agri-food production: an overview, Nanotechnology, science and applications, 7 (2014) 31.
[13] X. Lu, Sensing Techniques for Food Safety and Quality Control: Sensing Techniques for Food Safety and Quality Control, Royal Society of Chemistry 2017.
[14] B. Hosnedlova, J. Sochor, M. Baron, G. Bjørklund, R. Kizek, Application of nanotechnology based-biosensors in analysis of wine compounds and control of wine quality and safety: A critical review, Critical reviews in food science and nutrition, 60 (2020) 3271-3289.
[15] C. Dincer, R. Bruch, E. Costa-Rama, M.T. Fernández-Abedul, A. Merkoçi, A. Manz, G.A. Urban, F. Güder, Disposable sensors in diagnostics, food, and environmental monitoring, Adv. Mater. 31 (2019) 1806739.
[16] I. Anshori, H. Suzuki, Microfluidic device for high-sensitivity coulometric detection of proteins, Sens. Actuators B: Chem. 256 (2018) 835-838.

[17] J.B. Allen, R.F. Larry, Electrochemical methods fundamentals and applications, John Wiley & Sons2001.
[18] X. Guo, J. Kuhlmann, W.R. Heineman, Biosensors on enzymes, tissues, and cells, Environmental Analysis by Electrochemical Sensors and Biosensors, Springer2014, pp. 283-312.
[19] N.Z.M. Muslim, M. Ahmad, L.Y. Heng, B. Saad, Optical biosensor test strip for the screening and direct determination of l-glutamate in food samples, Sens. Actuators B: Chem. 161 (2012) 493-497.
[20] N. Akhtar, M.Y. Emran, M.A. Shenashen, H. Khalifa, T. Osaka, A. Faheem, T. Homma, H. Kawarada, S.A. El-Safty, Fabrication of photo-electrochemical biosensors for ultrasensitive screening of mono-bioactive molecules: the effect of geometrical structures and crystal surfaces, J. Mater. Chem. B, 5 (2017) 7985-7996.
[21] M.Y. Emran, M. Mekawy, N. Akhtar, M.A. Shenashen, I.M. EL-Sewify, A. Faheem, S.A. El-Safty, Broccoli-shaped biosensor hierarchy for electrochemical screening of noradrenaline in living cells, Biosens. Bioelectron. 100 (2018) 122-131.
[22] M.Y. Emran, M.A. Shenashen, H. Morita, S.A. El-Safty, One-step selective screening of bioactive molecules in living cells using sulfur-doped microporous carbon, Biosens. Bioelectron. 109 (2018) 237-245.
[23] C.M. Hung, H.V. Phuong, N. Van Duy, N.D. Hoa, N. Van Hieu, Comparative effects of synthesis parameters on the NO_2 gas-sensing performance of on-chip grown ZnO and Zn_2SnO_4 nanowire sensors, J. Alloys and Compds. 765 (2018) 1237-1242.
[24] C.M. Hung, N. Van Duy, V. Van Quang, N. Van Toan, N. Van Hieu, N.D. Hoa, Facile synthesis of ultrafine rGO/WO_3 nanowire nanocomposites for highly sensitive toxic NH3 gas sensors, Mater. Res. Bull.125 (2020) 110810.
[25] N. Van Hoang, C.M. Hung, N.D. Hoa, N. Van Duy, N. Van Hieu, Facile on-chip electrospinning of $ZnFe_2O_4$ nanofiber sensors with excellent sensing performance to H_2S down ppb level, J. Hazardous Mater. 360 (2018) 6-16.
[26] F. Liu, S. Li, J. He, J. Wang, R. You, Z. Yang, L. Zhao, P. Sun, X. Yan, X. Liang, Highly selective and stable mixed-potential type gas sensor based on stabilized zirconia and $Cd_2V_2O_7$ sensing electrode for NH3 detection, Sens. Actuators B: Chem. 279 (2019) 213-222.
[27] M. Stanisavljevic, S. Krizkova, M. Vaculovicova, R. Kizek, V. Adam, Quantum dots-fluorescence resonance energy transfer-based nanosensors and their application, Biosens. Bioelectron. 74 (2015) 562-574.

[28] A.A. Abdelwahab, A.H. Naggar, M. Abdelmotaleb, M.Y. Emran, Ruthenium Nanoparticles Uniformly-designed Chemically Treated Graphene Oxide Nanosheets for Simultaneous Voltammetric Determination of Dopamine and Acetaminophen, Electroanalysis, 32 (2020) 2156-2165.
[29] M.Y. Emran, S.A. El-Safty, M.M. Selim, T. Minowa, A. Elmarakbi, M.A. Shenashen, Non-metal sensory electrode design and protocol of DNA-nucleobases in living cells exposed to oxidative stresses, Anal. Chim. Acta, 1142 (2020) 143-156.
[30] M.Y. Emran, S.A. El-Safty, M.A. Shenashen, T. Minowa, A well-thought-out sensory protocol for screening of oxygen reactive species released from cancer cells, Sens. Actuators B: Chem. 284 (2019) 456-467.
[31] Y. Zhang, X. Bai, X. Wang, K.-K. Shiu, Y. Zhu, H. Jiang, Highly sensitive graphene–Pt nanocomposites amperometric biosensor and its application in living cell H_2O_2 detection, Anal. Chem. 86 (2014) 9459-9465.
[32] J. Wang, M. Yu, Y. Xia, X. Li, C. Yang, S. Komarneni, On-chip grown ZnO nanosheet-array with interconnected nanojunction interfaces for enhanced optoelectronic NO_2 gas sensing at room temperature, J. Coll. Interface Sci. 554 (2019) 19-28.
[33] M.R. Awual, T. Yaita, S.A. El-Safty, H. Shiwaku, S. Suzuki, Y. Okamoto, Copper (II) ions capturing from water using ligand modified a new type mesoporous adsorbent, Chem. Eng. J. 221 (2013) 322-330.
[34] M. Emran, S. El-Safty, M. Selim, M. Shenashen, Selective monitoring of ultra-trace guanine and adenine from hydrolyzed DNA using boron-doped carbon electrode surfaces, Sens. Actuators B: Chem. 329 (2021) 129192.
[35] M.Y. Emran, M.A. Shenashen, S.A. El-Safty, M.M. Selim, T. Minowa, A. Elmarakbi, Three-Dimensional Circular Surface Curvature of a Spherule-Based Electrode for Selective Signaling and Dynamic Mobility of Norepinephrine in Living Cells, ACS Appl. Bio Mater. 3 (2020) 8496–8506
[36] H. Khalifa, S. El-Safty, A. Reda, A. Elmarakbi, H. Metawa, M. Shenashen, Multifaceted geometric 3D mesopolytope cathodes and its directional transport gates for superscalable LIB models, Applied Materials Today, 19 (2020) 100590.
[37] H. Khalifa, S.A. El-Safty, A. Reda, M.A. Shenashen, A.I. Eid, Anisotropic alignments of hierarchical Li_2SiO_3/TiO_2@ nano-C anode//$LiMnPO_4$@ nano-C cathode architectures for full-cell lithium-ion battery, Nat. Sci. Rev. 7 (2020) 863-880.

[38] H. Nguyen, S.A. El-Safty, Meso-and macroporous Co_3O_4 nanorods for effective VOC gas sensors, J. Phy. Chem.C, 115 (2011) 8466-8474.
[39] D.G. Papageorgiou, I.A. Kinloch, R.J. Young, Mechanical properties of graphene and graphene-based nanocomposites, Prog. Mater. Sci. 90 (2017) 75-127.
[40] M. Emran, S. El-Safty, M. Selim, A. Reda, H. Morita, M. Shenashen, Electrochemical sensors-based phosphorus-doped carbon for determination of adenine DNA-nucleobases in living cells, Carbon, 173 (2021) 1093-1104 .
[41] M.Y. Emran, M.A. Shenashen, A.A. Abdelwahab, M. Abdelmottaleb, M. Khairy, S.A. El-Safty, Nanohexagonal Fe_2O_3 electrode for one-step selective monitoring of dopamine and uric acid in biological samples, Electrocatalysis, 9 (2018) 514-525.
[42] M. Israr-Qadir, S. Jamil-Rana, O. Nur, M. Willander, Zinc oxide-based self-powered potentiometric chemical sensors for biomolecules and metal ions, Sensors, 17 (2017) 1645.
[43] I. Simon, A. Savitsky, R. Mülhaupt, V. Pankov, C. Janiak, Nickel nanoparticle decorated reduced graphene oxide-WO3 nanocomposite-a promising candidate for gas sensing, Beilstein Archives, 2020 (2020) 145.
[44] D.M. Steinert, S.-J. Ernst, S.K. Henninger, C. Janiak, Metal-Organic Frameworks as Sorption Materials for Heat Transformation Processes, Eur. J. Inorg. Chem. 2020 (2020) 4502-4515.
[45] J. Huang, J. Liu, J. Wang, Optical properties of biomass-derived nanomaterials for sensing, catalytic, biomedical and environmental applications, TrAC Tren. Anal. Chem. 124 (2020) 115800.
[46] V.J. Toranzos, G.P. Ortiz, W.L. Mochán, J.O. Zerbino, Optical and electrical properties of nanostructured metallic electrical contacts, Mater. Res. Exp. 4 (2017) 015026.
[47] F. Ma, C.-c. Li, C.-y. Zhang, Development of quantum dot-based biosensors: principles and applications, J. Mater. Chem. B, 6 (2018) 6173-6190.
[48] X. Zhang, S. Yu, W. He, H. Uyama, Q. Xie, L. Zhang, F. Yang, Electrochemical sensor based on carbon-supported $NiCoO_2$ nanoparticles for selective detection of ascorbic acid, Biosens. Bioelectron. 55 (2014) 446-451.
[49] A. Duda-Chodak, M. Lukasiewicz, G. Zięć, A. Florkiewicz, A. Filipiak-Florkiewicz, Covid-19 pandemic and food: Present knowledge, risks, consumers fears and safety, Trends in Food Sci. Tech., 105 (2020) 145-160.
[50] M.L. Holshue, C. DeBolt, S. Lindquist, K.H. Lofy, J. Wiesman, H. Bruce, C. Spitters, K. Ericson, S. Wilkerson, A. Tural, First case of 2019 novel coronavirus in the United States, N Engl J Med 382 (2020) 929-936.

[51] K. Jalava, A. Kauppinen, H. Al-Hello, S. Räsänen, An outbreak of norovirus infection caused by ice cubes and a leaking air ventilation valve, Epidemiology & Infection, 147 (2019).
[52] W.H. Organization, COVID-19 weekly epidemiological update, 1 December 2020, (2020).
[53] H. Zhang, Z. Kang, H. Gong, D. Xu, J. Wang, Z. Li, X. Cui, J. Xiao, T. Meng, W. Zhou, The digestive system is a potential route of 2019-nCov infection: a bioinformatics analysis based on single-cell transcriptomes, BioRxiv, (2020).
[54] Y. Zhang, C. Chen, S. Zhu, C. Shu, D. Wang, J. Song, Y. Song, W. Zhen, Z. Feng, G. Wu, Isolation of 2019-nCoV from a stool specimen of a laboratory-confirmed case of the coronavirus disease 2019 (COVID-19), China CDC Weekly, 2 (2020) 123-124.
[55] Y. Dou, Z. Jiang, W. Deng, J. Su, S. Chen, H. Song, A. Aldalbahi, X. Zuo, S. Song, J. Shi, Portable detection of clenbuterol using a smartphone-based electrochemical biosensor with electric field-driven acceleration, J. Electroanal. Chem. 781 (2016) 339-344.
[56] J. Han, X. Zhang, S. He, P. Jia, Can the coronavirus disease be transmitted from food? A review of evidence, risks, policies and knowledge gaps, Env. Chem. Lett. 19 (2021) 5-16.
[57] S.M.H. Commission, Detection of SARS-CoV-2 on an imported chicken wing sample, 2020.
[58] O. mondiale de la Santé, COVID-19 et sécurité sanitaire des aliments: orientations pour les autorités compétentes responsables des systèmes nationaux de contrôle de la sécurité sanitaire des aliments: orientations provisoires, 22 avril 2020, Organisation mondiale de la Santé, 2020.
[59] V.K. Sharma, C. Jinadatha, E. Lichtfouse, Environmental chemistry is most relevant to study coronavirus pandemics, Springer, 2020.
[60] H. Eslami, M. Jalili, The role of environmental factors to transmission of SARS-CoV-2 (COVID-19), AMB Express, 10 (2020) 1-8.
[61] S. Zuber, H. Brüssow, COVID 19: Challenges for virologists in the food industry, Microbial Biotech., 13 (2020) 1689-1701.
[62] Z. Ceylan, R. Meral, T. Cetinkaya, Relevance of SARS-CoV-2 in food safety and food hygiene: potential preventive measures, suggestions and nanotechnological approaches, VirusDisease, 31 (2020) 154-160.
[63] M. Rizou, I.M. Galanakis, T.M. Aldawoud, C.M. Galanakis, Safety of foods, food supply chain and environment within the COVID-19 pandemic, Tren. food Sci. Tech. 102 (2020) 293-299.
[64] D. Fisher, A. Reilly, A.K.E. Zheng, A.R. Cook, D. Anderson, Seeding of outbreaks of COVID-19 by contaminated fresh and frozen food, BioRxiv, (2020).

[65] D.E. Harbourt, A.D. Haddow, A.E. Piper, H. Bloomfield, B.J. Kearney, D. Fetterer, K. Gibson, T. Minogue, Modeling the stability of severe acute respiratory syndrome coronavirus 2 (SARS-CoV-2) on skin, currency, and clothing, PLoS neglected tropical diseases, 14 (2020) e0008831.
[66] J. Gallagher, Are coronavirus tests flawed?, BBC NEWS, 13 (2020).
[67] Z. Li, Y. Yi, X. Luo, N. Xiong, Y. Liu, S. Li, R. Sun, Y. Wang, B. Hu, W. Chen, Development and clinical application of a rapid IgM-IgG combined antibody test for SARS-CoV-2 infection diagnosis, J. Med. Virology, (2020).
[68] J.-L. Wu, W.-P. Tseng, C.-H. Lin, T.-F. Lee, M.-Y. Chung, C.-H. Huang, S.-Y. Chen, P.-R. Hsueh, S.-C. Chen, Four point-of-care lateral flow immunoassays for diagnosis of COVID-19 and for assessing dynamics of antibody responses to SARS-CoV-2, Journal of Infection, 81 (2020) 435-442.
[69] M.A. Moyad, M.A. Combs, D.C. Crowley, J.E. Baisley, P. Sharma, A.S. Vrablic, M. Evans, Vitamin C with metabolites reduce oxalate levels compared to ascorbic acid: a preliminary and novel clinical urologic finding, Urol Nurs, 29 (2009) 95-102.
[70] C. Wilson, Ascorbic acid function and metabolism during colds, Ann. NY Acad. Sci, 258 (1975) 529-539.
[71] L.K. Massey, M. Liebman, S.A. Kynast-Gales, Ascorbate increases human oxaluria and kidney stone risk, J. Nutrition, 135 (2005) 1673-1677.
[72] V. Gérard, E. Ay, B. Graff, F. Morlet-Savary, C. Galopin, W. Mutilangi, J. Lalevée, Ascorbic acid derivatives as potential substitutes for ascorbic acid to reduce color degradation of drinks containing ascorbic acid and anthocyanins from natural extracts, J. Agri. Food Chem. 67 (2019) 12061-12071.
[73] M. Varvara, G. Bozzo, G. Celano, C. Disanto, C.N. Pagliarone, G.V. Celano, The use of ascorbic acid as a food additive: technical-legal issues, Italian J. Food Safety, 5 (2016).
[74] A. Ferro-Luzzi, E. Cialfa, C. Leclercq, E. Toti, The Mediterranean diet revisited. Focus on fruit and vegetables, Int. J. Food Sci. Nutrition, 45 (1994) 291-300.
[75] R.A. Jacob, G. Sotoudeh, Vitamin C function and status in chronic disease, Nutrition Clin. Care, 5 (2002) 66-74.
[76] D.-H. Lee, A.R. Folsom, L. Harnack, B. Halliwell, D.R. Jacobs Jr, Does supplemental vitamin C increase cardiovascular disease risk in women with diabetes?, Am. J. Clin. Nutrition, 80 (2004) 1194-1200.

[77] S.H. Lee, T. Oe, I.A. Blair, Vitamin C-induced decomposition of lipid hydroperoxides to endogenous genotoxins, Sci. 292 (2001) 2083-2086.
[78] M. Levine, S.C. Rumsey, R. Daruwala, J.B. Park, Y. Wang, Criteria and recommendations for vitamin C intake, Jama, 281 (1999) 1415-1423.
[79] M.W. Davey, M.v. Montagu, D. Inze, M. Sanmartin, A. Kanellis, N. Smirnoff, I.J.J. Benzie, J.J. Strain, D. Favell, J. Fletcher, Plant L-ascorbic acid: chemistry, function, metabolism, bioavailability and effects of processing, J. Sci. Food Agr. 80 (2000) 825-860.
[80] M. Gómez-Romero, D. Arráez-Román, A. Segura-Carretero, A. Fernández-Gutiérrez, Analytical determination of antioxidants in tomato: typical components of the Mediterranean diet, J. Sep. Sci., 30 (2007) 452-461.
[81] Y. Ogiri, F. Sun, S. Hayami, A. Fujimura, K. Yamamoto, M. Yaita, S. Kojo, Very low vitamin C activity of orally administered L-dehydroascorbic acid, J. Agri. Food Chem. 50 (2002) 227-229.
[82] K. Szabo, Z. Diaconeasa, A.-F. Cătoi, D.C. Vodnar, Screening of ten tomato varieties processing waste for bioactive components and their related antioxidant and antimicrobial activities, Antioxidants, 8 (2019) 292.
[83] V. Valpuesta, M.A. Botella, Biosynthesis of L-ascorbic acid in plants: new pathways for an old antioxidant, Trend. Plant Sci. 9 (2004) 573-577.
[84] S.A. El-Safty, M. Shenashen, Mercury-ion optical sensors, TrAC Trend. Anal. Chem. 38 (2012) 98-115.
[85] S.A. El-Safty, M. Shenashen, M. Ismael, M. Khairy, M.R. Awual, Optical mesosensors for monitoring and removal of ultra-trace concentration of Zn (II) and Cu (II) ions from water, Analyst, 137 (2012) 5278-5290.
[86] S. El-Safty, M. Shenashen, M. Ismael, M. Khairy, Mesocylindrical Aluminosilica Monolith Biocaptors for Size-Selective Macromolecule Cargos, Adv. Functional Mater. 22 (2012) 3013-3021.
[87] Y. Herbani, Isnaeni, Irmaniar, M.R. Ihsan, Y.P. Putra, T.E. Saraswati, Colloidal Au and Au/Ag nanoparticles prepared by laser ablation in liquid as a substrate of surface enhanced Raman scattering (SERS) in ascorbic acid detection, AIP Conference Proceedings, AIP Publishing LLC, 2256 (2020) 020012.
[88] I. Sebarchievici, A. Lascu, G. Fagadar-Cosma, A. Palade, I. Fringu, M. Birdeanu, B. Taranu, E. Fagadar-Cosma, Optical and electrochemical-mediated detection of ascorbic acid using manganese porphyrin and its gold hybrids, Comptes Rendus Chimie, 21 (2018) 327-338.

[89] J. Wang, X. Peng, D. Li, X. Jiang, Z. Pan, A. Chen, L. Huang, J. Hu, Ratiometric ultrasensitive fluorometric detection of ascorbic acid using a dually emitting CdSe@ SiO_2@CdTe quantum dot hybrid, Microchim. Acta, 185 (2018) 42.
[90] J.L. Cholula-Díaz, D. Lomelí-Marroquín, B. Pramanick, A. Nieto-Argüello, L.A. Cantú-Castillo, H. Hwang, Synthesis of colloidal silver nanoparticle clusters and their application in ascorbic acid detection by SERS, Coll. Surf. B: Biointerfaces, 163 (2018) 329-335.
[91] C.Y. Panicker, H.T. Varghese, D. Philip, FT-IR, FT-Raman and SERS spectra of Vitamin C, Spectrochimica Acta Part A: Molec. Biomolec. Spectrosc. 65 (2006) 802-804.
[92] G. Lin, W. Lu, W. Cui, L. Jiang, A simple synthesis method for gold nano-and microplate fabrication using a tree-type multiple-amine head surfactant, Crystal growth & design, 10 (2010) 1118-1123.
[93] J. Shuhai, W. Jun, J. Yang, Ordered silver nanoparticle arrays as surface-enhanced Raman spectroscopy substrates for label-free detection of vitamin C in serum, Sens. Actuators A: Phy. 201 (2013) 416-420.
[94] N. Gavrilenko, G. Mokrousov, O. Dzhiganskaya, An optical sensor for the determination of ascorbic acid, J. Anal. Chem. 59 (2004) 871-874.
[95] K. Xing, J. Ge, W.-X. Wang, X. Geng, X.-P. Shen, J.-L. Tang, L.-B. Qu, Y.-Q. Sun, Z.-H. Li, A turn-on fluorescent probe for sensitive detection of ascorbic acid based on SiNP–MnO 2 nanocomposites, New J. Chem. 43 (2019) 9466-9471.
[96] J. Bi, H. Wang, T. Kamal, B.-W. Zhu, M. Tan, A fluorescence turn-off-on chemosensor based on carbon nanocages for detection of ascorbic acid, RSC Adv. 7 (2017) 30481-30487.
[97] J.-J. Liu, Z.-T. Chen, D.-S. Tang, Y.-B. Wang, L.-T. Kang, J.-N. Yao, Graphene quantum dots-based fluorescent probe for turn-on sensing of ascorbic acid, Sens. Actuators B: Chem. 212 (2015) 214-219.
[98] D.C.M. Ferreira, G.F. Giordano, C.C.d.S.P. Soares, J.F.A. de Oliveira, R.K. Mendes, M.H. Piazzetta, A.L. Gobbi, M.B. Cardoso, Optical paper-based sensor for ascorbic acid quantification using silver nanoparticles, Talanta, 141 (2015) 188-194.
[99] S. Rostami, A. Mehdinia, A. Jabbari, Seed-mediated grown silver nanoparticles as a colorimetric sensor for detection of ascorbic acid, Spectrochim. Acta Part A: Mol. Biomol. Spectrosc.180 (2017) 204-210.
[100] B. Song, Z. Ye, Y. Yang, H. Ma, X. Zheng, D. Jin, J. Yuan, Background-free in-vivo Imaging of Vitamin C using Time-gateable Responsive Probe, Sci. Rep. 5 (2015) 1-10.

[101] Q. Tan, W. Kong, H. Sun, X. Qin, F. Qu, Fluorometric turn-on detection of ascorbic acid based on controlled release of polyallylamine-capped gold nanoclusters from MnO_2 nanosheets, Microchim. Acta, 186 (2019) 282.
[102] W. Xu, L. Yu, H. Xu, S. Zhang, W. Xu, Y. Lin, X. Zhu, Water-dispersed silicon quantum dots for on-off-on fluorometric determination of chromium (VI) and ascorbic acid, Microchim. Acta, 186 (2019) 673.
[103] Y. Wang, Y. Yang, W. Liu, F. Ding, P. Zou, X. Wang, Q. Zhao, H. Rao, A carbon dot-based ratiometric fluorometric and colorimetric method for determination of ascorbic acid and of the activity of ascorbic acid oxidase, Microchim. Acta, 186 (2019) 246.
[104] X. Liu, W. Na, H. Liu, X. Su, Fluorescence turn-off-on probe based on polypyrrole/graphene quantum composites for selective and sensitive detection of paracetamol and ascorbic acid, Biosens. Bioelectron. 98 (2017) 222-226.
[105] J.F.Y. Fong, S.F. Chin, S.M. Ng, A unique "turn-on" fluorescence signalling strategy for highly specific detection of ascorbic acid using carbon dots as sensing probe, Biosens. Bioelectron., 85 (2016) 844-852.
[106] H. Liu, W. Na, Z. Liu, X. Chen, X. Su, A novel turn-on fluorescent strategy for sensing ascorbic acid using graphene quantum dots as fluorescent probe, Biosens. Bioelectron. 92 (2017) 229-233.
[107] Y. Zhang, X. Fang, H. Zhao, Z. Li, A highly sensitive and selective detection of Cr (VI) and ascorbic acid based on nitrogen-doped carbon dots, Talanta, 181 (2018) 318-325.
[108] X. Gong, Y. Liu, Z. Yang, S. Shuang, Z. Zhang, C. Dong, An "on-off-on" fluorescent nanoprobe for recognition of chromium (VI) and ascorbic acid based on phosphorus/nitrogen dual-doped carbon quantum dot, Anal. Chim. Acta, 968 (2017) 85-96.
[109] H. Yang, L. He, Y. Long, H. Li, S. Pan, H. Liu, X. Hu, Fluorescent carbon dots synthesized by microwave-assisted pyrolysis for chromium (VI) and ascorbic acid sensing and logic gate operation, Spectrochim. Acta Part A: Mol.Biomol.Spectrosc. 205 (2018) 12-20.
[110] X. Luo, W. Zhang, Y. Han, X. Chen, L. Zhu, W. Tang, J. Wang, T. Yue, Z. Li, N, S co-doped carbon dots based fluorescent "on-off-on" sensor for determination of ascorbic acid in common fruits, Food Chem. 258 (2018) 214-221.
[111] D. Atias, Y. Liebes, V. Chalifa-Caspi, L. Bremand, L. Lobel, R.S. Marks, P. Dussart, Chemiluminescent optical fiber immunosensor for the detection of IgM antibody to dengue virus in humans, Sens. Actuators B: Chem.140 (2009) 206-215.

[112] L. Bøtter-Jensen, Luminescence techniques: instrumentation and methods, Rad. Measur. 27 (1997) 749-768.
[113] Z. Guo, F. Yang, L. Zhang, X. Zheng, Electrogenerated chemiluminescence energy transfer for the label-free detection of DNA, Sens. Actuators B: Chem. 177 (2013) 316-321.
[114] Z. Zhang, S. Zhang, X. Zhang, Recent developments and applications of chemiluminescence sensors, Anal. Chim. Acta, 541 (2005) 37-46.
[115] Y.P. Dong, T.T. Gao, X.F. Chu, J. Chen, C.M. Wang, Flow injection-chemiluminescence determination of ascorbic acid based on luminol–ferricyanide–gold nanoparticles system, J. Luminesc.154 (2014) 350-355.
[116] S. Zhao, Y. Huang, Y.-M. Liu, Microchip electrophoresis with chemiluminescence detection for assaying ascorbic acid and amino acids in single cells, J. Chromatog. A, 1216 (2009) 6746-6751.
[117] H. Chen, Q. Wang, Q. Shen, X. Liu, W. Li, Z. Nie, S. Yao, Nitrogen doped graphene quantum dots based long-persistent chemiluminescence system for ascorbic acid imaging, Biosens. Bioelectron. 91 (2017) 878-884.
[118] H. Chen, R. Li, L. Lin, G. Guo, J.-M. Lin, Determination of l-ascorbic acid in human serum by chemiluminescence based on hydrogen peroxide–sodium hydrogen carbonate–CdSe/CdS quantum dots system, Talanta, 81 (2010) 1688-1696.
[119] K. Dhara, R.M. Debiprosad, Review on nanomaterials-enabled electrochemical sensors for ascorbic acid detection, Anal. Biochem. 586 (2019) 113415.
[120] B. Liu, L. Luo, Y. Ding, X. Si, Y. Wei, X. Ouyang, D. Xu, Differential pulse voltammetric determination of ascorbic acid in the presence of folic acid at electro-deposited NiO/graphene composite film modified electrode, Electrochim. Acta, 142 (2014) 336-342.
[121] Y. Haldorai, S.R. Choe, Y.S. Huh, Y.-K. Han, A composite consisting of microporous carbon and cobalt (III) oxide and prepared from zeolitic imidazolate framework-67 for voltammetric determination of ascorbic acid, Microchim. Acta, 185 (2018) 116.
[122] H. Liu, C. Gu, C. Hou, Z. Yin, K. Fan, M. Zhang, Plasma-assisted synthesis of carbon fibers/ZnO core–shell hybrids on carbon fiber templates for detection of ascorbic acid and uric acid, Sens. Actuators B: Chem. 224 (2016) 857-862.
[123] S. Pakapongpan, J.P. Mensing, D. Phokharatkul, T. Lomas, A. Tuantranont, Highly selective electrochemical sensor for ascorbic acid based on a novel hybrid graphene-copper phthalocyanine-polyaniline nanocomposites, Electrochim. Acta, 133 (2014) 294-301.

[124] S.R. Dash, S.S. Bag, A.K. Golder, Synergized AgNPs formation using microwave in a bio-mediated route: Studies on particle aggregation and electrocatalytic sensing of ascorbic acid from biological entities, J. Electroanal. Chem. 827 (2018) 181-192.
[125] L. Contat-Rodrigo, C. Pérez-Fuster, J.V. Lidón-Roger, A. Bonfiglio, E. García-Breijo, Screen-printed Organic Electrochemical Transistors for the detection of ascorbic acid in food, Org. Electron., 45 (2017) 89-96.
[126] X. Li, C.-H. Zhou, Q.-j. Zi, Q.-E. Cao, An electrochemical signal transduction amplification strategy for ultrasensitive detection of ascorbic acid, J.Electroanal. Chem. 780 (2016) 321-326.
[127] C. Yan, X. Liu, R. Zhang, Y. Chen, G. Wang, A selective strategy for determination of ascorbic acid based on molecular imprinted copolymer of o-phenylenediamine and pyrrole, J.Electroanal. Chem. 780 (2016) 276-281.
[128] Y. Kong, X. Shan, J. Ma, M. Chen, Z. Chen, A novel voltammetric sensor for ascorbic acid based on molecularly imprinted poly (o-phenylenediamine-co-o-aminophenol), Anal. Chim. Acta, 809 (2014) 54-60.
[129] F.A. Harraz, M. Faisal, A.A. Ismail, S. Al-Sayari, A. Al-Salami, A. Al-Hajry, M. Al-Assiri, TiO_2/reduced graphene oxide nanocomposite as efficient ascorbic acid amperometric sensor, J.Electroanal. Chem. 832 (2019) 225-232.
[130] L. Liu, J. Zhai, C. Zhu, L. Han, W. Ren, S. Dong, One-step synthesis of functional pNR/rGO composite as a building block for enhanced ascorbic acid biosensing, Anal. Chim. Acta, 981 (2017) 34-40.
[131] A.T. Lawal, Graphene-based nano composites and their applications. A review, Biosens.and Bioelectron. 141 (2019) 111384.
[132] T.R. Das, S.K. Jena, R. Madhuri, P.K. Sharma, Polymeric iron oxide-graphene nanocomposite as a trace level sensor of vitamin C, Appl. Surf. Sci. 449 (2018) 304-313.
[133] Y. Sun, M. Luo, X. Meng, J. Xiang, L. Wang, Q. Ren, S. Guo, Graphene/intermetallic PtPb nanoplates composites for boosting electrochemical detection of H_2O_2 released from cells, Anal. Chem. 89 (2017) 3761-3767.
[134] C. de Gracia Lux, S. Joshi-Barr, T. Nguyen, E. Mahmoud, E. Schopf, N. Fomina, A. Almutairi, Biocompatible polymeric nanoparticles degrade and release cargo in response to biologically relevant levels of hydrogen peroxide, J. Am. Chem. Soc. 134 (2012) 15758-15764.

[135] Y. Xu, K. Li, W. Qin, B. Zhu, Z. Zhou, J. Shi, K. Wang, J. Hu, C. Fan, D. Li, Unraveling the role of hydrogen peroxide in α-synuclein aggregation using an ultrasensitive nanoplasmonic probe, Anal. Chem. 87 (2015) 1968-1973.
[136] M.M. Gaschler, B.R. Stockwell, Lipid peroxidation in cell death, Biochem. Biophy. Res. Commun. 482 (2017) 419-425.
[137] S.D. Jereil, K. Vijayalakshmi, A. Monamary, Substantial effect of Pd incorporation in MnO_2 synthesized by spray pyrolysis on MWCNTs/Ta electrode for better H_2O_2 sensitivity, Ceram. Int. 45 (2019) 3782-3790.
[138] J.F. Botero-Cadavid, A.G. Brolo, P. Wild, N. Djilali, Detection of hydrogen peroxide using an optical fiber-based sensing probe, Sens. Actuators B: Chem. 185 (2013) 166-173.
[139] C.K. Tagad, S.R. Dugasani, R. Aiyer, S. Park, A. Kulkarni, S. Sabharwal, Green synthesis of silver nanoparticles and their application for the development of optical fiber based hydrogen peroxide sensor, Sens. Actuators B: Chem. 183 (2013) 144-149.
[140] P. Bhatia, P. Yadav, B.D. Gupta, Surface plasmon resonance based fiber optic hydrogen peroxide sensor using polymer embedded nanoparticles, Sens. Actuators B: Chem. 182 (2013) 330-335.
[141] H.A. Khorami, J.F. Botero-Cadavid, P. Wild, N. Djilali, Spectroscopic detection of Hydrogen peroxide with an optical fiber probe using chemically deposited Prussian blue, Electrochim. Acta, 115 (2014) 416-424.
[142] I. Del Villar, I.R. Matias, F.J. Arregui, J. Echeverría, R.O. Claus, Strategies for fabrication of hydrogen peroxide sensors based on electrostatic self-assembly (ESA) method, Sens. Actuators B: Chem. 108 (2005) 751-757.
[143] L. Jianzhong, Z. Zhujun, L. Ling, A simplified enzyme-based fiber optic sensor for hydrogen peroxide and oxidase substrates, Talanta, 41 (1994) 1999-2002.
[144] Y. Zhu, H. Cao, L. Tang, X. Yang, C. Li, Immobilization of horseradish peroxidase in three-dimensional macroporous TiO 2 matrices for biosensor applications, Electrochim. Acta, 54 (2009) 2823-2827.
[145] F. Hu, Y. Huang, G. Zhang, R. Zhao, D. Zhang, A highly selective fluorescence turn-on detection of hydrogen peroxide and d-glucose based on the aggregation/deaggregation of a modified tetraphenylethylene, Tetrahedron lett. 55 (2014) 1471-1474.
[146] K. Ragavan, S.R. Ahmed, X. Weng, S. Neethirajan, Chitosan as a peroxidase mimic: Paper based sensor for the detection of hydrogen peroxide, Sens. Actuators B: Chem. 272 (2018) 8-13.

[147] M. Farrokhnia, S. Karimi, S. Momeni, S. Khalililaghab, Colorimetric sensor assay for detection of hydrogen peroxide using green synthesis of silver chloride nanoparticles: Experimental and theoretical evidence, Sens. Actuators B: Chem. 246 (2017) 979-987.
[148] L. Zhang, W. Hou, Q. Lu, M. Liu, C. Chen, Y. Zhang, S. Yao, Colorimetric detection of hydrogen peroxide and lactate based on the etching of the carbon based Au-Ag bimetallic nanocomposite synthesized by carbon dots as the reductant and stabilizer, Anal. Chim. Acta, 947 (2016) 23-31.
[149] Y. Wang, B. Zhou, S. Wu, K. Wang, X. He, Colorimetric detection of hydrogen peroxide and glucose using the magnetic mesoporous silica nanoparticles, Talanta, 134 (2015) 712-717.
[150] T. Niu, X. Deng, R. Wang, C. Zhou, GO-PtNi hybrid nanoenzyme mimics for the colorimetric detection of hydrogen peroxide, Mater. Today Chem. 7 (2018) 35-39.
[151] Z. Zhou, Y. Li, W. Su, B. Gu, H. Xu, C. Wu, P. Yin, H. Li, Y. Zhang, A dual-signal colorimetric and near-infrared fluorescence probe for the detection of exogenous and endogenous hydrogen peroxide in living cells Sens. Actuators B: Chem. 280 (2019) 120-128.
[152] D. Yu, P. Wang, Y. Zhao, A. Fan, Iodophenol blue-enhanced luminol chemiluminescence and its application to hydrogen peroxide and glucose detection, Talanta, 146 (2016) 655-661.
[153] Z. Zhang, J. Lai, K. Wu, X. Huang, S. Guo, L. Zhang, J. Liu, Peroxidase-catalyzed chemiluminescence system and its application in immunoassay, Talanta, 180 (2018) 260-270.
[154] Y. Lu, X. Shi, W. Fan, C.A. Black, Z. Lu, C. Fan, A fast-response two-photon fluorescent probe for imaging endogenous H2O2 in living cells and tissues, Spectrochim. Acta Part A: Mol. Biomol. Spectrosc. 190 (2018) 353-359.
[155] L. Tang, M. Tian, H. Chen, X. Yan, K. Zhong, Y. Bian, An ESIPT-based mitochondria-targeted ratiometric and NIR-emitting fluorescent probe for hydrogen peroxide and its bioimaging in living cells, Dyes and Pigments, 158 (2018) 482-489.
[156] L. He, X. Liu, Y. Zhang, L. Yang, Q. Fang, Y. Geng, W. Chen, X. Song, A mitochondria-targeting ratiometric fluorescent probe for imaging hydrogen peroxide with long-wavelength emission and large stokes shift, Sens. Actuators B: Chem. 276 (2018) 247-253.
[157] Y. Shen, X. Zhang, Y. Zhang, Y. Wu, C. Zhang, Y. Chen, J. Jin, H. Li, A mitochondria-targeted colorimetric and ratiometric fluorescent probe for hydrogen peroxide with a large emission shift and bio-imaging in living cells, Sens. Actuators B: Chem. 255 (2018) 42-48.

[158] K. Liu, H. Shang, X. Kong, M. Ren, J.-Y. Wang, Y. Liu, W. Lin, A novel near-infrared fluorescent probe for H2O2 in alkaline environment and the application for H_2O_2 imaging in vitro and in vivo, Biomaterials, 100 (2016) 162-171.
[159] J. Xu, Q. Li, Y. Yue, Y. Guo, S. Shao, A water-soluble BODIPY derivative as a highly selective "Turn-On" fluorescent sensor for H_2O_2 sensing in vivo, Biosens. Bioelectron. 56 (2014) 58-63.
[160] W. Chen, L. Hong, A.-L. Liu, J.-Q. Liu, X.-H. Lin, X.-H. Xia, Enhanced chemiluminescence of the luminol-hydrogen peroxide system by colloidal cupric oxide nanoparticles as peroxidase mimic, Talanta, 99 (2012) 643-648.
[161] H. Abdolmohammad-Zadeh, E. Rahimpour, A novel chemosensor for Ag (I) ion based on its inhibitory effect on the luminol–H_2O_2 chemiluminescence response improved by $CoFe_2O_4$ nano-particles, Sens. Actuators B: Chem. 209 (2015) 496-504.
[162] Y. Sheng, H. Yang, Y. Wang, L. Han, Y. Zhao, A. Fan, Silver nanoclusters-catalyzed luminol chemiluminescence for hydrogen peroxide and uric acid detection, Talanta, 166 (2017) 268-274.
[163] L. Ming, T. Peng, Y. Tu, Multiple enhancement of luminol electrochemiluminescence using electrodes functionalized with titania nanotubes and platinum black: ultrasensitive determination of hydrogen peroxide, resveratrol, and dopamine, Microchim. Acta, 183 (2016) 305-310.
[164] K. Wang, Q. Liu, X.-Y. Wu, Q.-M. Guan, H.-N. Li, Graphene enhanced electrochemiluminescence of CdS nanocrystal for H2O2 sensing, Talanta, 82 (2010) 372-376.
[165] T. Khajvand, M.J. Chaichi, A.H. Colagar, Sensitive assay of hexythiazox residue in citrus fruits using gold nanoparticles-catalysed luminol–H2O2 chemiluminescence, Food Chem.173 (2015) 514-520.
[166] Z. Yu, H. Li, X. Zhang, N. Liu, X. Zhang, NiO/graphene nanocomposite for determination of H2O2 with a low detection limit, Talanta, 144 (2015) 1-5.
[167] S. Kogularasu, M. Govindasamy, S.-M. Chen, M. Akilarasan, V. Mani, 3D graphene oxide-cobalt oxide polyhedrons for highly sensitive non-enzymatic electrochemical determination of hydrogen peroxide, Sens. Actuators B: Chem. 253 (2017) 773-783.
[168] W. Jia, M. Guo, Z. Zheng, T. Yu, E.G. Rodriguez, Y. Wang, Y. Lei, Electrocatalytic oxidation and reduction of H_2O_2 on vertically aligned Co_3O_4 nanowalls electrode: Toward H_2O_2 detection, J. Electroanal. Chem. 625 (2009) 27-32.

[169] J. Zhou, C. Liao, L. Zhang, Q. Wang, Y. Tian, Molecular hydrogel-stabilized enzyme with facilitated electron transfer for determination of H_2O_2 released from live cells, Anal. Chem. 86 (2014) 4395-4401.
[170] J. Cui, S. Ren, B. Sun, S. Jia, Optimization protocols and improved strategies for metal-organic frameworks for immobilizing enzymes: Current development and future challenges, Coordination Chemistry Reviews, 370 (2018) 22-41.
[171] G.H. Jin, E. Ko, M.K. Kim, V.-K. Tran, S.E. Son, Y. Geng, W. Hur, G.H. Seong, Graphene oxide-gold nanozyme for highly sensitive electrochemical detection of hydrogen peroxide, Sens. Actuators B: Chem. 274 (2018) 201-209.
[172] Y. Astuti, E. Topoglidis, J.R. Durrant, Use of microperoxidase-11 to functionalize tin dioxide electrodes for the optical and electrochemical sensing of hydrogen peroxide, Anal. Chim. Acta, 686 (2011) 126-132.
[173] C. Gong, J. Chen, Y. Shen, Y. Song, Y. Song, L. Wang, Microperoxidase-11/metal–organic framework/macroporous carbon for detecting hydrogen peroxide, RSC Adv. 6 (2016) 79798-79804.
[174] C. Gong, Y. Shen, J. Chen, Y. Song, S. Chen, Y. Song, L. Wang, Microperoxidase-11@ PCN-333 (Al)/three-dimensional macroporous carbon electrode for sensing hydrogen peroxide, Sens. Actuators B: Chem. 239 (2017) 890-897.
[175] N. Akhtar, S.A. El-Safty, M. Khairy, W.A. El-Said, Fabrication of a highly selective nonenzymatic amperometric sensor for hydrogen peroxide based on nickel foam/cytochrome c modified electrode, Sens. Actuators B: Chem. 207 (2015) 158-166.
[176] M.P. Bilibana, A.R. Williams, C. Rassie, C.E. Sunday, H. Makelane, L. Wilson, N. Ntshongontshi, A.N. Jijana, M. Masikini, P.G. Baker, Electrochemical aptatoxisensor responses on nanocomposites containing electro-deposited silver nanoparticles on poly (Propyleneimine) dendrimer for the detection of microcystin-LR in freshwater, Sensors, 16 (2016) 1901.
[177] H. Heli, J. Pishahang, Cobalt oxide nanoparticles anchored to multiwalled carbon nanotubes: synthesis and application for enhanced electrocatalytic reaction and highly sensitive nonenzymatic detection of hydrogen peroxide, Electrochim. Acta, 123 (2014) 518-526.
[178] S. Barkaoui, M. Haddaoui, H. Dhaouadi, N. Raouafi, F. Touati, Hydrothermal synthesis of urchin-like Co_3O_4 nanostructures and their electrochemical sensing performance of H_2O_2, J. Solid State Chem. 228 (2015) 226-231.

[179] Y. Ni, Y. Liao, M. Zheng, S. Shao, In-situ growth of Co_3O_4 nanoparticles on mesoporous carbon nanofibers: a new nanocomposite for nonenzymatic amperometric sensing of H_2O_2, Microchim. Acta, 184 (2017) 3689-3695.
[180] J. Wang, H. Gao, F. Sun, Q. Hao, C. Xu, Highly sensitive detection of hydrogen peroxide based on nanoporous Fe_2O_3/CoOcomposites, Biosens. Bioelectron. 42 (2013) 550-555.
[181] M.-Y. Wang, T. Shen, M. Wang, D.-E. Zhang, Z.-w. Tong, J. Chen, One-pot synthesis of α-Fe_2O_3 nanoparticles-decorated reduced graphene oxide for efficient nonenzymatic H_2O_2 biosensor, Sens. Actuators B: Chem. 190 (2014) 645-650.
[182] M. Yuan, J. Li, Y. Yu, Y. Fu, A. Fong, J. Hu, Fabrication of a Fe_2O_3 Nanoparticles Implantation-modified Electrode and its Applications in Electrochemical Sensing, Electroanalysis, 28 (2016) 954-961.
[183] B. Zhang, X. Zhang, D. Huang, S. Li, H. Yuan, M. Wang, Y. Shen, Co9S8 hollow spheres for enhanced electrochemical detection of hydrogen peroxide, Talanta, 141 (2015) 73-79.
[184] H. Guan, Y. Liu, Z. Bai, J. Zhang, S. Yuan, B. Zhang, Ag nanoparticles embedded in N-doped carbon nanofibers: a superior electrocatalyst for hydrogen peroxide detection, Mater. Chem. Phys. 213 (2018) 335-342.
[185] X. Liu, T. Shen, Z. Zhao, Y. Qin, P. Zhang, H. Luo, Z.-X. Guo, Graphene/gold nanoparticle aerogel electrode for electrochemical sensing of hydrogen peroxide, Mater. Lett. 229 (2018) 368-371.
[186] H. Dai, D. Chen, P. Cao, Y. Li, N. Wang, S. Sun, T. Chen, H. Ma, M. Lin, Molybdenum sulfide/nitrogen-doped carbon nanowire-based electrochemical sensor for hydrogen peroxide in living cells, Sens. Actuators B: Chem. 276 (2018) 65-71.
[187] H. Dai, Y. Chen, X. Niu, C. Pan, H. Chen, X. Chen, High-performance electrochemical biosensor for nonenzymatic H2O2 sensing based on Au@C-Co_3O_4 heterostructures, Biosens. Bioelectron. 118 (2018) 36-43.
[188] Z. Wu, L.-P. Sun, Z. Zhou, Q. Li, L.-H. Huo, H. Zhao, Efficient nonenzymatic H2O2 biosensor based on ZIF-67 MOF derived Co nanoparticles embedded N-doped mesoporous carbon composites, Sens. Actuators B: Chem. 276 (2018) 142-149.
[189] X. Wu, F. Li, C. Zhao, X. Qian, One-step construction of hierarchical $Ni(OH)_2$/RGO/Cu_2O on Cu foil for ultra-sensitive non-enzymatic glucose and hydrogen peroxide detection, Sens. Actuators B: Chem. 274 (2018) 163-171.

[190] K. Vijayalakshmi, S.D. Jereil, K. Alagusundaram, Electron beam and spray technologies fabrication of hybrid MnO_2/CNT/Ta nanocomposite for the electrochemical detection of H_2O_2, Ceram.Int. 43 (2017) 14464-14472.
[191] J.S. Easow, T. Selvaraju, Unzipped catalytic activity of copper in realizing bimetallic Ag@ Cu nanowires as a better amperometric H_2O_2 sensor, Electrochim. Acta, 112 (2013) 648-654.
[192] S.G. Leonardi, D. Aloisio, N. Donato, P.A. Russo, M.C. Ferro, N. Pinna, G. Neri, Amperometric sensing of H2O2 using Pt–TiO_2/reduced graphene oxide nanocomposites, ChemElectroChem, 1 (2014) 617-624.
[193] H. Liu, Q. Chen, X. Cheng, Y. Wang, Y. Zhang, G. Fan, Sustainable and scalable in-situ fabrication of Au nanoparticles and Fe_3O_4 hybrids as highly efficient electrocatalysts for the enzyme-free sensing of H_2O_2 in neutral and basic solutions, Sens. Actuators B: Chem. 314 (2020) 128067.
[194] M.A. Riaz, Z. Yuan, A. Mahmood, F. Liu, X. Sui, J. Chen, Q. Huang, X. Liao, L. Wei, Y. Chen, Hierarchically porous carbon nanofibers embedded with cobalt nanoparticles for efficient H2O2 detection on multiple sensor platforms, Sens. Actuators B: Chem. 319 (2020) 128243.
[195] X.R. Li, B. Wang, J.J. Xu, H.Y. Chen, Noncovalent Assembly of Picket-Fence Porphyrin on Carbon Nanotubes as Effective Peroxidase-Like Catalysts for Detection of Hydrogen Peroxide in Beverages, Electroanalysis, 23 (2011) 2955-2963.
[196] F. Gao, B. Jiang, Z. Cang, N. Wang, B. Han, Q. Li, Y. Chen, Y. Chen, F. Xia, H. Zhai, C. Chen, M. Lu, Y. Meng, Y. Lu, Z. Shen, Serum Uric Acid Is Associated with Erectile Dysfunction: A Population-Based Cross-Sectional Study in Chinese Men, Sci. Rep. 7 (2017) 2087.
[197] B.N. Ames, R. Cathcart, E. Schwiers, P. Hochstein, Uric acid provides an antioxidant defense in humans against oxidant- and radical-caused aging and cancer: a hypothesis, Proceedings of the National Academy of Sciences of the United States of America, 78 (1981) 6858-6862.
[198] C.-C. Chang, C.-H. Wu, L.-K. Liu, R.-H. Chou, C.-S. Kuo, P.-H. Huang, L.-K. Chen, S.-J. Lin, Association between serum uric acid and cardiovascular risk in nonhypertensive and nondiabetic individuals: The Taiwan I-Lan Longitudinal Aging Study, Scie.Rep. 8 (2018) 5234.
[199] H. Kono, C.J. Chen, F. Ontiveros, K.L. Rock, Uric acid promotes an acute inflammatory response to sterile cell death in mice, J. Clin. Inv. 120 (2010) 1939-1949.
[200] A.C. Gagliardi, M.H. Miname, R.D. Santos, Uric acid: A marker of increased cardiovascular risk, Atherosclerosis, 202 (2009) 11-17.

[201] H. Sun, N. Wang, C. Chen, X. Nie, B. Han, Q. Li, C. Zhu, Y. Chen, F. Xia, Y. Chen, H. Zhai, B. Jiang, B. Hu, Y. Lu, Cadmium exposure and its association with serum uric acid and hyperuricemia, Sci. Rep. 7 (2017) 550-550.
[202] N.E. Azmi, A.H.A. Rashid, J. Abdullah, N.A. Yusof, H. Sidek, Fluorescence biosensor based on encapsulated quantum dots/enzymes/sol-gel for non-invasive detection of uric acid, J. Luminesc. 202 (2018) 309-315.
[203] M.W. Abbas, R.A. Soomro, N.H. Kalwar, M. Zahoor, A. Avci, E. Pehlivan, K.R. Hallam, M. Willander, Carbon quantum dot coated Fe_3O_4 hybrid composites for sensitive electrochemical detection of uric acid, Microchem. J.146 (2019) 517-524.
[204] F. Yang, Z. Yu, X. Li, P. Ren, G. Liu, Y. Song, J. Wang, Design and synthesis of a novel lanthanide fluorescent probe (TbIII-dtpa-bis(2,6-diaminopurine)) and its application to the detection of uric acid in urine sample, Spectrochim. Acta Part A: Mol. Biomol. Spectrosc. 203 (2018) 461-471.
[205] D. Jin, M.-H. Seo, B.T. Huy, Q.-T. Pham, M.L. Conte, D. Thangadurai, Y.-I. Lee, Quantitative determination of uric acid using CdTe nanoparticles as fluorescence probes, Biosens. Bioelectron. 77 (2016) 359-365.
[206] C.-Y. Wang, C.-W. Huang, T.-T. Wei, M.-Y. Wu, Y.-W. Lin, Fluorescent detection of uric acid in biological samples through the inhibition of cobalt(II) catalyzed Amplex UltraRed, Sens. Actuators B: Chem. 244 (2017) 357-364.
[207] H.-F. Lu, J.-Y. Li, M.-M. Zhang, D. Wu, Q.-L. Zhang, A highly selective and sensitive colorimetric uric acid biosensor based on Cu(II)-catalyzed oxidation of 3,3′,5,5′-tetramethylbenzidine, Sens. Actuators B: Chem. 244 (2017) 77-83.
[208] J. Wang, X. Fang, Y. Zhang, X. Cui, H. Zhao, X. Li, Z. Li, A simple and rapid colorimetric probe for uric acid detection based on redox reaction of 3,3′,5,5′-tetramethylbenzidine with HAuCl4, Coll. Surf. A: Physicochem. Eng. Asp. 555 (2018) 565-571.
[209] C. Vakh, S. Koronkiewicz, S. Kalinowski, L. Moskvin, A. Bulatov, An automatic chemiluminescence method based on the multi-pumping flow system coupled with the fluidized reactor and direct-injection detector: Determination of uric acid in saliva samples, Talanta, 167 (2017) 725-732.
[210] J. Yu, S. Wang, L. Ge, S. Ge, A novel chemiluminescence paper microfluidic biosensor based on enzymatic reaction for uric acid determination, Biosens. Bioelectron. 26 (2011) 3284-3289.

[211] M. Saqib, L. Qi, P. Hui, A. Nsabimana, M.I. Halawa, W. Zhang, G. Xu, Development of luminol-N-hydroxyphthalimide chemiluminescence system for highly selective and sensitive detection of superoxide dismutase, uric acid and Co2+, Biosens. Bioelectron. 99 (2018) 519-524.
[212] B.J. Matsoso, B.K. Mutuma, C. Billing, K. Ranganathan, T. Lerotholi, G. Jones, N.J. Coville, Investigating the electrochemical behaviour and detection of uric acid on ITO electrodes modified with differently doped N-graphene films, J. Electroanal. Chem. 833 (2019) 160-168.
[213] M.Y. Emran, M.A. Shenashen, A.A. Abdelwahab, H. Khalifa, M. Mekawy, N. Akhtar, M. Abdelmottaleb, S.A. El-Safty, Design of hierarchical electrocatalytic mediator for one step, selective screening of biomolecules in biological fluid samples, J. Appl. Electrochem. 48 (2018) 529-542.
[214] A.H. Wolfe, J.A. Patz, Reactive nitrogen and human health: acute and long-term implications, Ambio, 31 (2002) 120-125.
[215] J. Vinoth Kumar, R. Karthik, S.-M. Chen, P. Balasubramanian, V. Muthuraj, V. Selvam, A Novel Cerium Tungstate Nanosheets Modified Electrode for the Effective Electrochemical Detection of Carcinogenic Nitrite Ions, Electroanalysis, 29 (2017) 2385-2394.
[216] V.Y. Titov, Y.M. Petrenko, Proposed Mechanism of Nitrite-Induced Methemoglobinemia, Biochemistry (Moscow), 70 (2005) 473-483.
[217] A. Pandikumar, S. Manonmani, R. Ramaraj, TiO2–Au nanocomposite materials embedded in polymer matrices and their application in the photocatalytic reduction of nitrite to ammonia, Catal. Sci.Tech. 2 (2012) 345-353.
[218] A. Casula, A. Llopis-Lorente, A. Garau, F. Isaia, M. Kubicki, V. Lippolis, F. Sancenón, R. Martínez-Máñez, A. Owczarzak, C. Santi, A new class of silica-supported chromo-fluorogenic chemosensors for anion recognition based on a selenourea scaffold, Chem. Commun. 53 (2017) 3729-3732.
[219] V.V. Kumar, S.P. Anthony, Highly selective silver nanoparticles based label free colorimetric sensor for nitrite anions, Anal. Chim. Acta, 842 (2014) 57-62.
[220] X. Hu, J. Shi, Y. Shi, X. Zou, H.E. Tahir, M. Holmes, W. Zhang, X. Huang, Z. Li, Y. Xu, A dual-mode sensor for colorimetric and fluorescent detection of nitrite in hams based on carbon dots-neutral red system, Meat Sci. 147 (2019) 127-134.
[221] N.S.M. Noor, L.L. Tan, L.Y. Heng, K.F. Chong, S.N. Tajuddin, Acrylic microspheres-based optosensor for visual detection of nitrite, Food Chem. 207 (2016) 132-138.

[222] J. Nam, I.-B. Jung, B. Kim, S.-M. Lee, S.-E. Kim, K.-N. Lee, D.-S. Shin, A colorimetric hydrogel biosensor for rapid detection of nitrite ions, Sens. Actuators B: Chem. 270 (2018) 112-118.
[223] T.M. Cardoso, P.T. Garcia, W.K. Coltro, Colorimetric determination of nitrite in clinical, food and environmental samples using microfluidic devices stamped in paper platforms, Anal. Meth. 7 (2015) 7311-7317.
[224] Y. Zhan, Y. Zeng, L. Li, F. Luo, B. Qiu, Z. Lin, L. Guo, Ratiometric fluorescent hydrogel test kit for on-spot visual detection of nitrite, ACS Sensors, 4 (2019) 1252-1260.
[225] H.-H. Ren, Y. Fan, B. Wang, L.-P. Yu, Polyethylenimine-capped CdS quantum dots for sensitive and selective detection of nitrite in vegetables and water, J. Agric. Food Chem. 66 (2018) 8851-8858.
[226] H. Wang, X. Jing, X. Bi, B. Bai, X. Wang, Quantitative Detection of Nitrite in Food Samples Based on Digital Image Colourimetry by Smartphone, ChemistrySelect, 5 (2020) 9952-9956.
[227] Y. Haldorai, S.-K. Hwang, A.-I. Gopalan, Y.S. Huh, Y.-K. Han, W. Voit, G. Sai-Anand, K.-P. Lee, Direct electrochemistry of cytochrome c immobilized on titanium nitride/multi-walled carbon nanotube composite for amperometric nitrite biosensor, Biosens. Bioelectron. 79 (2016) 543-552.
[228] T. Islam, M.M. Hasan, S.S. Akter, N.H. Alharthi, M.R. Karim, M.A. Aziz, M.D. Hossain, A.S. Ahammad, Fabrication of Ni–Co-Based Heterometallo-Supramolecular Polymer Films and the Study of Electron Transfer Kinetics for the Nonenzymatic Electrochemical Detection of Nitrite, ACS Appl. Polymer Mater. 2 (2019) 273-284.
[229] Y. Ma, Y. Wang, D. Xie, Y. Gu, H. Zhang, G. Wang, Y. Zhang, H. Zhao, P.K. Wong, NiFe-layered double hydroxide nanosheet arrays supported on carbon cloth for highly sensitive detection of nitrite, ACS Appl. Mater. Interfaces, 10 (2018) 6541-6551.
[230] W. Zhu, Y. Zhang, J. Gong, Y. Ma, J. Sun, T. Li, J. Wang, Surface engineering of carbon fiber paper toward exceptionally high-performance and stable electrochemical nitrite sensing, ACS Sensors, 4 (2019) 2980-2987.
[231] Z. Meng, B. Liu, J. Zheng, Q. Sheng, H. Zhang, Electrodeposition of cobalt oxide nanoparticles on carbon nanotubes, and their electrocatalytic properties for nitrite electrooxidation, Microchim. Acta, 175 (2011) 251-257.
[232] J. Wang, N. Hui, A nanocomposite consisting of flower-like cobalt nanostructures, graphene oxide and polypyrrole for amperometric sensing of nitrite, Microchim. Acta, 184 (2017) 2411-2418.

[233] L. Fu, S. Yu, L. Thompson, A. Yu, Development of a novel nitrite electrochemical sensor by stepwise in situ formation of palladium and reduced graphene oxide nanocomposites, RSC Adv.5 (2015) 40111-40116.
[234] R. Ahmad, T. Mahmoudi, M.-S. Ahn, J.-Y. Yoo, Y.-B. Hahn, Fabrication of sensitive non-enzymatic nitrite sensor using silver-reduced graphene oxide nanocomposite, J. Coll. Interface Sci.516 (2018) 67-75.
[235] M. Ghanei-Motlagh, M.A. Taher, A novel electrochemical sensor based on silver/halloysite nanotube/molybdenum disulfide nanocomposite for efficient nitrite sensing, Biosens. Bioelectron. 109 (2018) 279-285.
[236] C. Rajkumar, B. Thirumalraj, S.-M. Chen, S. Palanisamy, Novel electrochemical preparation of gold nanoparticles decorated on a reduced graphene oxide–fullerene composite for the highly sensitive electrochemical detection of nitrite, RSC Adv. 6 (2016) 68798-68805.
[237] S. Zhang, Q. Sheng, J. Zheng, Synthesis of Au nanoparticles dispersed on halloysite nanotubes–reduced graphene oxide nanosheets and their application for electrochemical sensing of nitrites, New J. Chem., 40 (2016) 9672-9678.
[238] Y. Ma, X. Song, X. Ge, H. Zhang, G. Wang, Y. Zhang, H. Zhao, In situ growth of α-Fe 2 O 3 nanorod arrays on 3D carbon foam as an efficient binder-free electrode for highly sensitive and specific determination of nitrite, J. Mater. Chem. A, 5 (2017) 4726-4736.
[239] A. Gill, J. Zajda, M.E. Meyerhoff, Comparison of electrochemical nitric oxide detection methods with chemiluminescence for measuring nitrite concentration in food samples, Anal. Chim. Acta, 1077 (2019) 167-173.
[240] A. Üzer, Ş. Sağlam, Z. Can, E. Erçağ, R. Apak, Electrochemical determination of food preservative nitrite with gold nanoparticles/p-aminothiophenol-modified gold electrode, Int. J. Mol. Sci. 17 (2016) 1253.
[241] M.-L. Zhang, D.-K. Huang, Z. Cao, Y.-Q. Liu, J.-L. He, J.-F. Xiong, Z.-M. Feng, Y.-L. Yin, Determination of trace nitrite in pickled food with a nano-composite electrode by electrodepositing ZnO and Pt nanoparticles on MWCNTs substrate, LWT-Food Sci.Tech. 64 (2015) 663-670.
[242] H. Rao, Y. Liu, J. Zhong, Z. Zhang, X. Zhao, X. Liu, Y. Jiang, P. Zou, X. Wang, Y. Wang, Gold nanoparticle/chitosan@ N, S co-doped multiwalled carbon nanotubes sensor: fabrication, characterization, and electrochemical detection of catechol and nitrite, ACS Sust. Chem. Eng. 5 (2017) 10926-10939.

[243] R. Madhuvilakku, S. Alagar, R. Mariappan, S. Piraman, Glassy carbon electrodes modified with reduced graphene oxide-MoS2-poly (3, 4-ethylene dioxythiophene) nanocomposites for the non-enzymatic detection of nitrite in water and milk, Anal. Chim.Acta, 1093 (2020) 93-105.
[244] J. Jackowetz, R.M. de Orduña, Metabolism of SO_2 binding compounds by Oenococcus oeni during and after malolactic fermentation in white wine, Int. J. Food Microbio. 155 (2012) 153-157.
[245] R. McFeeters, A. Barish, Sulfite analysis of fruits and vegetables by high-performance liquid chromatography (HPLC) with ultraviolet spectrophotometric detection, Journal of Agricultural and Food Chem. 51 (2003) 1513-1517.
[246] G. Carrabs, G. Smaldone, L. Carosielli, M. Girasole, M. Iammarino, E. Chiaravalle, Detection of sulfites in fresh meat preparation commercialised at retail in Lazio Region, Italian J. Food safety, 6 (2017).
[247] T. D'Amore, A. Di Taranto, G. Berardi, V. Vita, G. Marchesani, A.E. Chiaravalle, M. Iammarino, Sulfites in meat: Occurrence, activity, toxicity, regulation, and detection. A comprehensive review, Comprehensive Reviews in Food Sci. Food Safety, 19 (2020) 2701-2720.
[248] H. Tian, J. Qian, Q. Sun, H. Bai, W. Zhang, Colorimetric and ratiometric fluorescent detection of sulfite in water via cationic surfactant-promoted addition of sulfite to α, β-unsaturated ketone, Anal. Ahim. Acta, 788 (2013) 165-170.
[249] P. Kaur, H. Kaur, K. Singh, A 'turn-off'emission based chemosensor for HSO 4−–formation of a hydrogen-bonded complex, Analyst, 138 (2013) 425-428.
[250] K. Kobiro, Y. Inoue, A new chiral probe for sulfate anion: uv, cd, fluorescence, and nmr spectral studies of 1: 1 and 2: 1 complex formation and structure of chiral guanidinium− p-dimethylaminobenzoate conjugate with sulfate anion, J. Am. Chem. Soc.,125 (2003) 421-427.
[251] W. Lu, J. Shu, Z. Wang, N. Huang, W. Song, The intrinsic oxidase-like activity of Ag2O nanoparticles and its application for colorimetric detection of sulfite, Mater. Lett. 154 (2015) 33-36.
[252] H. Zhang, S. Xue, G. Feng, A colorimetric and near-infrared fluorescent turn-on probe for rapid detection of sulfite, Sens. Actuators B: Chem. 231 (2016) 752-758.
[253] T. Gao, X. Cao, P. Ge, J. Dong, S. Yang, H. Xu, Y. Wu, F. Gao, W. Zeng, A self-assembled fluorescent organic nanoprobe and its application for sulfite detection in food samples and living systems, Org. Biomol. Chem. 15 (2017) 4375-4382.
[254] F. Zhou, H. Feng, H. Li, Y. Wang, Z. Zhang, W. Kang, H. Jia, X. Yang, Q. Meng, R. Zhang, Red-emission probe for ratiometric fluorescent detection of bisulfite and its application in live animals and food samples, ACS Omega, 5 (2020) 5452-5459.

[255] L. Fang, L. Zhang, Z. Chen, C. Zhu, J. Liu, J. Zheng, Ammonium citrate derived carbon quantum dot as on-off-on fluorescent sensor for detection of chromium (VI) and sulfites, Mater. Lett. 191 (2017) 1-4.
[256] J.P. Winiarski, M.R. de Barros, H.A. Magosso, C.L. Jost, Electrochemical reduction of sulfite based on gold nanoparticles/silsesquioxane-modified electrode, Electrochim. Acta, 251 (2017) 522-531.
[257] S. Devaramani, P. Malingappa, Synthesis and characterization of cobalt nitroprusside nano particles: application to sulfite sensing in food and water samples, Electrochim. Acta, 85 (2012) 579-587.
[258] B. Devadas, M. Sivakumar, S.M. Chen, S. Cheemalapati, An electrochemical approach: Switching Structures of rare earth metal Praseodymium hexacyanoferrate and its application to sulfite sensor in Red Wine, Electrochim. Acta, 176 (2015) 350-358.
[259] S. Devaramani, P.S. Adarakatti, P. Malingappa, Covalent anchoring of cobalt hexacyanoferrate particles on graphitic carbon: A simple and renewable robust pellet electrode as an electrochemical interface for amperometric quantification of sulfite, Electrochim. Acta, 231 (2017) 650-658.
[260] P. Manusha, S. Senthilkumar, Design and synthesis of phenothiazine based imidazolium ionic liquid for electrochemical nonenzymatic detection of sulfite in food samples, J. Mol. Liq., 301 (2020) 112412.
[261] Z. Wu, F. Guo, L. Huang, L. Wang, Electrochemical nonenzymatic sensor based on cetyltrimethylammonium bromide and chitosan functionalized carbon nanotube modified glassy carbon electrode for the determination of hydroxymethanesulfinate in the presence of sulfite in foods, Food Chem. 259 (2018) 213-218.
[262] R. Wang, Y. Mao, H. Qu, W. Chen, A. Ma, L. Zheng, Highly sensitive and selective sulfite sensors based on solution-gated graphene transistors with multi-walled carbon nanotube functionalized gate electrodes, Food Chem. 290 (2019) 101-106.
[263] A. Turner, Heavy metals in the glass and enamels of consumer container bottles, Env. Sci. Tech., 53 (2019) 8398-8404.
[264] B.W. Redan, Processing aids in food and beverage manufacturing: Potential source of elemental and trace metal contaminants, J. Agric. Food Chem. 68 (2020) 13001–13007
[265] A.S. Saleemi, M. Hafeez, A. Munawar, N. Akhtar, W. Abbas, M.E. Mazhar, Z. Shafiq, A.P. Davis, S.-L. Lee, Synthesis and sensing efficiency of CN-wrapped ZnFe 2 O 4 microsphere–ionic

liquid composites towards ultra-high sensitive arsenic (iii) monitoring of ground drinking water, J. Mater. Chem. C, 8 (2020) 12984-12992.
[266] M.A. Baki, M.M. Hossain, J. Akter, S.B. Quraishi, M.F.H. Shojib, A.A. Ullah, M.F. Khan, Concentration of heavy metals in seafood (fishes, shrimp, lobster and crabs) and human health assessment in Saint Martin Island, Bangladesh, Ecotoxic. Env. safety, 159 (2018) 153-163.
[267] E.P. Nardi, F.S. Evangelista, L. Tormen, T.D. Saint, A.J. Curtius, S.S. de Souza, F. Barbosa Jr, The use of inductively coupled plasma mass spectrometry (ICP-MS) for the determination of toxic and essential elements in different types of food samples, Food Chem. 112 (2009) 727-732.
[268] M.R. Awual, S.A. El-Safty, A. Jyo, Removal of trace arsenic (V) and phosphate from water by a highly selective ligand exchange adsorbent, J. Env. Sci. 23 (2011) 1947-1954.
[269] M.R. Awual, M. Ismael, T. Yaita, S.A. El-Safty, H. Shiwaku, Y. Okamoto, S. Suzuki, Trace copper (II) ions detection and removal from water using novel ligand modified composite adsorbent, Chem. Eng. J. 222 (2013) 67-76.
[270] S. El-Safty, A. Shahat, M.R. Awual, M. Mekawy, Large three-dimensional mesocage pores tailoring silica nanotubes as membrane filters: nanofiltration and permeation flux of proteins, J. Mater. Chem. 21 (2011) 5593-5603.
[271] S.A. El-Safty, D. Prabhakaran, A.A. Ismail, H. Matsunaga, F. Mizukami, Nanosensor design packages: a smart and compact development for metal ions sensing responses, Adv. Functional Mater. 17 (2007) 3731-3745.
[272] D. Zhang, W. Jiang, Y. Zhao, Y. Dong, X. Feng, L. Chen, Carbon dots rooted PVDF membrane for fluorescence detection of heavy metal ions, Appl. Surf. Sci. 494 (2019) 635-643.
[273] K. Radhakrishnan, S. Sivanesan, P. Panneerselvam, Turn-On fluorescence sensor based detection of heavy metal ion using carbon dots@ graphitic-carbon nitride nanocomposite probe, J. Photochem. Photobio. A: Chem. 389 (2020) 112204.
[274] S.L. Ting, S.J. Ee, A. Ananthanarayanan, K.C. Leong, P. Chen, Graphene quantum dots functionalized gold nanoparticles for sensitive electrochemical detection of heavy metal ions, Electrochim. Acta, 172 (2015) 7-11.
[275] M. Baghayeri, A. Amiri, B. Maleki, Z. Alizadeh, O. Reiser, A simple approach for simultaneous detection of cadmium (II) and lead (II) based on glutathione coated magnetic nanoparticles as a highly selective electrochemical probe, Sens. Actuators B: Chem. 273 (2018) 1442-1450.

[276] S.A. El-Safty, M.R. Awual, M. Shenashen, A. Shahat, Simultaneous optical detection and extraction of cobalt (II) from lithium ion batteries using nanocollector monoliths, Sens. Actuators B: Chem. 176 (2013) 1015-1025.
[277] S.A. El-Safty, A.A. Ismail, H. Matsunaga, F. Mizukami, Optical nanosensor design with uniform pore geometry and large particle morphology, Chem.–A Eur. J. 13 (2007) 9245-9255.
[278] S. Goswami, S. Das, K. Aich, An ICT based highly selective and sensitive sulfur-free sensor for naked eye as well as fluorogenic detection of Hg2+ in mixed aqueous media, Tetrahedron Lett. 54 (2013) 4620-4623.
[279] S.A. El-Safty, M. Shenashen, M. Ismael, M. Khairy, M.R. Awual, Mesoporous aluminosilica sensors for the visual removal and detection of Pd (II) and Cu (II) ions, Microp. Mesop. Mater. 166 (2013) 195-205.
[280] M. Shenashen, S. El-Safty, E. Elshehy, Architecture of optical sensor for recognition of multiple toxic metal ions from water, J. Hazardous Mater..260 (2013) 833-843.
[281] H. Gomaa, H. Khalifa, M. Selim, M. Shenashen, S. Kawada, A.S. Alamoudi, A. Azzam, A. Alhamid, S. El-Safty, Selective, photoenhanced trapping/detrapping of arsenate anions using mesoporous blobfish head TiO2 monoliths, ACS Sust. Chem. Eng. 5 (2017) 10826-10839.
[282] M.A. Shenashen, S.A. El-Safty, E.A. Elshehy, M. Khairy, Hexagonal-Prism-Shaped Optical Sensor/Captor for the Optical Recognition and Sequestration of PdII Ions from Urban Mines, Eur. J. Inorg. Chem. 2015 (2015) 179-191.
[283] M.A. Shenashen, S. Kawada, M.M. Selim, W.M. Morsy, H. Yamaguchi, A.A. Alhamid, N. Ohashi, I. Ichinose, S.A. El-Safty, Bushy sphere dendrites with husk-shaped branches axially spreading out from the core for photo-catalytic oxidation/remediation of toxins, Nanoscale, 9 (2017) 7947-7959.
[284] H. Gomaa, M. Shenashen, H. Yamaguchi, A. Alamoudi, S. El-Safty, Extraction and recovery of Co 2+ ions from spent lithium-ion batteries using hierarchical mesosponge γ-Al 2 O 3 monolith extractors, Green Chem. 20 (2018) 1841-1857.
[285] A.A.E. Soliman, M.A. Shenashen, I.M. El-Sewify, G.M. Taha, M.A. El-Taher, H. Yamaguchi, A.S. Alamoudi, M.M. Selim, S.A. El-Safty, Mesoporous organic–inorganic core–shell necklace cages for potentially capturing Cd^{2+} ions from water sources, ChemistrySelect, 2 (2017) 6135-6142.
[286] M.R. Awual, M.M. Hasan, A.M. Asiri, M.M. Rahman, Novel optical composite material for efficient vanadium (III) capturing from wastewater, J. Mol. Liq. 283 (2019) 704-712.

[287] M.R. Awual, M.M. Hasan, J. Iqbal, A. Islam, M.A. Islam, A.M. Asiri, M.M. Rahman, Naked-eye lead (II) capturing from contaminated water using innovative large-pore facial composite materials, Microchem. J. 154 (2020) 104585.
[288] M.R. Awual, M.M. Hasan, A. Islam, M.M. Rahman, A.M. Asiri, M.A. Khaleque, M.C. Sheikh, Offering an innovative composited material for effective lead (II) monitoring and removal from polluted water, J. Cleaner Prod. 231 (2019) 214-223.
[289] S. Jimenez-Falcao, A. Villalonga, J. Parra-Nieto, A. Llopis-Lorente, P. Martinez-Ruiz, R. Martinez-Mañez, R. Villalonga, Dithioacetal-mechanized mesoporous nanosensor for Hg (II) determination, Microp. Mesop. Mater. 297 (2020) 110054.
[290] H.E. Okda, S. El Sayed, R.C. Ferreira, R.C. Gonçalves, S.P. Costa, M.M.M. Raposo, R. Martínez-Máñez, F. Sancenón, N, N-Diphenylanilino-heterocyclic aldehyde-based chemosensors for UV-vis/NIR and fluorescence Cu (II) detection, New J. Chem. 43 (2019) 7393-7402.
[291] L. Shi, Y. Bao, Y. Zhang, C. Zhang, G. Zhang, C. Dong, S. Shuang, Orange emissive carbon nanodots for fluorescent and colormetric bimodal discrimination of Cu^{2+} and pH, Analyst, 146 (2021) 1907-1914
[292] S. Goswami, S. Maity, A.K. Das, A.C. Maity, Single chemosensor for highly selective colorimetric and fluorometric dual sensing of Cu (II) as well as 'NIRF'to acetate ion, Tetrahedron Lett. 54 (2013) 6631-6634.
[293] A. Sayed, I.M. Othman, M. Hamam, H. Gomaa, M.I. Gadallah, M. Mostfa, H.R.H. Ali, M.Y. Emran, M. Abdel-Hakim, M. Mahross, A novel fluorescent sensor for fast and highly selective turn-off detection of Fe^{3+} in water and pharmaceutical samples using synthesized azopyrazole-benzenesulfonamide derivative, J. Mol. Struct.1225 (2021) 129175.
[294] I.M. El-Sewify, M.A. Shenashen, A. Shahat, M.M. Selim, M.M. Khalil, S.A. El-Safty, Sensitive and selective fluorometric determination and monitoring of Zn^{2+} ions using supermicroporous Zr-MOFs chemosensors, Microchem. J. 139 (2018) 24-33.
[295] G.D. O'Neil, M.E. Newton, J.V. Macpherson, Direct identification and analysis of heavy metals in solution (Hg, Cu, Pb, Zn, Ni) by use of in situ electrochemical X-ray fluorescence, Anal. Chem. 87 (2015) 4933-4940.
[296] I.M. El-Sewify, M.A. Shenashen, A. Shahat, H. Yamaguchi, M.M. Selim, M.M.H. Khalil, S.A. El-Safty, Ratiometric Fluorescent Chemosensor for Zn^{2+} Ions in Environmental Samples Using Supermicroporous Organic-Inorganic Structures as Potential Platforms, ChemistrySelect, 2 (2017) 11083-11090.

[297] I.M. El-Sewify, M.A. Shenashen, A. Shahat, H. Yamaguchi, M.M. Selim, M.M. Khalil, S.A. El-Safty, Dual colorimetric and fluorometric monitoring of Bi^{3+} ions in water using supermicroporous Zr-MOFs chemosensors, J .Luminesc.198 (2018) 438-448.
[298] S.O. Tümay, V. Şanko, E. Demirbas, A. Şenocak, Fluorescence determination of trace level of cadmium with pyrene modified nanocrystalline cellulose in food and soil samples, Food Chem. Toxic., 146 (2020) 111847.
[299] A.A. Gouda, S.M. Al Ghannam, Impregnated multiwalled carbon nanotubes as efficient sorbent for the solid phase extraction of trace amounts of heavy metal ions in food and water samples, Food Chem. 202 (2016) 409-416.
[300] T.L. Read, M.B. Joseph, J.V. Macpherson, Manipulation and measurement of pH sensitive metal–ligand binding using electrochemical proton generation and metal detection, Chem. Commun. 52 (2016) 1863-1866.
[301] Y. Zhou, L. Tang, G. Zeng, C. Zhang, Y. Zhang, X. Xie, Current progress in biosensors for heavy metal ions based on DNAzymes/DNA molecules functionalized nanostructures: A review, Sens. Actuators B: Chem. 223 (2016) 280-294.
[302] J. Xu, Z. Cao, Y. Zhang, Z. Yuan, Z. Lou, X. Xu, X. Wang, A review of functionalized carbon nanotubes and graphene for heavy metal adsorption from water: Preparation, application, and mechanism, Chemosphere, 195 (2018) 351-364.
[303] J. Wei, D. Yang, H. Chen, Y. Gao, H. Li, Stripping voltammetric determination of mercury (II) based on SWCNT-PhSH modified gold electrode, Sens. Actuators B: Chem. 190 (2014) 968-974.
[304] S. Wu, K. Li, X. Dai, Z. Zhang, F. Ding, S. Li, An ultrasensitive electrochemical platform based on imprinted chitosan/gold nanoparticles/graphene nanocomposite for sensing cadmium (II) ions, Microchem. J. 155 (2020) 104710.
[305] L. Wang, X. Peng, H. Fu, C. Huang, Y. Li, Z. Liu, Recent advances in the development of electrochemical aptasensors for detection of heavy metals in food, Biosens. Bioelectron. 147 (2020) 111777.
[306] X.-M. Bi, H.-R. Wang, L.-Q. Ge, D.-M. Zhou, J.-Z. Xu, H.-Y. Gu, N. Bao, Gold-coated nanostructured carbon tape for rapid electrochemical detection of cadmium in rice with in situ electrodeposition of bismuth in paper-based analytical devices, Sens. Actuators B: Chem. 260 (2018) 475-479.

[307] W. Wu, M. Jia, Z. Zhang, X. Chen, Q. Zhang, W. Zhang, P. Li, L. Chen, Sensitive, selective and simultaneous electrochemical detection of multiple heavy metals in environment and food using a lowcost Fe_3O_4 nanoparticles/fluorinated multi-walled carbon nanotubes sensor, Ecotoxic. Env. safety, 175 (2019) 243-250.
[308] L. Huang, W. Huang, R. Shen, Q. Shuai, Chitosan/thiol functionalized metal–organic framework composite for the simultaneous determination of lead and cadmium ions in food samples, Food Chem. 330 (2020) 127212.
[309] S.-W. Lv, J.-M. Liu, C.-Y. Li, N. Zhao, Z.-H. Wang, S. Wang, A novel and universal metal-organic frameworks sensing platform for selective detection and efficient removal of heavy metal ions, Chem. Eng. J. 375 (2019) 122111.
[310] X. Wang, Y. Qi, Y. Shen, Y. Yuan, L. Zhang, C. Zhang, Y. Sun, A ratiometric electrochemical sensor for simultaneous detection of multiple heavy metal ions based on ferrocene-functionalized metal-organic framework, Sens. Actuators B: Chem. 310 (2020) 127756.
[311] A. Jurek, E. Leitner, Analytical determination of bisphenol A (BPA) and bisphenol analogues in paper products by LC-MS/MS, Food Add. Contam. Part A, 35 (2018) 2256-2269.
[312] T. Geens, D. Aerts, C. Berthot, J.-P. Bourguignon, L. Goeyens, P. Lecomte, G. Maghuin-Rogister, A.-M. Pironnet, L. Pussemier, M.-L. Scippo, A review of dietary and non-dietary exposure to bisphenol-A, Food Chem. Toxic. 50 (2012) 3725-3740.
[313] S. Kitamura, T. Suzuki, S. Sanoh, R. Kohta, N. Jinno, K. Sugihara, S.i. Yoshihara, N. Fujimoto, H. Watanabe, S. Ohta, Comparative study of the endocrine-disrupting activity of bisphenol A and 19 related compounds, Toxic. Sci.84 (2005) 249-259.
[314] J.-M. Molina-Molina, E. Amaya, M. Grimaldi, J.-M. Sáenz, M. Real, M.F. Fernandez, P. Balaguer, N. Olea, In vitro study on the agonistic and antagonistic activities of bisphenol-S and other bisphenol-A congeners and derivatives via nuclear receptors, Toxic. Appl. Pharmacol. 272 (2013) 127-136.
[315] C.R. Armendáriz, Á. Daschner, E.G. Fandos, M. José, G. Muñoz, M.V. Moreno-Arribas, P.T. Oliag, J.B.G. de Castro, Report of the Scientific Committee of the Spanish Agency for Food Safety and Nutrition (AESAN) on the presence and safety of plastics as contaminants in food. Reference number: AESAN-2019-007.
[316] N. González, S.C. Cunha, R. Ferreira, J.O. Fernandes, M. Marquès, M. Nadal, J.L. Domingo, Concentrations of nine bisphenol analogues in food purchased from Catalonia (Spain): Comparison of canned and non-canned foodstuffs, Food Chem. Toxic. 136 (2020) 110992.

[317] R. Braunrath, D. Podlipna, S. Padlesak, M. Cichna-Markl, Determination of bisphenol A in canned foods by immunoaffinity chromatography, HPLC, and fluorescence detection, J. Agric. Food Chem. 53 (2005) 8911-8917.
[318] F. Sun, L. Kang, X. Xiang, H. Li, X. Luo, R. Luo, C. Lu, X. Peng, Recent advances and progress in the detection of bisphenol A, Anal. Bioanal. Chem. 408 (2016) 6913-6927.
[319] S.-H. Rajabnejad, H. Badibostan, A. Verdian, G.R. Karimi, E. Fooladi, J. Feizy, Aptasensors as promising new tools in bisphenol A detection-An invisible pollution in food and environment, Microchem. J. 155 (2020) 104722.
[320] À. Ribes, E. Aznar, A. Bernardos, M.D. Marcos, P. Amorós, R. Martínez-Máñez, F. Sancenón, Fluorogenic Sensing of Carcinogenic Bisphenol A using Aptamer-Capped Mesoporous Silica Nanoparticles, Chem.–A Eur. J., 23 (2017) 8581-8584.
[321] E. Sundaram, A. Manna, K.L. Servarayan, V.S. Vasantha, Colorimetric Detection and Bio-Magnification of Bisphenol A in Fish Organs and Water Sources using 3', 6'-bis (diethylamino)-2-((3, 4, 5trimethyl benzylidene) amino) spiro [isoindoline-1, 9'-xanthen]-3-one (BTSIXO)-Fe^{3+} ion Conjugate, Food Chem. 345 (2021) 128627.
[322] M. Jia, J. Sha, Z. Li, W. Wang, H. Zhang, High affinity truncated aptamers for ultra-sensitive colorimetric detection of bisphenol A with label-free aptasensor, Food Chem. 317 (2020) 126459.
[323] E.-H. Lee, S.K. Lee, M.J. Kim, S.-W. Lee, Simple and rapid detection of bisphenol A using a gold nanoparticle-based colorimetric aptasensor, Food Chem. 287 (2019) 205-213.
[324] D. Zhang, J. Yang, J. Ye, L. Xu, H. Xu, S. Zhan, B. Xia, L. Wang, Colorimetric detection of bisphenol A based on unmodified aptamer and cationic polymer aggregated gold nanoparticles, Anal. Biochem. 499 (2016) 51-56.
[325] Q. Kong, Y. Wang, L. Zhang, S. Ge, J. Yu, A novel microfluidic paper-based colorimetric sensor based on molecularly imprinted polymer membranes for highly selective and sensitive detection of bisphenol A, Sens. Actuators B: Chem. 243 (2017) 130-136.
[326] E.-S. Lee, G.B. Kim, S.-H. Ryu, H. Kim, H.H. Yoo, M.Y. Yoon, J.-W. Lee, M.C. Gye, Y.-P. Kim, Fluorescing aptamer-gold nanosensors for enhanced sensitivity to bisphenol A, Sens. Actuators B: Chem. 260 (2018) 371-379.
[327] E.-H. Lee, H.J. Lim, S.-D. Lee, A. Son, Highly sensitive detection of bisphenol A by NanoAptamer assay with truncated aptamer, ACS Appl. Mater. Iinterfaces, 9 (2017) 14889-14898.

[328] S.G. Kim, J.S. Lee, J. Jun, D.H. Shin, J. Jang, Ultrasensitive bisphenol a field-effect transistor sensor using an aptamer-modified multichannel carbon nanofiber transducer, ACS Appl. Mater. Iinterfaces, 8 (2016) 6602-6610.
[329] Y. Zhu, Y. Cai, L. Xu, L. Zheng, L. Wang, B. Qi, C. Xu, Building an aptamer/graphene oxide FRET biosensor for one-step detection of bisphenol A, ACS Appl. Mater. Iinterfaces, 7 (2015) 7492-7496.
[330] Y. Li, J. Xu, L. Wang, Y. Huang, J. Guo, X. Cao, F. Shen, Y. Luo, C. Sun, Aptamer-based fluorescent detection of bisphenol A using nonconjugated gold nanoparticles and CdTe quantum dots, Sens. Actuators B: Chem. 222 (2016) 815-822.
[331] L. Jiang, I. Santiago, J. Foord, A Comparative Study of Fouling-free Nanodiamond and Nanocarbon Electrochemical Sensors for Sensitive Bisphenol A Detection, Carbon, (2020).
[332] A.U. Alam, M.J. Deen, Bisphenol A Electrochemical Sensor Using Graphene Oxide and β-Cyclodextrin-Functionalized Multi-Walled Carbon Nanotubes, Anal. Chem. 92 (2020) 5532-5539.
[333] H. Yin, Y. Zhou, J. Xu, S. Ai, L. Cui, L. Zhu, Amperometric biosensor based on tyrosinase immobilized onto multiwalled carbon nanotubes-cobalt phthalocyanine-silk fibroin film and its application to determine bisphenol A, Anal. Chim. Acta, 659 (2010) 144-150.
[334] I. Kazane, K. Gorgy, C. Gondran, N. Spinelli, A. Zazoua, E. Defrancq, S. Cosnier, Highly sensitive bisphenol-A electrochemical aptasensor based on poly (pyrrole-nitrilotriacetic acid)-aptamer film, Anal. Chem. 88 (2016) 7268-7273.
[335] D.-N. Pei, A.-Y. Zhang, X.-Q. Pan, Y. Si, H.-Q. Yu, Electrochemical sensing of bisphenol a on facet-tailored TiO_2 single crystals engineered by inorganic-framework molecular imprinting sites, Anal. Chem. 90 (2018) 3165-3173.
[336] A. Thamilselvan, V. Rajagopal, V. Suryanarayanan, Highly sensitive and selective amperometric determination of BPA on carbon black/f-MWCNT composite modified GCE, J. Alloys Compds.786 (2019) 698-706.
[337] Ş. Ulubay Karabiberoğlu, Sensitive voltammetric determination of bisphenol A based on a glassy carbon electrode modified with copper oxide-zinc oxide decorated on graphene oxide, Electroanalysis, 31 (2019) 91-102.
[338] L. Hu, C.-C. Fong, X. Zhang, L.L. Chan, P.K. Lam, P.K. Chu, K.-Y. Wong, M. Yang, Au nanoparticles decorated TiO2 nanotube arrays as a recyclable sensor for photoenhanced electrochemical detection of bisphenol A, Env. Sci. Tech. 50 (2016) 4430-4438.

[339] X. Li, C. Li, C. Wu, K. Wu, Strategy for highly sensitive electrochemical sensing: in situ coupling of a metal–organic framework with ball-mill-exfoliated graphene, Anal. Chem. 91 (2019) 6043-6050.
[340] A. Derbalah, S. El-Safty, M. Shenashen, N.A. Ghany, Mesocage collector cavities as nanopockets for remediation and real assessment of carbamate pesticides in aquatic water, Nano-Structures & Nano-Objects, 3 (2015) 17-27.
[341] A. Derbalah, S.A. El-Safty, M.A. Shenashen, N.A.A. Ghany, Mesoporous alumina nanoparticles as host tunnel-like pores for removal and recovery of insecticides from environmental samples, ChemPlusChem, 80 (2015) 1119.
[342] A. Derbalah, S.A. El-Safty, M.A. Shenashen, M. Khairy, Hierarchical nanohexagon ceramic sheet layers as platform adsorbents for hydrophilic and hydrophobic insecticides from agricultural wastewater, ChemPlusChem, 80 (2015) 1769-1778.
[343] A. Derbalah, M. Shenashen, A. Hamza, A. Mohamed, S. El Safty, Toxicity of some metal oxides nanoparticles on male rats with respect to biochemical and histological changes, Int. J. Adv. Res. Biol. Sci, 4 (2017) 68-75.
[344] M.-L. Xu, Y. Gao, X.X. Han, B. Zhao, Detection of pesticide residues in food using surface-enhanced Raman spectroscopy: a review, J. Agric. Food Chem. 65 (2017) 6719-6726.
[345] M.-L. Xu, J.-B. Liu, J. Lu, Determination and control of pesticide residues in beverages: a review of extraction techniques, chromatography, and rapid detection methods, Appl. Spectrosc. Rev. 49 (2014) 97-120.
[346] E. Watanabe, S. Miyake, Y. Yogo, Review of enzyme-linked immunosorbent assays (ELISAs) for analyses of neonicotinoid insecticides in agro-environments, J. Agric. Food Chem. 61 (2013) 12459-12472.
[347] J.V. Rohit, H. Basu, R.K. Singhal, S.K. Kailasa, Development of p-nitroaniline dithiocarbamate capped gold nanoparticles-based microvolume UV–vis spectrometric method for facile and selective detection of quinalphos insecticide in environmental samples, Sens. Actuators B: Chem. 237 (2016) 826-835.
[348] R. Bala, M. Kumar, K. Bansal, R.K. Sharma, N. Wangoo, Ultrasensitive aptamer biosensor for malathion detection based on cationic polymer and gold nanoparticles, Biosens. Bioelectron. 85 (2016) 445-449.
[349] E.P. Hoppmann, W.Y. Wei, I.M. White, Highly sensitive and flexible inkjet printed SERS sensors on paper, Meth. 63 (2013) 219-224.

[350] Y. Qian, G. Meng, Q. Huang, C. Zhu, Z. Huang, K. Sun, B. Chen, Flexible membranes of Ag-nanosheet-grafted polyamide-nanofibers as effective 3D SERS substrates, Nanoscale, 6 (2014) 4781-4788.
[351] J. Chen, Y. Huang, P. Kannan, L. Zhang, Z. Lin, J. Zhang, T. Chen, L. Guo, Flexible and adhesive surface enhance Raman scattering active tape for rapid detection of pesticide residues in fruits and vegetables, Anal. Chem. 88 (2016) 2149-2155.
[352] C.-L. Lee, C.-H. Chen, C.-W. Chen, Graphene nanosheets as ink particles for inkjet printing on flexible board, Chem. Eng. J. 230 (2013) 296-302.
[353] B. Li, L. Yu, J. Qi, L. Fu, P. Zhang, L. Chen, Controlling capillary-driven fluid transport in paper-based microfluidic devices using a movable valve, Anal. Chem. 89 (2017) 5707-5712.
[354] Y. Ma, Y. Wang, Y. Luo, H. Duan, D. Li, H. Xu, E.K. Fodjo, Rapid and sensitive on-site detection of pesticide residues in fruits and vegetables using screen-printed paper-based SERS swabs, Anal. Meth. 10 (2018) 4655-4664.
[355] E.H. Koh, C. Mun, C. Kim, S.-G. Park, E.J. Choi, S.H. Kim, J. Dang, J. Choo, J.-W. Oh, D.-H. Kim, M13 bacteriophage/silver nanowire surface-enhanced raman scattering sensor for sensitive and selective pesticide detection, ACS Appl. Mater. Interfaces, 10 (2018) 10388-10397.
[356] M. Lee, K. Oh, H.-K. Choi, S.G. Lee, H.J. Youn, H.L. Lee, D.H. Jeong, Subnanomolar sensitivity of filter paper-based SERS sensor for pesticide detection by hydrophobicity change of paper surface, ACS Sensors, 3 (2018) 151-159.
[357] G.-H. Yao, R.-P. Liang, C.-F. Huang, Y. Wang, J.-D. Qiu, Surface plasmon resonance sensor based on magnetic molecularly imprinted polymers amplification for pesticide recognition, Anal. Chem. 85 (2013) 11944-11951.
[358] H. Borah, S. Gogoi, S. Kalita, P. Puzari, A broad spectrum amperometric pesticide biosensor based on glutathione S-transferase immobilized on graphene oxide-gelatin matrix, J. Electroanal. Chem. 828 (2018) 116-123.
[359] M.B. Colovic, D.Z. Krstic, T.D. Lazarevic-Pasti, A.M. Bondzic, V.M. Vasic, Acetylcholinesterase inhibitors: pharmacology and toxicology, Current Neuropharmacol. 11 (2013) 315-335.
[360] B. McGleenon, K. Dynan, A. Passmore, Acetylcholinesterase inhibitors in Alzheimer's disease, British J. Clin. Pharmacol. 48 (1999) 471.

[361] M.K. da Silva, H.C. Vanzela, L.M. Defavari, I. Cesarino, Determination of carbamate pesticide in food using a biosensor based on reduced graphene oxide and acetylcholinesterase enzyme, Sens. Actuators B: Chem. 277 (2018) 555-561.
[362] D. Song, Y. Li, X. Lu, M. Sun, H. Liu, G. Yu, F. Gao, Palladium-copper nanowires-based biosensor for the ultrasensitive detection of organophosphate pesticides, Anal. Chim. Acta, 982 (2017) 168-175.
[363] L. Zhou, X. Zhang, L. Ma, J. Gao, Y. Jiang, Acetylcholinesterase/chitosan-transition metal carbides nanocomposites-based biosensor for the organophosphate pesticides detection, Bioch. Eng. J. 128 (2017) 243-249.
[364] X. Lu, L. Tao, D. Song, Y. Li, F. Gao, Bimetallic Pd@Au nanorods based ultrasensitive acetylcholinesterase biosensor for determination of organophosphate pesticides, Sens. Actuators B: Chem.255 (2018) 2575-2581.
[365] W. Cheng, Z. Zheng, J. Yang, M. Chen, Q. Yao, Y. Chen, W. Gao, The visible light-driven and self-powered photoelectrochemical biosensor for organophosphate pesticides detection based on nitrogen doped carbon quantum dots for the signal amplification, Electrochim. Acta, 296 (2019) 627-636.
[366] C. Sahub, T. Tuntulani, T. Nhujak, B. Tomapatanaget, Effective biosensor based on graphene quantum dots via enzymatic reaction for directly photoluminescence detection of organophosphate pesticide, Sens. Actuators B: Chem. 258 (2018) 88-97.
[367] Q. Lang, L. Han, C. Hou, F. Wang, A. Liu, A sensitive acetylcholinesterase biosensor based on gold nanorods modified electrode for detection of organophosphate pesticide, Talanta, 156 (2016) 34-41.
[368] A.I. Dar, S. Walia, A. Acharya, Citric acid-coated gold nanoparticles for visual colorimetric recognition of pesticide dimethoate, J. Nanoparticle Res.18 (2016) 233.
[369] N. Chen, H. Liu, Y. Zhang, Z. Zhou, W. Fan, G. Yu, Z. Shen, A. Wu, A colorimetric sensor based on citrate-stabilized AuNPs for rapid pesticide residue detection of terbuthylazine and dimethoate, Sens. Actuators B: Chem. 255 (2018) 3093-3101.
[370] M. Sedki, R.Y. Hassan, A. Hefnawy, I.M. El-Sherbiny, Sensing of bacterial cell viability using nanostructured bioelectrochemical system: rGO-hyperbranched chitosan nanocomposite as a novel microbial sensor platform, Sens. Actuators B: Chem. 252 (2017) 191-200.

[371] D. Song, H. Liu, Q. Dong, Z. Bian, H. Wu, Y. Lei, Digital, Rapid, Accurate, and Label-Free Enumeration of Viable Microorganisms Enabled by Custom-Built On-Glass-Slide Culturing Device and Microscopic Scanning, Sensors, 18 (2018) 3700.
[372] S.O. Kim, S.S. Kim, Bacterial pathogen detection by conventional culture-based and recent alternative (polymerase chain reaction, isothermal amplification, enzyme linked immunosorbent assay, bacteriophage amplification, and gold nanoparticle aggregation) methods in food samples: A review, J. Food Safety, (2020) e12870.
[373] N. Farzad, S. Opper, K. Taisma, E.S. Kirkor, A. Senejani, S.K. Sinha, Highly Selective Bionanosensor for Quick Detection of Bacterial Pathogens in Food, Bioph. J.116 (2019) 316a.
[374] M. Ruiz-Rico, É. Pérez-Esteve, A. Bernardos, F. Sancenón, R. Martínez-Máñez, M.D. Marcos, J.M. Barat, Enhanced antimicrobial activity of essential oil components immobilized on silica particles, Food Chem.233 (2017) 228-236.
[375] A. Yamagishi, K. Tanabe, M. Yokokawa, Y. Morimoto, M. Kinoshita, H. Suzuki, Microfluidic device coupled with a microfabricated oxygen electrode for the measurement of bactericidal activity of neutrophil-like cells, Anal. Chim. Acta, 985 (2017) 1-6.
[376] A.M. Azzam, M.A. Shenashen, B.B. Mostafa, W.A. Kandeel, S.A. El-Safty, Antibacterial Activity of Magnesium Oxide Nano-hexagonal Sheets for Wastewater Remediation, Env. Prog. Sust. En. 38 (2019) S260-S266.
[377] A.M. Azzam, M.A. Shenashen, M.M. Selim, A.S. Alamoudi, S.A. El-Safty, Hexagonal Mg (OH) 2 nanosheets as antibacterial agent for treating contaminated water sources, ChemistrySelect, 2 (2017) 11431-11437.
[378] P.W. van der Wielen, D. van der Kooij, Effect of water composition, distance and season on the adenosine triphosphate concentration in unchlorinated drinking water in the Netherlands, Water Res. 44 (2010) 4860-4867.
[379] Y. Shinozaki, Y. Harada, Rapid detection of bacteria in green tea using a novel pretreatment method in a bioluminescence assay, J. Food protection, 77 (2014) 941-947.
[380] R.S. Santos, N. Guimarães, P. Madureira, N.F. Azevedo, Optimization of a peptide nucleic acid fluorescence in situ hybridization (PNA-FISH) method for the detection of bacteria and disclosure of a formamide effect, J. Biotech. 187 (2014) 16-24.
[381] J.Y. Park, M.-C. Lim, K. Park, G. Ok, H.-J. Chang, N. Lee, T.J. Park, S.-W. Choi, Detection of E. coli O157: H7 in Food Using Automated Immunomagnetic Separation Combined with Real-Time PCR, Processes, 8 (2020) 908.

[382] Y. Wang, Z. Ye, C. Si, Y. Ying, Monitoring of Escherichia coli O157: H7 in food samples using lectin based surface plasmon resonance biosensor, Food Chem. 136 (2013) 1303-1308.
[383] R.B. Jamal, S. Shipovskov, E.E. Ferapontova, Electrochemical Immuno-and Aptamer-Based Assays for Bacteria: Pros and Cons over Traditional Detection Schemes, Sensors, 20 (2020) 5561.
[384] W. Wu, J. Li, D. Pan, J. Li, S. Song, M. Rong, Z. Li, J. Gao, J. Lu, Gold nanoparticle-based enzyme-linked antibody-aptamer sandwich assay for detection of Salmonella Typhimurium, ACS Appl. Mater. Interfaces, 6 (2014) 16974-16981.
[385] L. Wang, Q. Liu, Z. Hu, Y. Zhang, C. Wu, M. Yang, P. Wang, A novel electrochemical biosensor based on dynamic polymerase-extending hybridization for E. coli O157: H7 DNA detection, Talanta, 78 (2009) 647-652.
[386] O. Tokel, U.H. Yildiz, F. Inci, N.G. Durmus, O.O. Ekiz, B. Turker, C. Cetin, S. Rao, K. Sridhar, N. Natarajan, Portable microfluidic integrated plasmonic platform for pathogen detection, Sci. Rep.5 (2015) 1-9.
[387] G.C. Shi, M.L. Wang, Y.Y. Zhu, L. Shen, W.L. Ma, Y.H. Wang, R.F. Li, Dragonfly wing decorated by gold nanoislands as flexible and stable substrates for surface-enhanced Raman scattering (SERS), Sci. Rep. 8 (2018) 1-11.
[388] B. Højris, S.C.B. Christensen, H.-J. Albrechtsen, C. Smith, M. Dahlqvist, A novel, optical, on-line bacteria sensor for monitoring drinking water quality, Scientific reports, 6 (2016) 23935.
[389] M. Yu, L. Wu, T. Huang, S. Wang, X. Yan, Rapid detection and enumeration of total bacteria in drinking water and tea beverages using a laboratory-built high-sensitivity flow cytometer, Anal. Meth. 7 (2015) 3072-3079.
[390] R.L. Phillips, O.R. Miranda, C.C. You, V.M. Rotello, U.H. Bunz, Rapid and efficient identification of bacteria using gold-nanoparticle–poly (para-phenyleneethynylene) constructs, Ang. Chem. Int. Ed. 47 (2008) 2590-2594.
[391] B. Duncan, N.D. Le, C. Alexander, A. Gupta, G. Yesilbag Tonga, M. Yazdani, R.F. Landis, L.-S. Wang, B. Yan, S. Burmaoglu, Sensing by Smell: Nanoparticle–Enzyme Sensors for Rapid and Sensitive Detection of Bacteria with Olfactory Output, ACS Nano, 11 (2017) 5339-5343.
[392] Y. Sun, L. Fang, Y. Wan, Z. Gu, Pathogenic detection and phenotype using magnetic nanoparticle-urease nanosensor, Sens. Actuators B: Chem. 259 (2018) 428-432.
[393] Y. Wan, Y. Sun, P. Qi, P. Wang, D. Zhang, Quaternized magnetic nanoparticles–fluorescent polymer system for detection and identification of bacteria, Biosens. Bioelectron. 55 (2014) 289-293.

[394] A.J. Hall, Noroviruses: the perfect human pathogens?, Oxford University Press, 2012.
[395] L. Liu, M.D. Moore, A survey of analytical techniques for noroviruses, Foods, 9 (2020) 318.
[396] J. Vinjé, Advances in laboratory methods for detection and typing of norovirus, J. Clin. Microb., 53 (2015) 373-381.
[397] V. Velusamy, K. Arshak, O. Korostynska, K. Oliwa, C. Adley, An overview of foodborne pathogen detection: In the perspective of biosensors, Biotech. Adv. 28 (2010) 232-254.
[398] P. Arora, A. Sindhu, H. Kaur, N. Dilbaghi, A. Chaudhury, An overview of transducers as platform for the rapid detection of foodborne pathogens, Appl. Microb. Biotech. 97 (2013) 1829-1840.
[399] J. Guo, D. Liu, Z. Yang, W. Weng, E.W.C. Chan, Z. Zeng, K.-Y. Wong, P. Lin, S. Chen, A photoelectrochemical biosensor for rapid and ultrasensitive norovirus detection, Bioelectrochem. 136 (2020) 107591.
[400] S. Chung, L.E. Breshears, A. Gonzales, C.M. Jennings, C.M. Morrison, W.Q. Betancourt, K.A. Reynolds, J.-Y. Yoon, Norovirus detection in water samples at the level of single virus copies per microliter using a smartphone-based fluorescence microscope, Nat. Protocols, 16 (2021) 1452-1475.
[401] H.A. Alhadrami, S. Al-Amer, Y. Aloraij, F. Alhamlan, R. Chinnappan, K.M. Abu-Salah, S. Almatrrouk, M.M. Zourob, Development of a Simple, Fast, and Cost-Effective Nanobased Immunoassay Method for Detecting Norovirus in Food Samples, ACS Omega, 5 (2020) 12162-12165.
[402] I.M. Khoris, K. Takemura, J. Lee, T. Hara, F. Abe, T. Suzuki, E.Y. Park, Enhanced colorimetric detection of norovirus using in-situ growth of Ag shell on Au NPs, Biosens. Bioelectron. 126 (2019) 425-432.
[403] J. Lee, M. Morita, K. Takemura, E.Y. Park, A multi-functional gold/iron-oxide nanoparticle-CNT hybrid nanomaterial as virus DNA sensing platform, Biosens. Bioelectron. 102 (2018) 425-431.
[404] S.H. Baek, M.W. Kim, C.Y. Park, C.-S. Choi, S.K. Kailasa, J.P. Park, T.J. Park, Development of a rapid and sensitive electrochemical biosensor for detection of human norovirus via novel specific binding peptides, Biosens. Bioelectron.123 (2019) 223-229.
[405] S.A. Hong, J. Kwon, D. Kim, S. Yang, A rapid, sensitive and selective electrochemical biosensor with concanavalin A for the preemptive detection of norovirus, Biosens. Bioelectron. 64 (2015) 338-344.

[406] S. Hirano, J. Saito, T. Yukawa, D. Sano, A. Okamoto, S. Okabe, M. Kitajima, Improvement of Electrochemical Conditions for Detecting Redox Reaction of $K_3[Fe(CN)_6]$ toward the Application in Norovirus Aptasensor, Electrochemistry, 88 (2020) 205-209.
[407] A. Giamberardino, M. Labib, E.M. Hassan, J.A. Tetro, S. Springthorpe, S.A. Sattar, M.V. Berezovski, M.C. DeRosa, Ultrasensitive norovirus detection using DNA aptasensor technology, PLoS One, 8 (2013) e79087-e79087.
[408] T. Azad, S. Ahmed, Common milk adulteration and their detection techniques, Int. J. Food Contamination, 3 (2016) 1-9.
[409] H. Xin, R. Stone, Chinese probe unmasks high-tech adulteration with melamine, Scie. 322 (2008) 1310-1311.
[410] J.S. Garcia, G.B. Sanvido, S.A. Saraiva, J.J. Zacca, R.G. Cosso, M.N. Eberlin, Bovine milk powder adulteration with vegetable oils or fats revealed by MALDI-QTOF MS, Food Chem. 131 (2012) 722-726.
[411] C. Kolar, I. Cho, W. Watrous, Vegetable protein application in yogurt, coffee creamers and whip toppings, Journal of the American Oil Chemists' Society, 56 (1979) 389-391.
[412] P.F. Scholl, S.M. Farris, M.M. Mossoba, Rapid turbidimetric detection of milk powder adulteration with plant proteins, J. Agric. Food Chem. 62 (2014) 1498-1505.
[413] R. Sanchez-Monge, G. Lopez-Torrejón, C. Pascual, J. Varela, M. Martin-Esteban, G. Salcedo, Vicilin and convicilin are potential major allergens from pea, Clin. Exp. Allergy, 34 (2004) 1747-1753.
[414] D. Dawson, J. Morrill, P. Reddy, H. Minocha, H. Ramsey, Soy protein concentrate and heated soy flours as protein sources in milk replacer for preruminant calves, J. Dairy Sci. 71 (1988) 1301-1309.
[415] L. Sánchez, M.D. Pérez, P. Puyol, M. Calvo, G. Brett, Collaborators:, Determination of Vegetal Proteins in Milk Powder by Enzyme-Linked Immunosorbent Assay: Interlaboratory Study, J. AOAC INT. 85 (2019) 1390-1397.
[416] J.E. Jablonski, J.C. Moore, J.M. Harnly, Nontargeted Detection of Adulteration of Skim Milk Powder with Foreign Proteins Using UHPLC–UV, J.Agric. Food Chem. 62 (2014) 5198-5206.
[417] R. Siciliano, B. Rega, A. Amoresano, P. Pucci, Modern mass spectrometric methodologies in monitoring milk quality, Anal. Chem.72 (2000) 408-415.
[418] I. Recio, M.-L. Pérez-Rodríguez, M. Ramos, L. Amigo, Capillary electrophoretic analysis of genetic variants of milk proteins from different species, J. Chromatog. A, 768 (1997) 47-56.

[419] F. Gustavsson, A.J. Buitenhuis, M. Johansson, H.P. Bertelsen, M. Glantz, N.A. Poulsen, H. Lindmark Månsson, H. Stålhammar, L.B. Larsen, C. Bendixen, M. Paulsson, A. Andrén, Effects of breed and casein genetic variants on protein profile in milk from Swedish Red, Danish Holstein, and Danish Jersey cows, J. Dairy Sci. 97 (2014) 3866-3877.
[420] I.P. Hurley, R.C. Coleman, H.E. Ireland, J.H. Williams, Measurement of bovine IgG by indirect competitive ELISA as a means of detecting milk adulteration, J. Dairy Sci. 87 (2004) 543-549.
[421] J. Bania, M. Ugorski, A. Polanowski, E. Adamczyk, Application of polymerase chain reaction for detection of goats' milk adulteration by milk of cow, Jo. Dairy Res.68 (2001) 333-336.
[422] I. López-Calleja, I. González, V. Fajardo, M. Rodriguez, P. Hernandez, T. García, R. Martín, Rapid detection of cows' milk in sheeps' and goats' milk by a species-specific polymerase chain reaction technique, J. Dairy Sci. 87 (2004) 2839-2845.
[423] C. Maudet, P. Taberlet, Detection of cows' milk in goats' cheeses inferred from mitochondrial DNA polymorphism, J. Dairy Res. 68 (2001) 229-235.
[424] M.T. Bottero, T. Civera, A. Anastasio, R.M. Turi, S. Rosati, Identification of cow's milk in "buffalo" cheese by duplex polymerase chain reaction, J. Food protection, 65 (2002) 362-366.
[425] A. Sroor, N.W. el-Dine, A. el-Shershaby, A.S. Abdel-Haleem, Major and trace elemental analysis in milk powder by inductively coupled plasma-optical emission spectrometry (ICP-OES) and instrumental neutron activation analysis (INAA), Journal of environmental sciences (China), 15 (2003) 570-576.
[426] M.L. Astolfi, E. Marconi, C. Protano, S. Canepari, Comparative elemental analysis of dairy milk and plant-based milk alternatives, Food Control, 116 (2020) 107327.
[427] T. Hoffman, R. Jaćimović, L.J. Bay, J. Griboff, M. Jagodic, M. Monferrán, N. Ogrinc, I. Podkolzin, D. Wunderlin, J. Almirall, Development of a method for the elemental analysis of milk powders using laser ablation-inductively coupled plasma-mass spectrometry (LA-ICP-MS) and its potential use in geographic sourcing, Talanta, 186 (2018) 670-677.
[428] A. Kim, S.J. Barcelo, R.S. Williams, Z. Li, Melamine sensing in milk products by using surface enhanced Raman scattering, Anal. Chem. 84 (2012) 9303-9309.
[429] R. Wei, R. Wang, Q. Zeng, M. Chen, T. Liu, High-performance liquid chromatographic method for the determination of cyromazine and melamine residues in milk and pork, J. Chromatog. Sci. 47 (2009) 581-584.

[430] T.-H. Tsai, S. Thiagarajan, S.-M. Chen, Detection of melamine in milk powder and human urine, J. Agric. Food Chem. 58 (2010) 4537-4544.
[431] X. Dai, X. Fang, F. Su, M. Yang, H. Li, J. Zhou, R. Xu, Accurate analysis of urea in milk and milk powder by isotope dilution gas chromatography–mass spectrometry, J. Chromatog. B, 878 (2010) 1634-1638.
[432] K. Ai, Y. Liu, L. Lu, Hydrogen-bonding recognition-induced color change of gold nanoparticles for visual detection of melamine in raw milk and infant formula, J. Am.Chem. Soc.131 (2009) 9496-9497.
[433] Y. Cheng, Y. Dong, J. Wu, X. Yang, H. Bai, H. Zheng, D. Ren, Y. Zou, M. Li, Screening melamine adulterant in milk powder with laser Raman spectrometry, J. Food Comp. Anal. 23 (2010) 199-202.
[434] P. O'mahony, Finding horse meat in beef products—a global problem, QJM: Int. J. Medicine, 106 (2013) 595-597.
[435] Y.C. Li, S.Y. Liu, F.B. Meng, D.Y. Liu, Y. Zhang, W. Wang, J.M. Zhang, Comparative review and the recent progress in detection technologies of meat product adulteration, Comprehensive Reviews in Food Science and Food Safety, 19 (2020) 2256-2296.
[436] J. Ha, S. Kim, J. Lee, S. Lee, H. Lee, Y. Choi, H. Oh, Y. Yoon, Identification of Pork Adulteration in Processed Meat Products Using the Developed Mitochondrial DNA-Based Primers, Korean J Food Sci Anim Resour, 37 (2017) 464-468.
[437] M.E. Ali, M.A. Razzak, S.B. Abd Hamid, M.M. Rahman, M. Al Amin, N.R. Abd Rashid, Multiplex PCR assay for the detection of five meat species forbidden in Islamic foods, Food Chem. 177 (2015) 214-224.
[438] W. Wang, J. Liu, Q. Zhang, X. Zhou, B. Liu, Multiplex PCR assay for identification and quantification of bovine and equine in minced meats using novel specific nuclear DNA sequences, Food Control, 105 (2019) 29-37.
[439] M.M. Hossain, M.E. Ali, S.B. Abd Hamid, S. Mustafa, M.N. Mohd Desa, I. Zaidul, Double gene targeting multiplex polymerase chain reaction–restriction fragment length polymorphism assay discriminates beef, buffalo, and pork substitution in frankfurter products, J. Agric. Food Chem. 64 (2016) 6343-6354.
[440] M.E. Ali, M.N.U. Ahamad, M.M. Hossain, S. Sultana, Multiplex polymerase chain reaction-restriction fragment length polymorphism assay discriminates of rabbit, rat and squirrel meat in frankfurter products, Food Control, 84 (2018) 148-158.

[441] M.M. Hossain, M.E. Ali, S.B. Abd Hamid, S. Mustafa, M.N.M. Desa, I. Zaidul, Targeting double genes in multiplex PCR for discriminating bovine, buffalo and porcine materials in food chain, Food Control, 73 (2017) 175-184.
[442] H. Li, R. Bai, Z. Zhao, L. Tao, M. Ma, Z. Ji, M. Jian, Z. Ding, X. Dai, F. Bao, Application of droplet digital PCR to detect the pathogens of infectious diseases, Biosc. Rep.38 (2018) BSR20181170.
[443] N. Seddaoui, A. Amine, A sensitive colorimetric immunoassay based on poly (dopamine) modified magnetic nanoparticles for meat authentication, LWT, 122 (2020) 109045.
[444] C.P. Thienes, J. Masiri, L.A. Benoit, B. Barrios-Lopez, S.A. Samuel, D.P. Cox, A.P. Dobritsa, C. Nadala, M. Samadpour, Quantitative Detection of Pork Contamination in Cooked Meat Products by ELISA, J.AOAC INT.101 (2019) 810-816.
[445] J. Mandli, I. El Fatimi, N. Seddaoui, A. Amine, Enzyme immunoassay (ELISA/immunosensor) for a sensitive detection of pork adulteration in meat, Food Chem. 255 (2018) 380-389.
[446] M.Y. Emran, M.A. Shenashen, S.A. El-Safty, A. Reda, M.M. Selim, Microporous P-doped carbon spheres sensory electrode for voltammetry and amperometry adrenaline screening in human fluids, Microchim. Acta, 188 (2021) 138.
[447] M.Y. Emran, M.A. Shenashen, S.A. El-Safty, M.M. Selim, Design of porous S-doped carbon nanostructured electrode sensor for sensitive and selective detection of guanine from DNA samples, Microp. Mesop. Mater. 320 (2021) 111097.
[448] M.Y. Emran, E. Talat, S.A. El-Safty, M.A. Shenashen, E.M. Saad, Influence of hollow sphere surface heterogeneity and geometry of N-doped carbon on sensitive monitoring of acetaminophen in human fluids and pharmaceutical products, New J. Chem. 45 (2021) 5452-5462.
[449] S.A. Lim, M.U. Ahmed, A label free electrochemical immunosensor for sensitive detection of porcine serum albumin as a marker for pork adulteration in raw meat, Food Chem.206 (2016) 197-203.
[450] M. Mansouri, B. Khalilzadeh, A. Barzegari, S. Shoeibi, S. Isildak, N. Bargahi, Y. Omidi, S. Dastmalchi, M.-R. Rashidi, Design a highly specific sequence for electrochemical evaluation of meat adulteration in cooked sausages, Biosens. Bioelectron. 150 (2020) 111916.
[451] A.V. Mohan, J.R. Windmiller, R.K. Mishra, J. Wang, Continuous minimally-invasive alcohol monitoring using microneedle sensor arrays, Biosens. Bioelectron. 91 (2017) 574-579.

[452] W. Roberts, S.A. McKee, Mobile alcohol biosensors and pharmacotherapy development research, Alcohol, 81 (2019) 149-160.
[453] P.C. Pandey, S. Shukla, S.A. Skoog, R.D. Boehm, R.J. Narayan, Current advancements in transdermal biosensing and targeted drug delivery, Sensors, 19 (2019) 1028.
[454] N. Kummer, W.E. Lambert, N. Samyn, C.P. Stove, Alternative sampling strategies for the assessment of alcohol intake of living persons, Clin. Biochem. 49 (2016) 1078-1091.
[455] M. Gamella, S. Campuzano, J. Manso, G.G. de Rivera, F. López-Colino, A. Reviejo, J. Pingarrón, A novel non-invasive electrochemical biosensing device for in situ determination of the alcohol content in blood by monitoring ethanol in sweat, Anal. Chim. Acta, 806 (2014) 1-7.
[456] A. Martín, J. Kim, J.F. Kurniawan, J.R. Sempionatto, J.R. Moreto, G. Tang, A.S. Campbell, A. Shin, M.Y. Lee, X. Liu, Epidermal microfluidic electrochemical detection system: Enhanced sweat sampling and metabolite detection, ACS sensors, 2 (2017) 1860-1868.
[457] J.R. Sempionatto, L.C. Brazaca, L. García-Carmona, G. Bolat, A.S. Campbell, A. Martin, G. Tang, R. Shah, R.K. Mishra, J. Kim, Eyeglasses-based tear biosensing system: Non-invasive detection of alcohol, vitamins and glucose, Biosens. Bioelectron.137 (2019) 161-170.
[458] A. Economou, C. Kokkinos, M. Prodromidis, Flexible plastic, paper and textile lab-on-a chip platforms for electrochemical biosensing, Lab on a Chip, 18 (2018) 1812-1830.
[459] J. Kim, Wearable Electrochemical Biosensors for Healthcare Monitoring Applications, UC San Diego, 2018.
[460] A.P. Selvam, S. Muthukumar, V. Kamakoti, S. Prasad, A wearable biochemical sensor for monitoring alcohol consumption lifestyle through Ethyl glucuronide (EtG) detection in human sweat, Scie. Rep. 6 (2016) 23111.
[461] K. Churski, A. Ruszczak, S. Jakiela, P. Garstecki, Droplet microfluidic technique for the study of fermentation, Micromachines, 6 (2015) 1514-1525.
[462] J. Kim, I. Jeerapan, S. Imani, T.N. Cho, A. Bandodkar, S. Cinti, P.P. Mercier, J. Wang, Noninvasive alcohol monitoring using a wearable tattoo-based iontophoretic-biosensing system, ACS Sensors, 1 (2016) 1011-1019.
[463] H. Zhu, U. Sikora, A. Ozcan, Quantum dot enabled detection of Escherichia coli using a cell-phone, Analyst, 137 (2012) 2541-2544.
[464] S.K. Ludwig, H. Zhu, S. Phillips, A. Shiledar, S. Feng, D. Tseng, L.A. van Ginkel, M.W. Nielen, A. Ozcan, Cellphone-based detection platform for rbST biomarker analysis in milk extracts using a microsphere fluorescence immunoassay, Anal. Bioanal. Chem. 406 (2014) 6857-6866.

[465] A.F. Coskun, J. Wong, D. Khodadadi, R. Nagi, A. Tey, A. Ozcan, A personalized food allergen testing platform on a cellphone, Lab on a Chip, 13 (2013) 636-640.
[466] G.F. Giordano, M.B. Vicentini, R.C. Murer, F. Augusto, M.F. Ferrão, G.A. Helfer, A.B. da Costa, A.L. Gobbi, L.W. Hantao, R.S. Lima, Point-of-use electroanalytical platform based on homemade potentiostat and smartphone for multivariate data processing, Electrochim. Acta, 219 (2016) 170-177.
[467] X.-Y. Xu, B. Yan, X. Lian, Wearable glove sensor for non-invasive organophosphorus pesticide detection based on a double-signal fluorescence strategy, Nanoscale, 10 (2018) 13722-13729.
[468] P. Wang, L. Wu, Z. Lu, Q. Li, W. Yin, F. Ding, H. Han, Gecko-inspired nanotentacle surface-enhanced Raman spectroscopy substrate for sampling and reliable detection of pesticide residues in fruits and vegetables, Anal. Chem. 89 (2017) 2424-2431.
[469] J. Kim, S. Imani, W.R. de Araujo, J. Warchall, G. Valdés-Ramírez, T.R. Paixão, P.P. Mercier, J. Wang, Wearable salivary uric acid mouthguard biosensor with integrated wireless electronics, Biosens. Bioelectron. 74 (2015) 1061-1068.
[470] P. Kassal, J. Kim, R. Kumar, W.R. de Araujo, I.M. Steinberg, M.D. Steinberg, J. Wang, Smart bandage with wireless connectivity for uric acid biosensing as an indicator of wound status, Electroch. Commun. 56 (2015) 6-10.

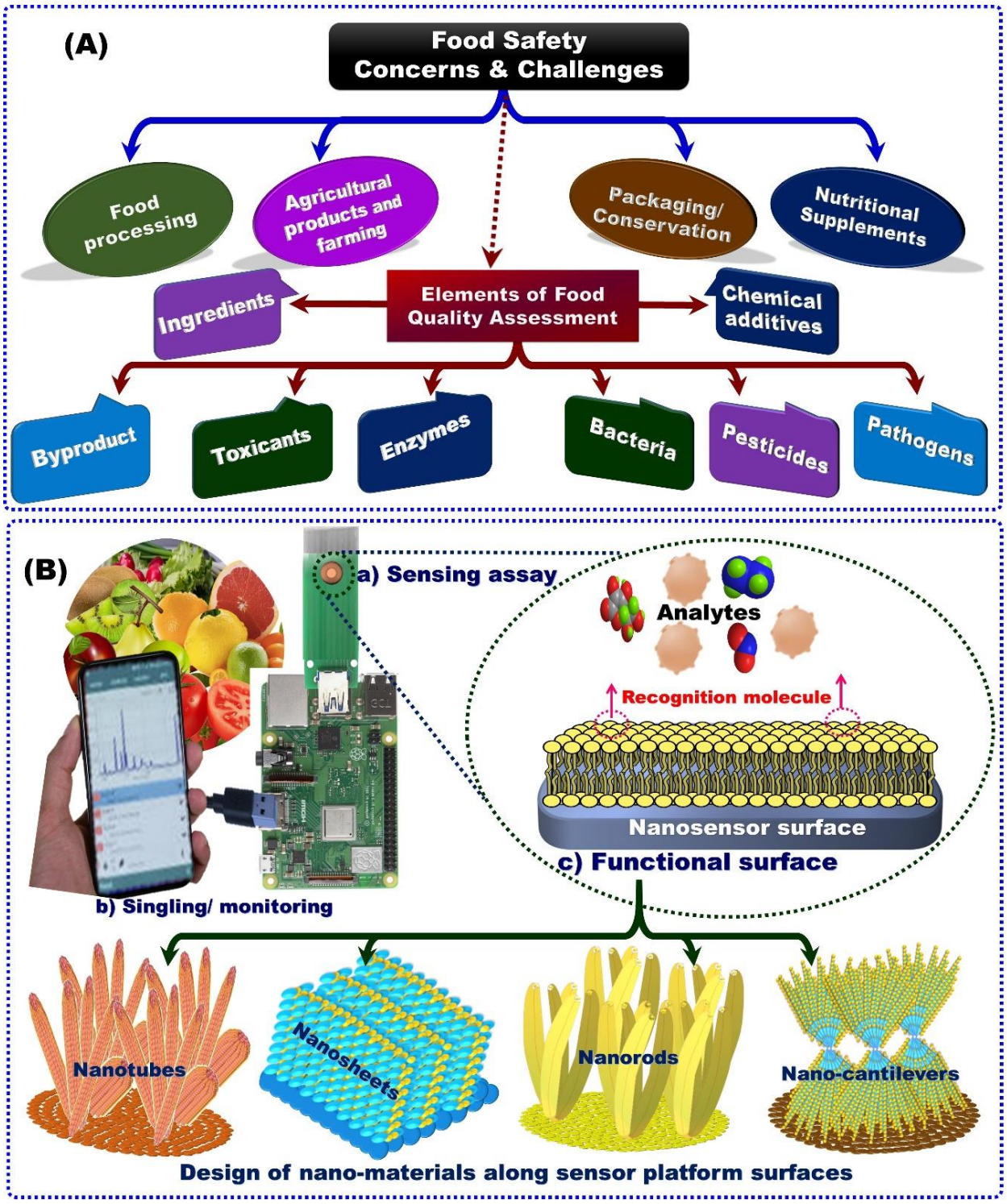
(A)
Food Safety Concerns & Challenges
Food processing
Agricultural products and farming
Packaging/ Conservation
Nutritional Supplements
Ingredients
Elements of Food Quality Assessment
Chemical additives
Byproduct
Toxicants
Enzymes
Bacteria
Pesticides
Pathogens
(B)
a) Sensing assay
Analytes
Recognition molecule
Nanosensor surface
c) Functional surface
b) Singling/ monitoring
Nanotubes
Nanosheets
Nanorods
Nano-cantilevers
Design of nano-materials along sensor platform surfaces

Scheme 1

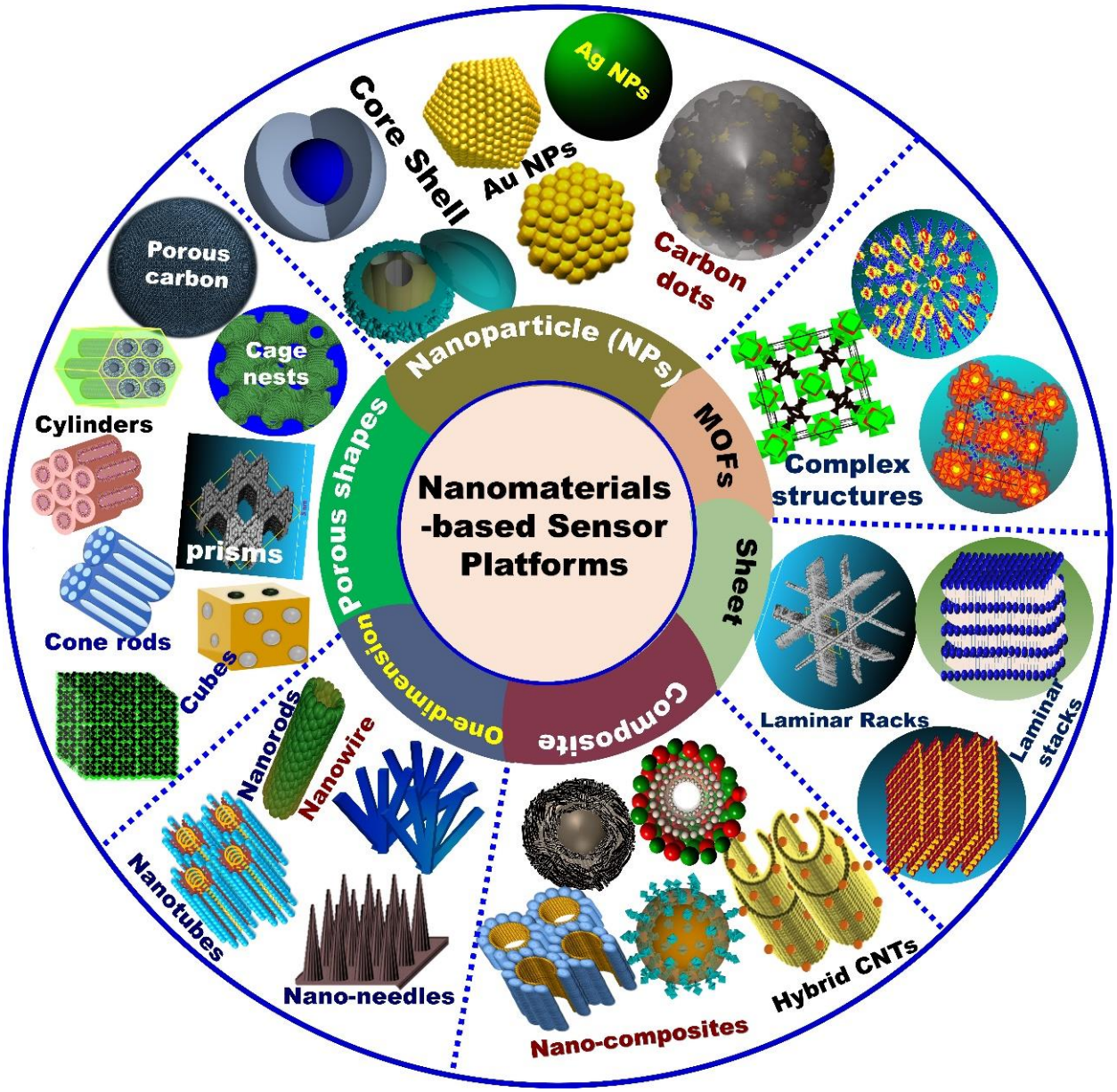
Nanomaterials -based Sensor Platforms
Nanoparticle (NPs)
MOFs
Sheet
Composite
One-dimension
Porous shapes
Core Shell
Ag NPs
Au NPs
Carbon dots
Porous carbon
Cage nests
Cylinders
prisms
Cone rods
Cubes
Nanorods
Nanowire
Nanotubes
Nano-needles
Complex structures
Laminar Racks
Laminar stacks
Hybrid CNTs
Nano-composites

Scheme 2

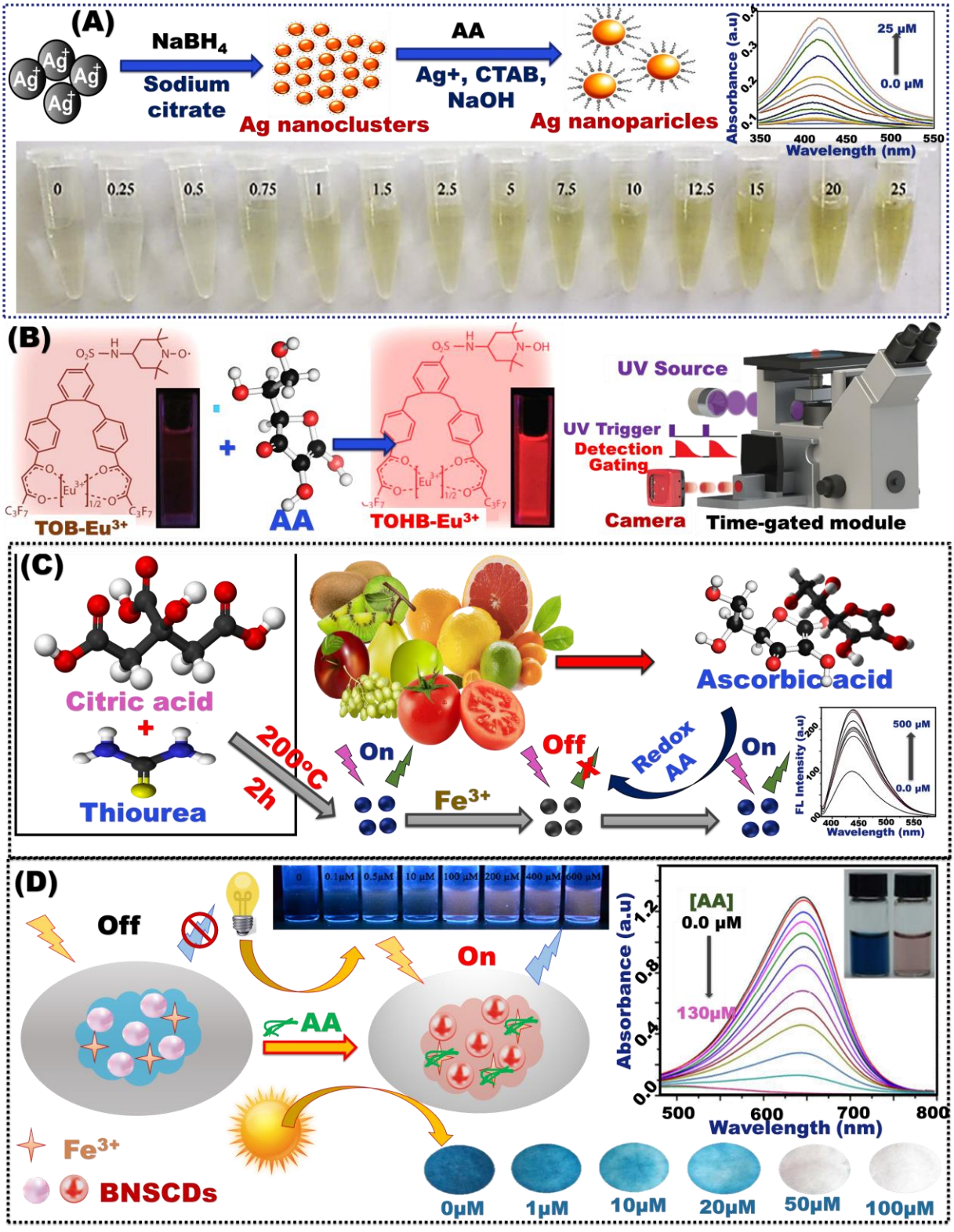
(A)
NaBH4
Sodium citrate
Ag nanoclusters
AA
Ag+, CTAB, NaOH
Ag nanoparicles
25 μM
0.0 μM
Absorbance (a.u)
Wavelength (nm)
0
0.25
0.5
0.75
1
1.5
2.5
5
7.5
10
12.5
15
20
25
(B)
TOB-Eu3+
AA
TOHB-Eu3+
UV Source
UV Trigger
Detection Gating
Camera
Time-gated module
(C)
Citric acid
Thiourea
200°C
2h
Ascorbic acid
On
Off
Fe3+
Redox AA
On
500 μM
0.0 μM
FL Intensity (a.u)
Wavelength (nm)
(D)
Off
On
AA
Fe3+
BNSCDs
[AA]
0.0 μM
130μM
Absorbance (a.u)
Wavelength (nm)
0μM
1μM
10μM
20μM
50μM
100μM

Scheme 3

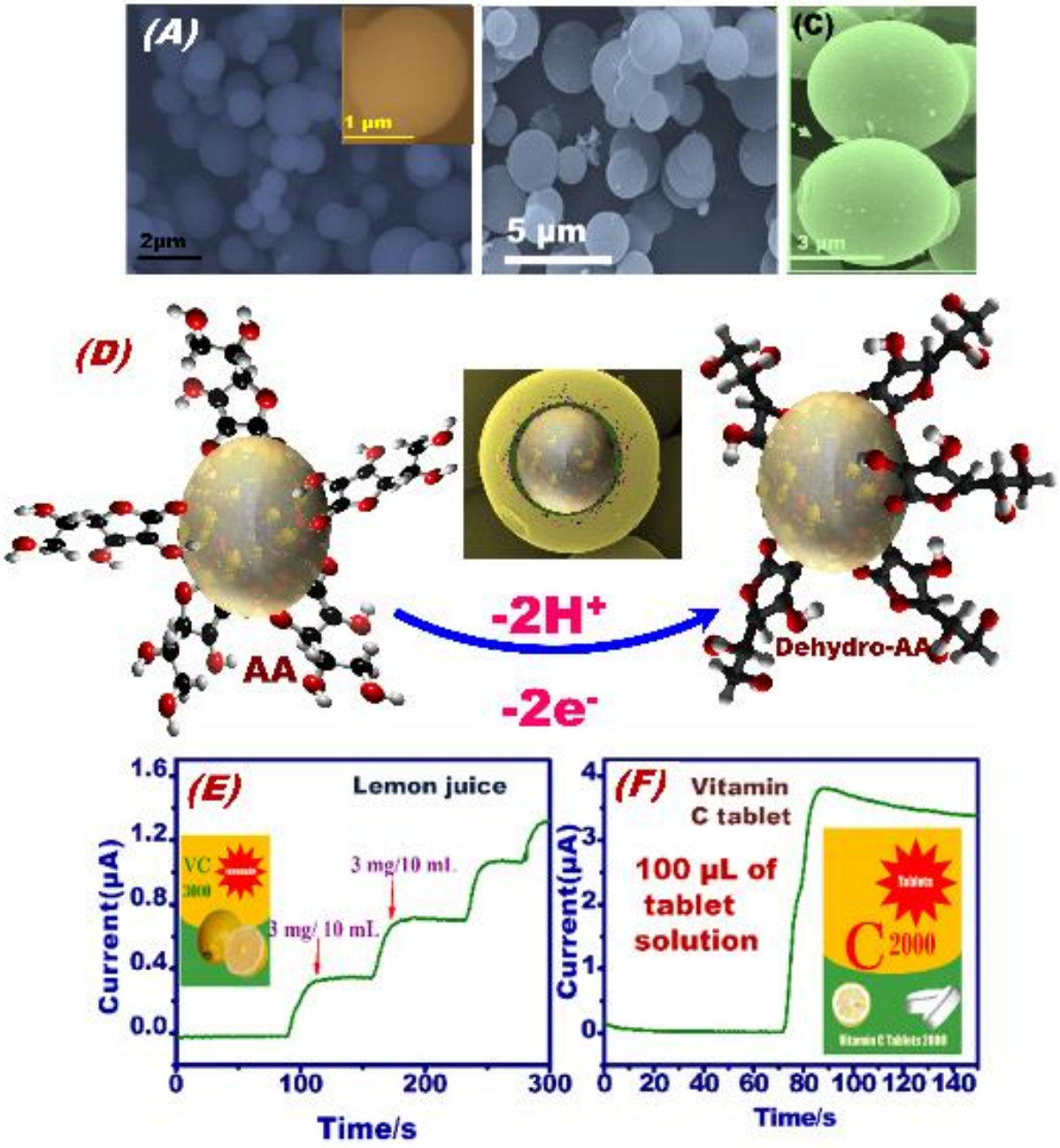
(A)
1 μm
2μm
5 μm
(C)
3 μm
(D)
AA
-2H+
-2e-
Dehydro-AA
(E)
Lemon juice
VC
3 mg/10 mL
3 mg/ 10 mL
Current(μA)
Time/s
(F)
Vitamin
C tablet
100 μL of
tablet
solution
C 2000
Current(μA)
Time/s

Scheme 4

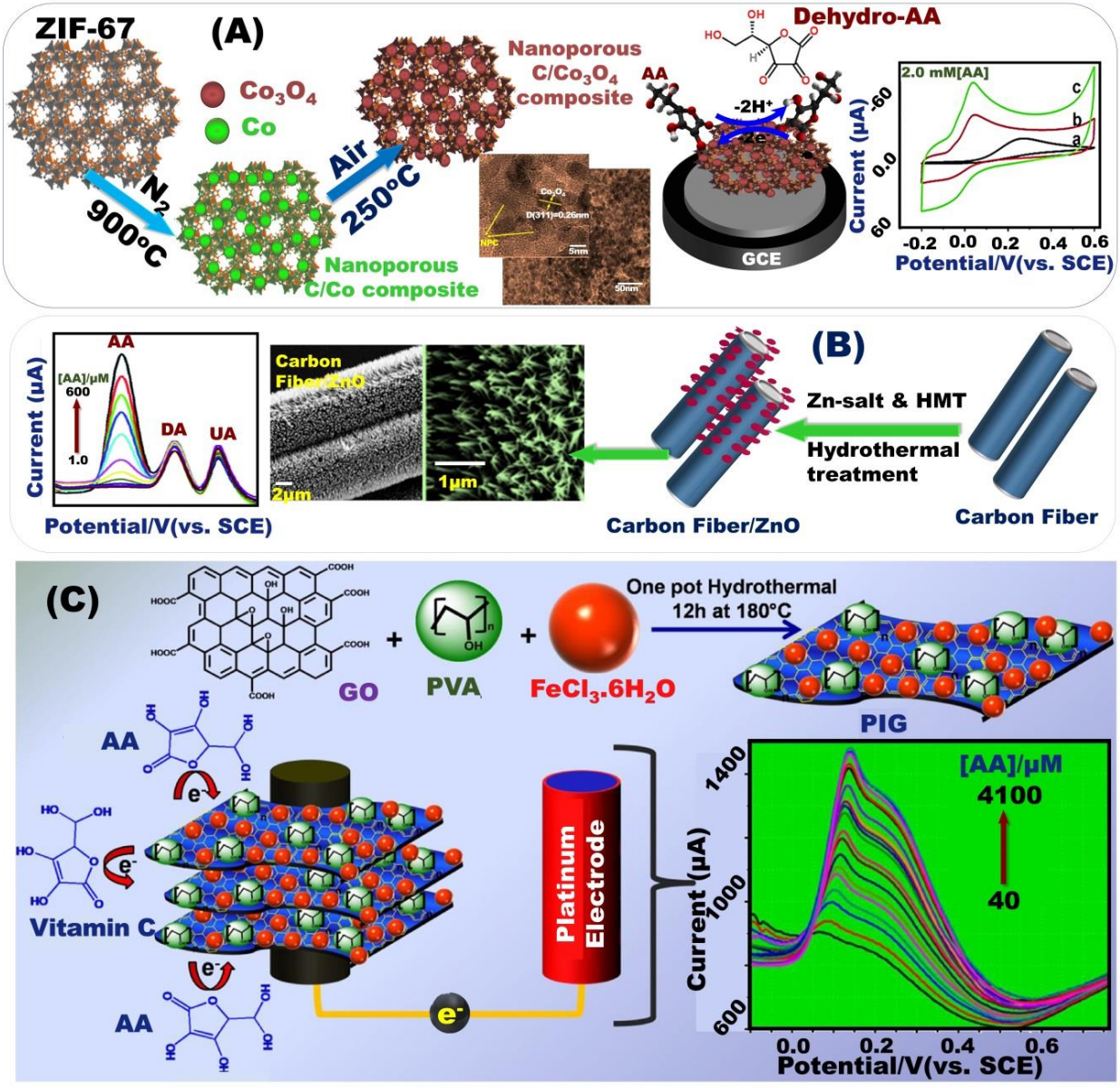
ZIF-67
(A)
Co_3O_4
Co
N_2
900°C
Air
250°C
Nanoporous C/Co composite
Nanoporous C/Co_3O_4 composite
AA
Dehydro-AA
-2H+
2e
GCE
2.0 mM[AA]
Current (μA)
Potential/V(vs. SCE)
AA
[AA]/μM
600
1.0
DA
UA
Current (μA)
Potential/V(vs. SCE)
Carbon Fiber/ZnO
2μm
1μm
(B)
Zn-salt & HMT
Hydrothermal treatment
Carbon Fiber/ZnO
Carbon Fiber
(C)
GO
PVA
$FeCl_3.6H_2O$
One pot Hydrothermal
12h at 180°C
PIG
AA
Vitamin C
AA
e-
Platinum Electrode
[AA]/μM
4100
40
Current (μA)
Potential/V(vs. SCE)

Scheme 5

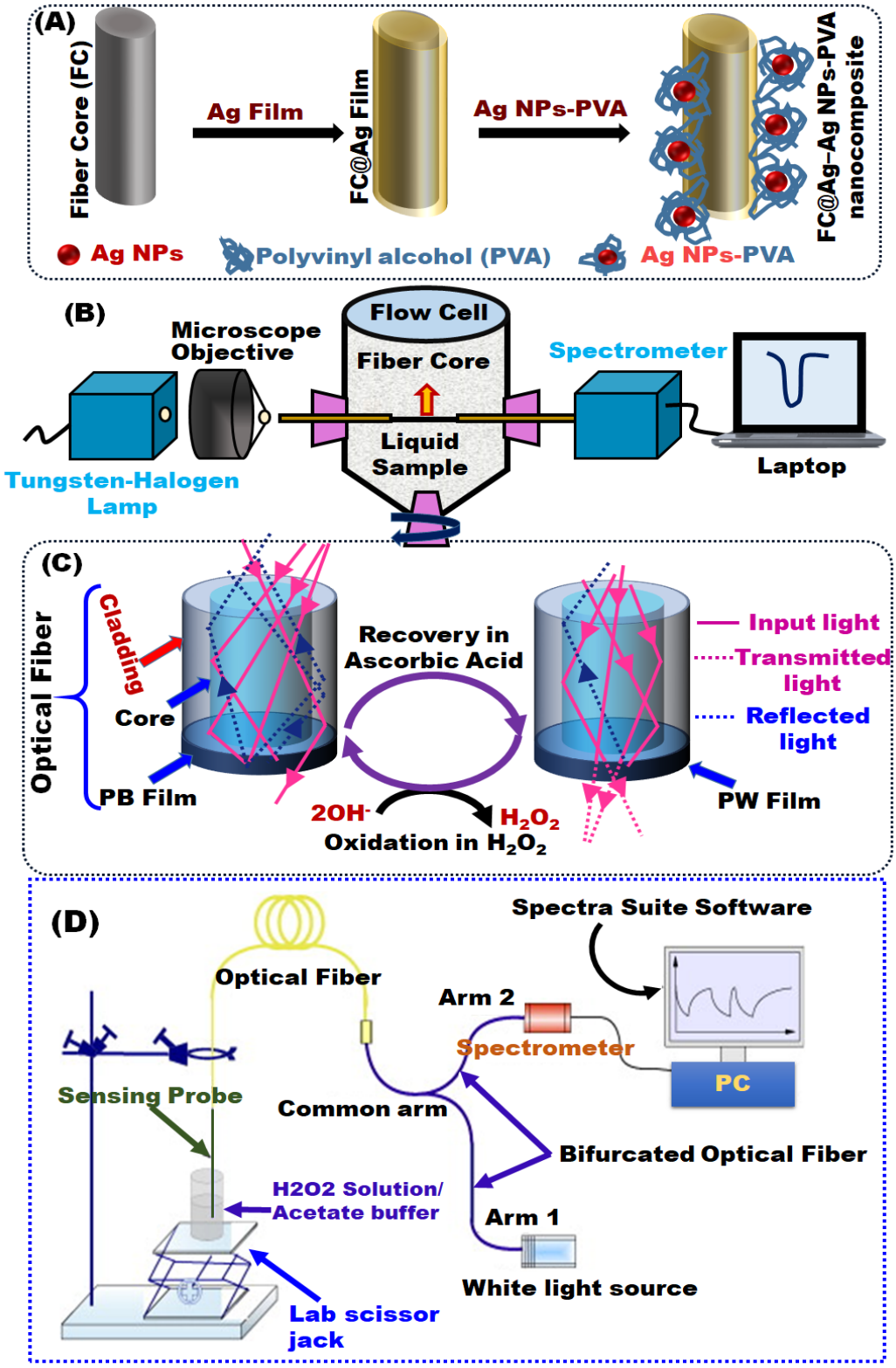
(A)
Fiber Core (FC)
Ag Film
FC@Ag Film
Ag NPs-PVA
FC@Ag–Ag NPs-PVA nanocomposite
Ag NPs
Polyvinyl alcohol (PVA)
Ag NPs-PVA
(B)
Microscope Objective
Flow Cell
Fiber Core
Liquid Sample
Spectrometer
Laptop
Tungsten-Halogen Lamp
(C)
Optical Fiber
Cladding
Core
PB Film
Recovery in Ascorbic Acid
2OH-
H2O2
Oxidation in H2O2
Input light
Transmitted light
Reflected light
PW Film
(D)
Spectra Suite Software
Optical Fiber
Arm 2
Spectrometer
PC
Sensing Probe
Common arm
Bifurcated Optical Fiber
H2O2 Solution/ Acetate buffer
Arm 1
White light source
Lab scissor jack

Scheme 6

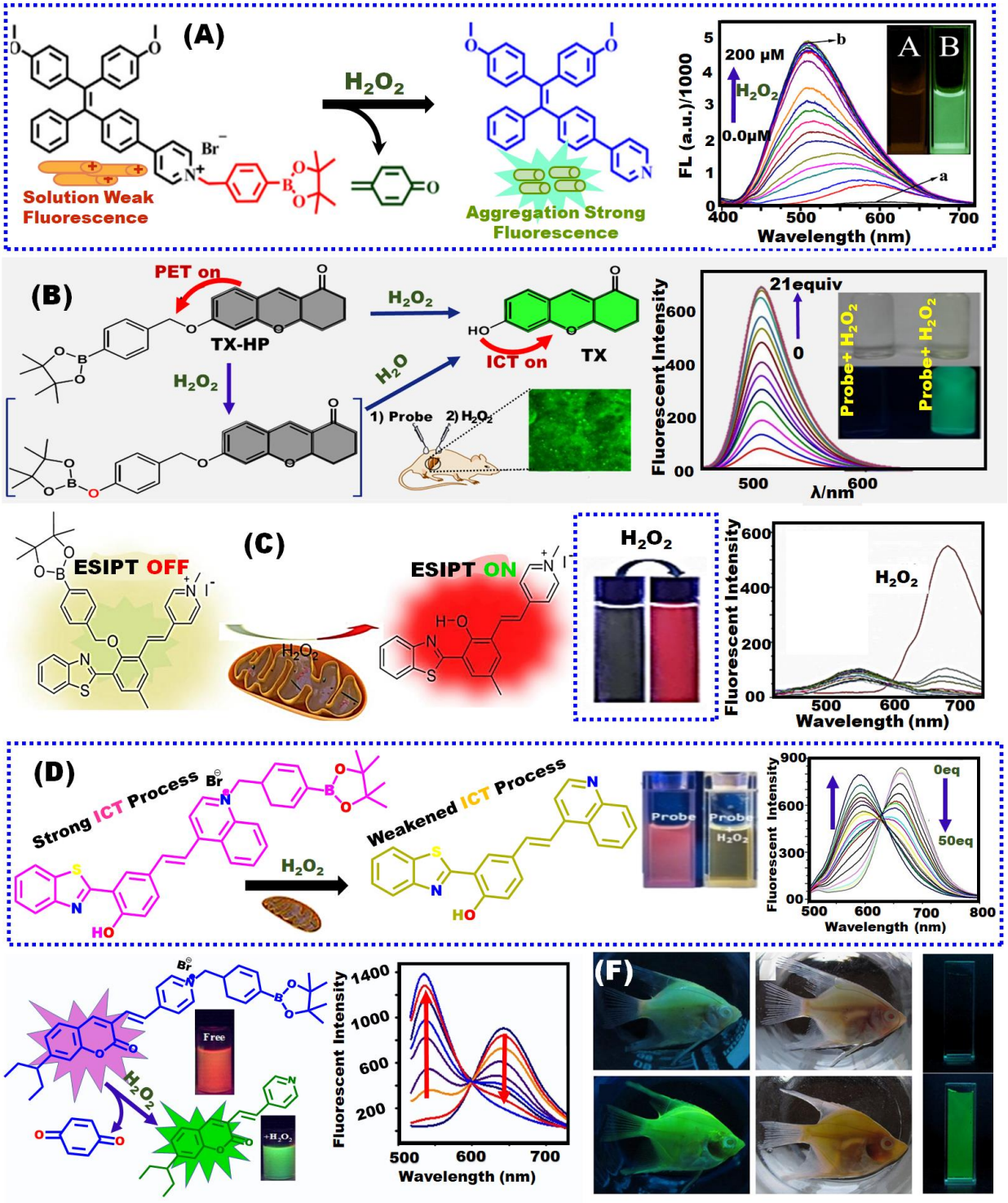
(A)
H_2O_2
Solution Weak Fluorescence
Aggregation Strong Fluorescence
200 μM
H_2O_2
0.0μM
FL (a.u.)/1000
Wavelength (nm)
A B
(B)
PET on
TX-HP
ICT on
TX
1) Probe 2) H_2O_2
21equiv
0
Probe+ H_2O_2
Fluorescent Intensity
λ/nm
(C)
ESIPT OFF
ESIPT ON
H_2O_2
Fluorescent Intensity
Wavelength (nm)
(D)
Strong ICT Process
Weakened ICT Process
Probe
Probe H_2O_2
0eq
50eq
Fluorescent Intensity
Wavelength (nm)
Free
Fluorescent Intensity
Wavelength (nm)
(F)

Scheme 7

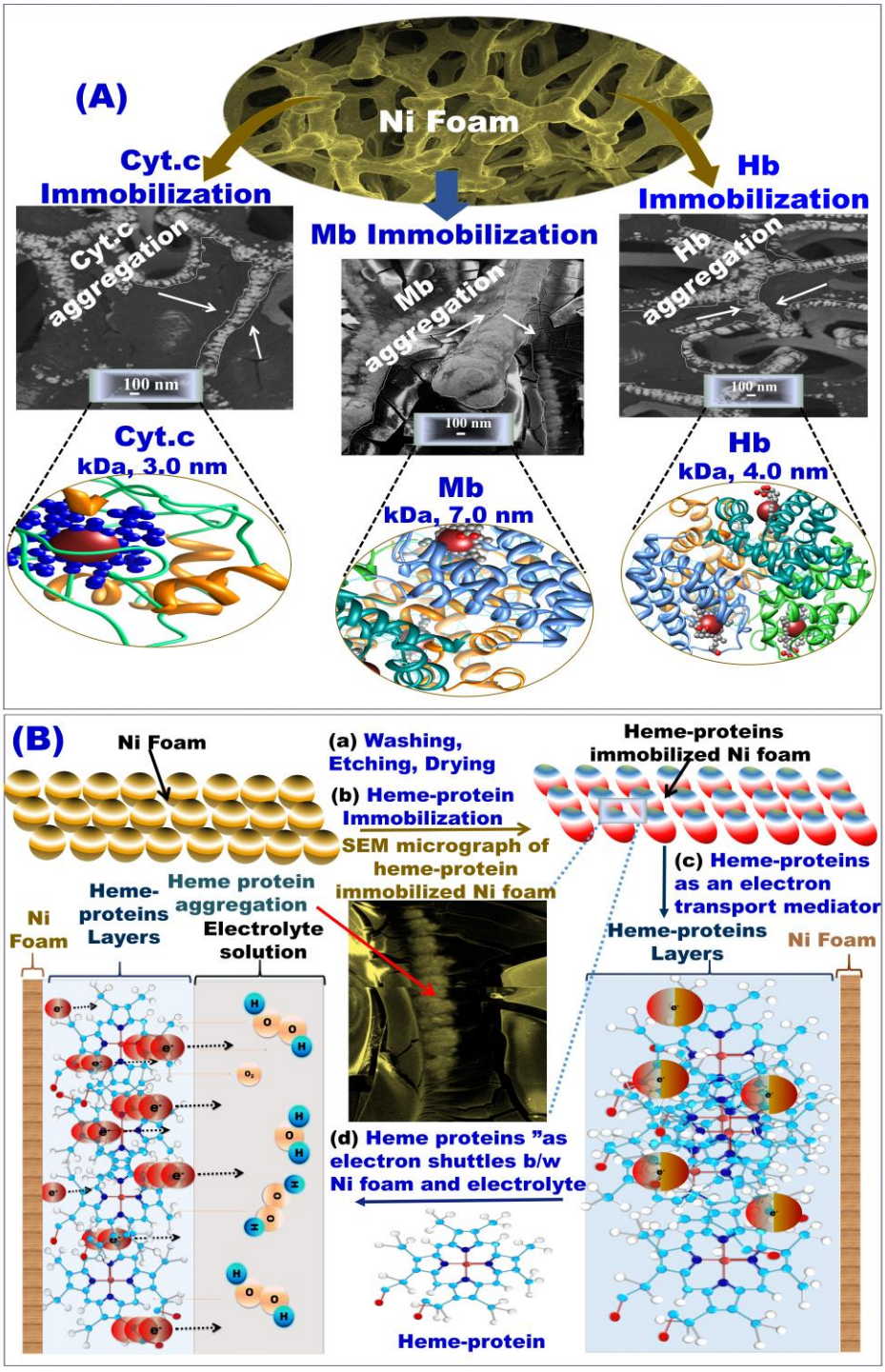
(A)
Ni Foam
Cyt.c Immobilization
Mb Immobilization
Hb Immobilization
Cyt.c aggregation
Mb aggregation
Hb aggregation
100 nm
Cyt.c
kDa, 3.0 nm
Mb
kDa, 7.0 nm
Hb
kDa, 4.0 nm
(B)
Ni Foam
(a) Washing, Etching, Drying
(b) Heme-protein Immobilization
SEM micrograph of heme-protein immobilized Ni foam
Heme-proteins immobilized Ni foam
(c) Heme-proteins as an electron transport mediator
Heme-proteins Layers
Heme protein aggregation
Electrolyte solution
Ni Foam
(d) Heme proteins "as electron shuttles b/w Ni foam and electrolyte
Heme-protein

Scheme 8

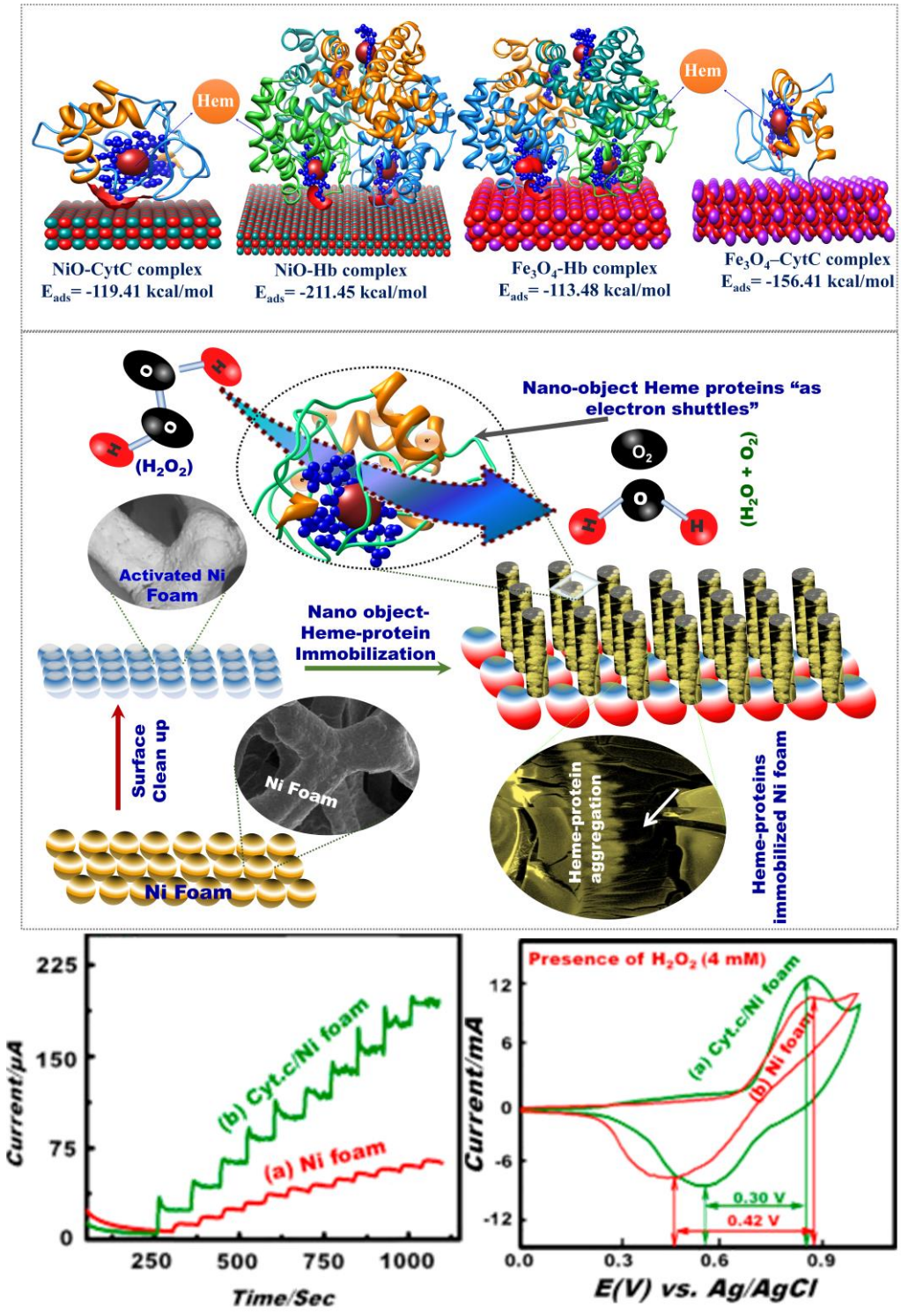
Hem
NiO-CytC complex
E_{ads}= -119.41 kcal/mol
NiO-Hb complex
E_{ads}= -211.45 kcal/mol
Fe_3O_4-Hb complex
E_{ads}= -113.48 kcal/mol
Hem
Fe_3O_4–CytC complex
E_{ads}= -156.41 kcal/mol
(H_2O_2)
Nano-object Heme proteins "as electron shuttles"
O_2
$(H_2O + O_2)$
Activated Ni Foam
Nano object-Heme-protein Immobilization
Surface Clean up
Ni Foam
Ni Foam
Heme-protein aggregation
Heme-proteins immobilized Ni foam
Current/μA
225
150
75
0
250
500
750
1000
Time/Sec
(b) Cyt.c/Ni foam
(a) Ni foam
Presence of H_2O_2 (4 mM)
Current/mA
12
6
0
-6
-12
0.0
0.3
0.6
0.9
E(V) vs. Ag/AgCl
(a) Cyt.c/Ni foam
(b) Ni foam
0.30 V
0.42 V

Scheme 9

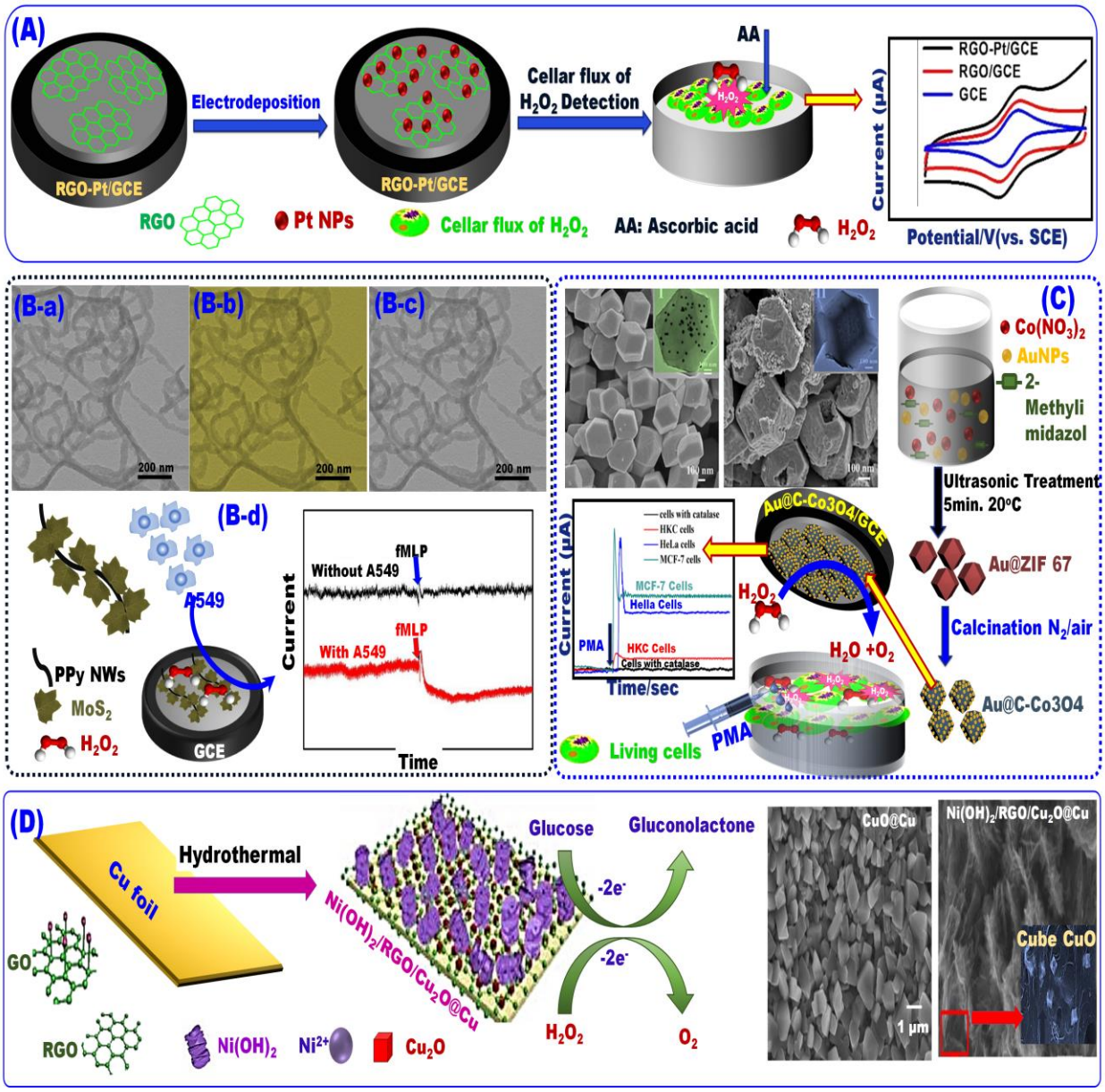
(A)
Electrodeposition
RGO-Pt/GCE
RGO-Pt/GCE
Cellar flux of H_2O_2 Detection
AA
RGO-Pt/GCE
RGO/GCE
GCE
Current (μA)
Potential/V(vs. SCE)
RGO
Pt NPs
Cellar flux of H_2O_2
AA: Ascorbic acid
H_2O_2
(B-a)
(B-b)
(B-c)
200 nm
(B-d)
A549
PPy NWs
MoS_2
H_2O_2
GCE
fMLP
Without A549
fMLP
With A549
Current
Time
(C)
$Co(NO_3)_2$
AuNPs
2-Methyli midazol
Ultrasonic Treatment 5min. 20°C
Au@ZIF 67
Calcination N_2/air
Au@C-Co3O4
Au@C-Co3O4/GCE
cells with catalase
HKC cells
HeLa cells
MCF-7 cells
MCF-7 Cells
Hella Cells
HKC Cells
Cells with catalase
PMA
Current (μA)
Time/sec
H_2O_2
$H_2O + O_2$
Living cells
PMA
(D)
Cu foil
Hydrothermal
GO
RGO
$Ni(OH)_2$
Ni^{2+}
Cu_2O
$Ni(OH)_2$/RGO/Cu_2O@Cu
Glucose
Gluconolactone
-2e⁻
-2e⁻
H_2O_2
O_2
CuO@Cu
1 μm
$Ni(OH)_2$/RGO/Cu_2O@Cu
Cube CuO

Scheme 10

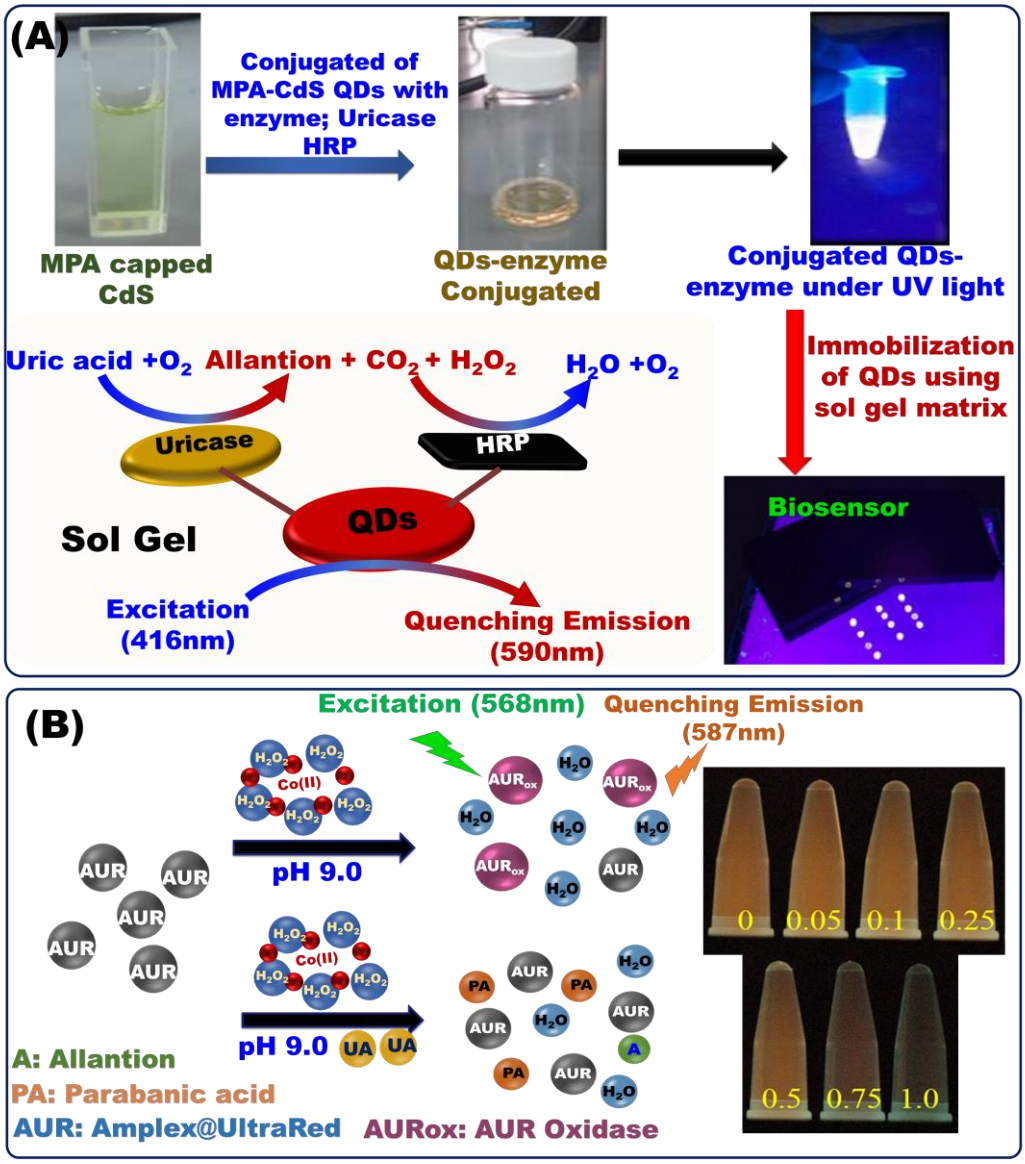
(A)
Conjugated of MPA-CdS QDs with enzyme; Uricase HRP
MPA capped CdS
QDs-enzyme Conjugated
Conjugated QDs-enzyme under UV light
Uric acid +O2
Allantion + CO2 + H2O2
H2O +O2
Uricase
HRP
QDs
Sol Gel
Excitation (416nm)
Quenching Emission (590nm)
Immobilization of QDs using sol gel matrix
Biosensor
(B)
Excitation (568nm)
Quenching Emission (587nm)
Co(II)
pH 9.0
AUR
AURox
PA
UA
A: Allantion
PA: Parabanic acid
AUR: Amplex@UltraRed
AURox: AUR Oxidase
0
0.05
0.1
0.25
0.5
0.75
1.0

Scheme 11

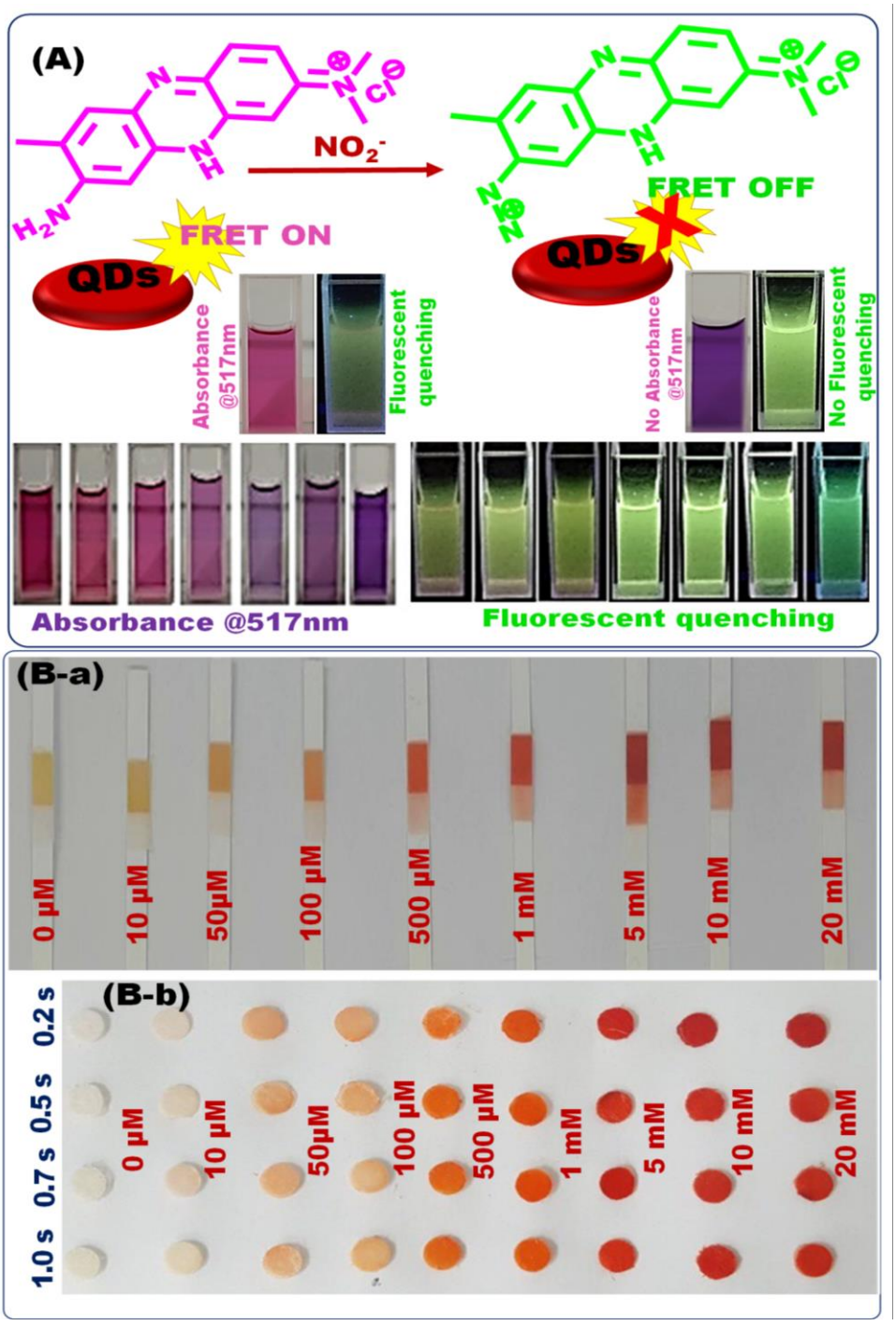
(A)
NO_2^-
FRET ON
FRET OFF
QDs
QDs
Absorbance @517nm
Fluorescent quenching
No Absorbance @517nm
No Fluorescent quenching
Absorbance @517nm
Fluorescent quenching
(B-a)
0 μM
10 μM
50μM
100 μM
500 μM
1 mM
5 mM
10 mM
20 mM
(B-b)
0.2 s
0.5 s
0.7 s
1.0 s
0 μM
10 μM
50μM
100 μM
500 μM
1 mM
5 mM
10 mM
20 mM

Scheme 12

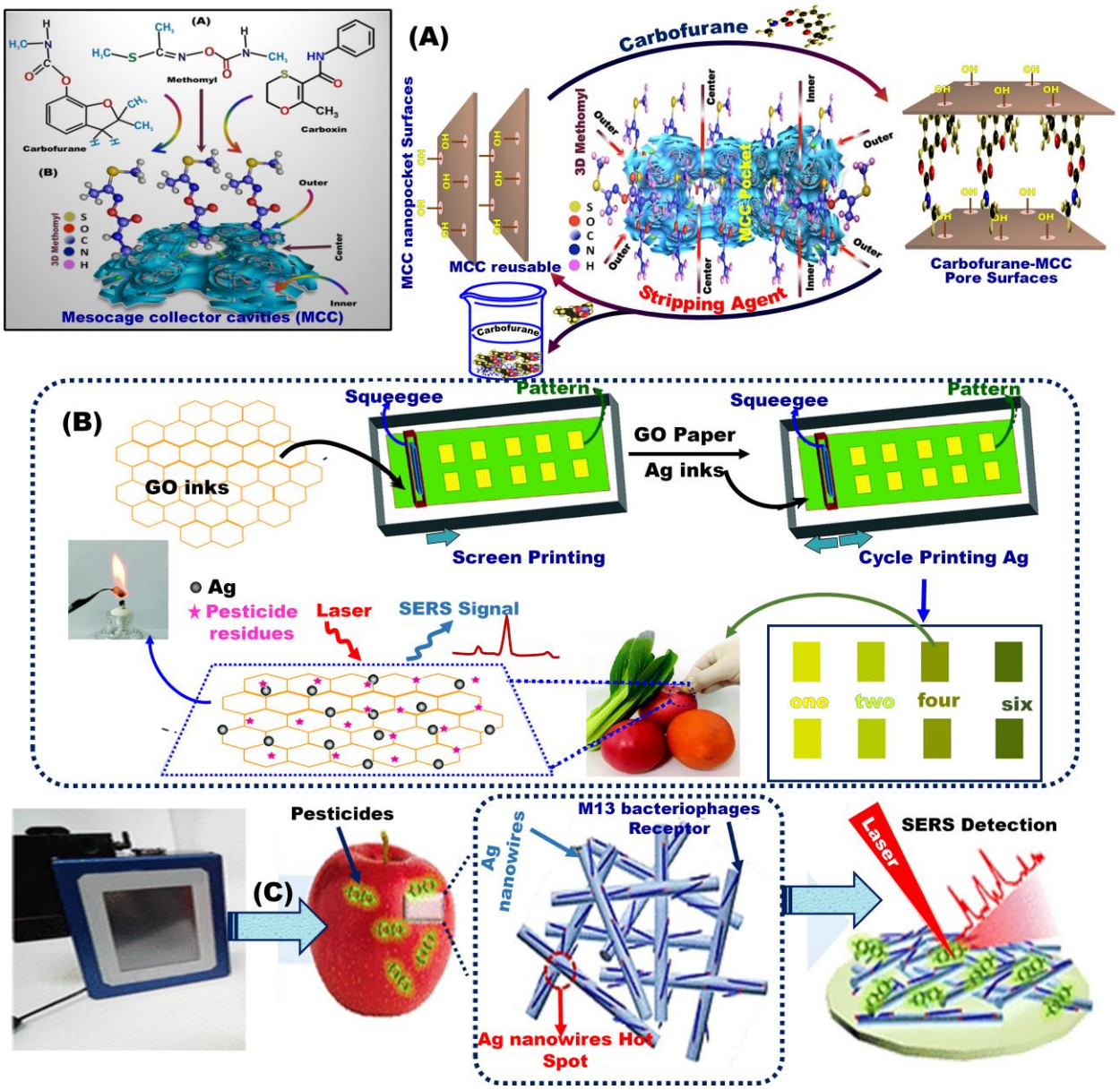
(A)
Methomyl
Carboxin
Carbofurane
(B)
Outer
Center
Inner
3D Methomyl
Mesocage collector cavities (MCC)
(A)
Carbofurane
MCC nanopocket Surfaces
MCC reusable
3D Methomyl
Outer
Center
Inner
MCC pocket
Stripping Agent
Carbofurane-MCC
Pore Surfaces
(B)
GO inks
Squeegee
Pattern
Screen Printing
GO Paper
Ag inks
Cycle Printing Ag
Ag
Pesticide residues
Laser
SERS Signal
one
two
four
six
(C)
Pesticides
M13 bacteriophages
Receptor
Ag nanowires
Ag nanowires Hot Spot
SERS Detection
Laser

Scheme 13

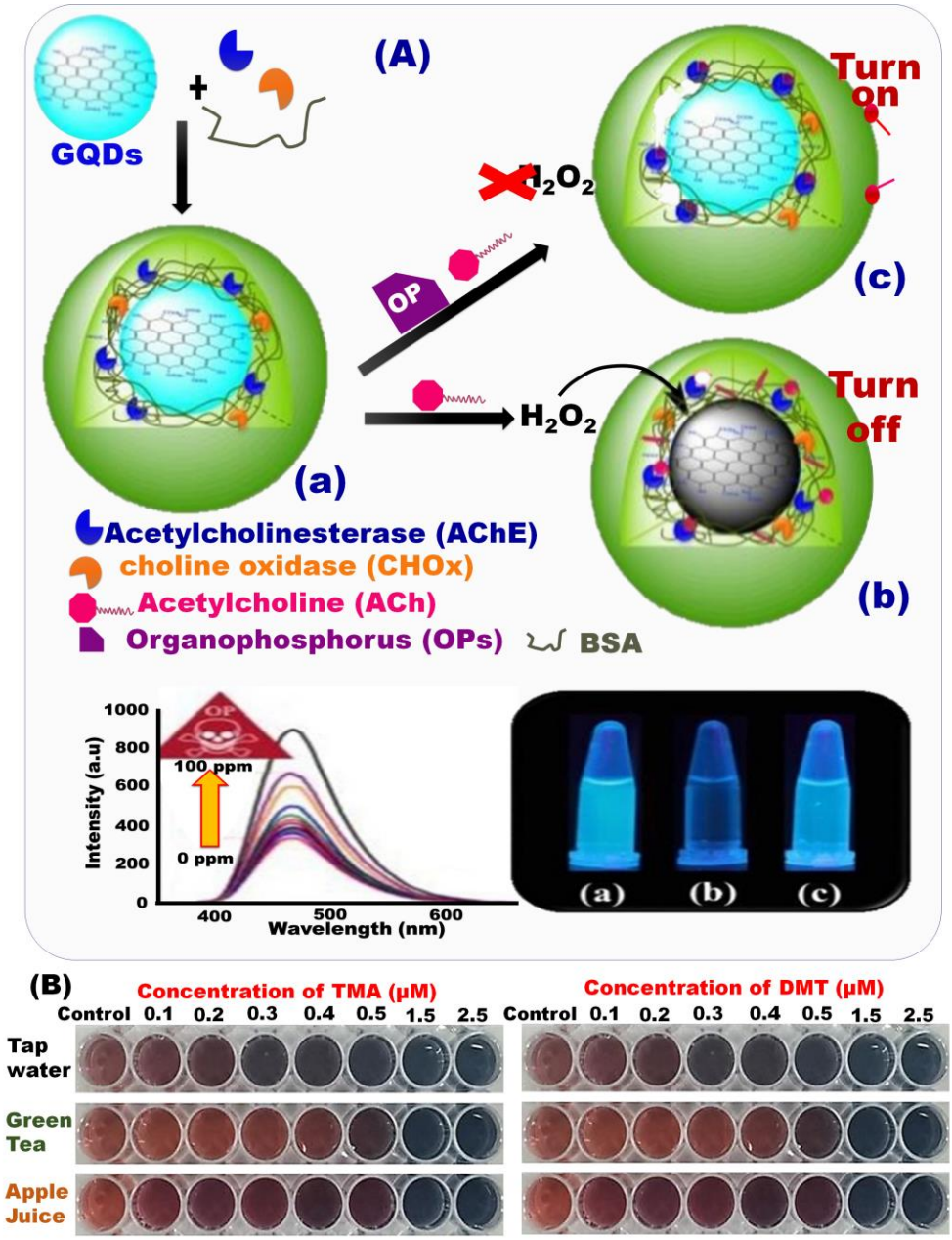
(A)
GQDs
Turn on
H_2O_2
OP
(c)
H_2O_2
Turn off
(a)
(b)
Acetylcholinesterase (AChE)
choline oxidase (CHOx)
Acetylcholine (ACh)
Organophosphorus (OPs)
BSA
Intensity (a.u)
1000
800
600
400
200
0
OP
100 ppm
0 ppm
400
500
600
Wavelength (nm)
(a)
(b)
(c)
(B)
Concentration of TMA (μM)
Concentration of DMT (μM)
Control 0.1 0.2 0.3 0.4 0.5 1.5 2.5
Control 0.1 0.2 0.3 0.4 0.5 1.5 2.5
Tap water
Green Tea
Apple Juice

Scheme 14

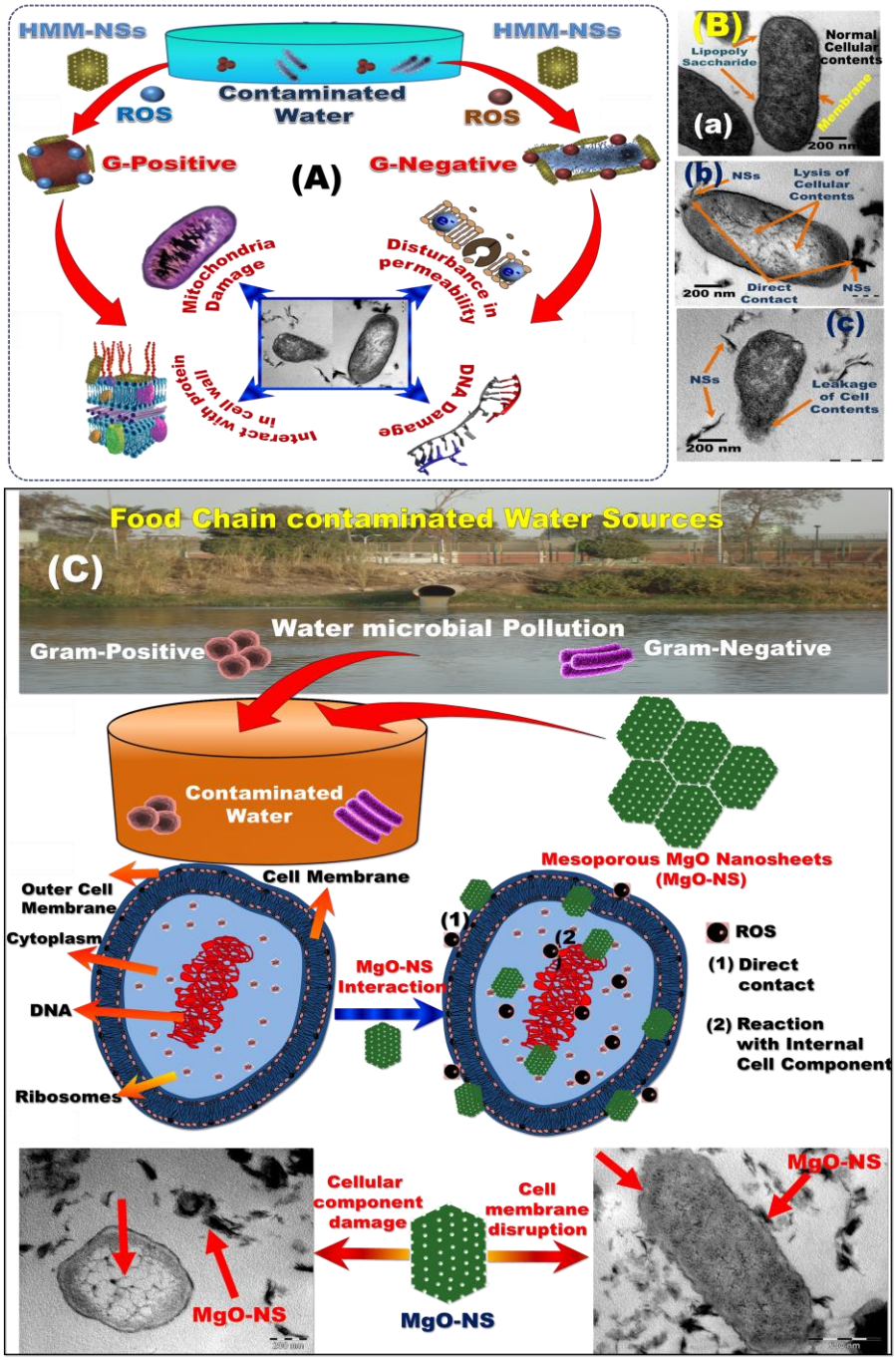
HMM-NSs
HMM-NSs
Contaminated Water
ROS
ROS
G-Positive
(A)
G-Negative
Mitochondria Damage
Disturbance in permeability
Interact with protein in cell wall
DNA Damage
(B)
Lipopoly Saccharide
Normal Cellular contents
Membrane
(a)
200 nm
(b)
NSs
Lysis of Cellular Contents
200 nm
Direct Contact
NSs
(c)
NSs
Leakage of Cell Contents
200 nm
Food Chain contaminated Water Sources
(C)
Water microbial Pollution
Gram-Positive
Gram-Negative
Contaminated Water
Outer Cell Membrane
Cell Membrane
Cytoplasm
DNA
Ribosomes
MgO-NS Interaction
Mesoporous MgO Nanosheets (MgO-NS)
(1)
(2
ROS
(1) Direct contact
(2) Reaction with Internal Cell Component
MgO-NS
Cellular component damage
Cell membrane disruption
MgO-NS
MgO-NS

Scheme 15

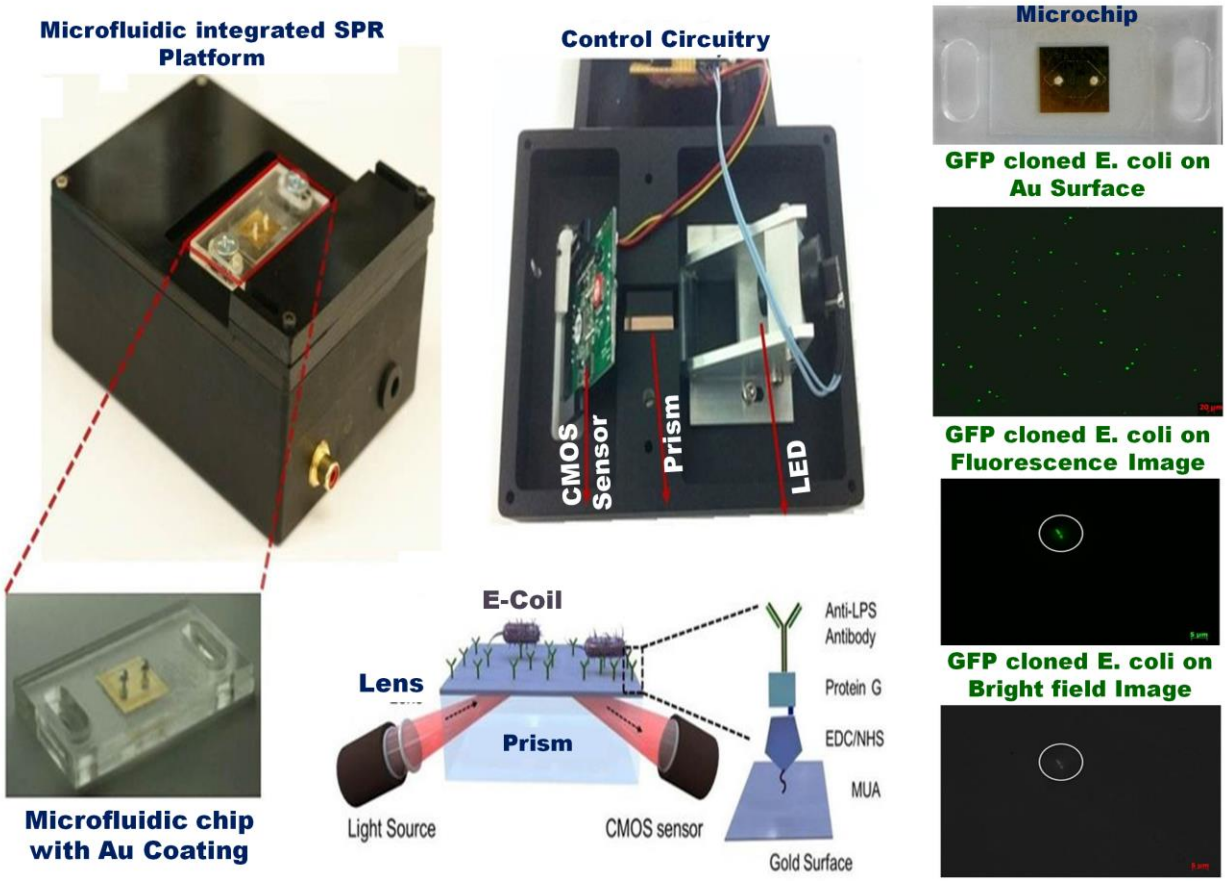
Microfluidic integrated SPR Platform
Control Circuitry
Microchip
GFP cloned E. coli on Au Surface
CMOS Sensor
Prism
LED
GFP cloned E. coli on Fluorescence Image
GFP cloned E. coli on Bright field Image
E-Coil
Anti-LPS Antibody
Protein G
EDC/NHS
MUA
Lens
Prism
Light Source
CMOS sensor
Gold Surface
Microfluidic chip with Au Coating

Scheme 16

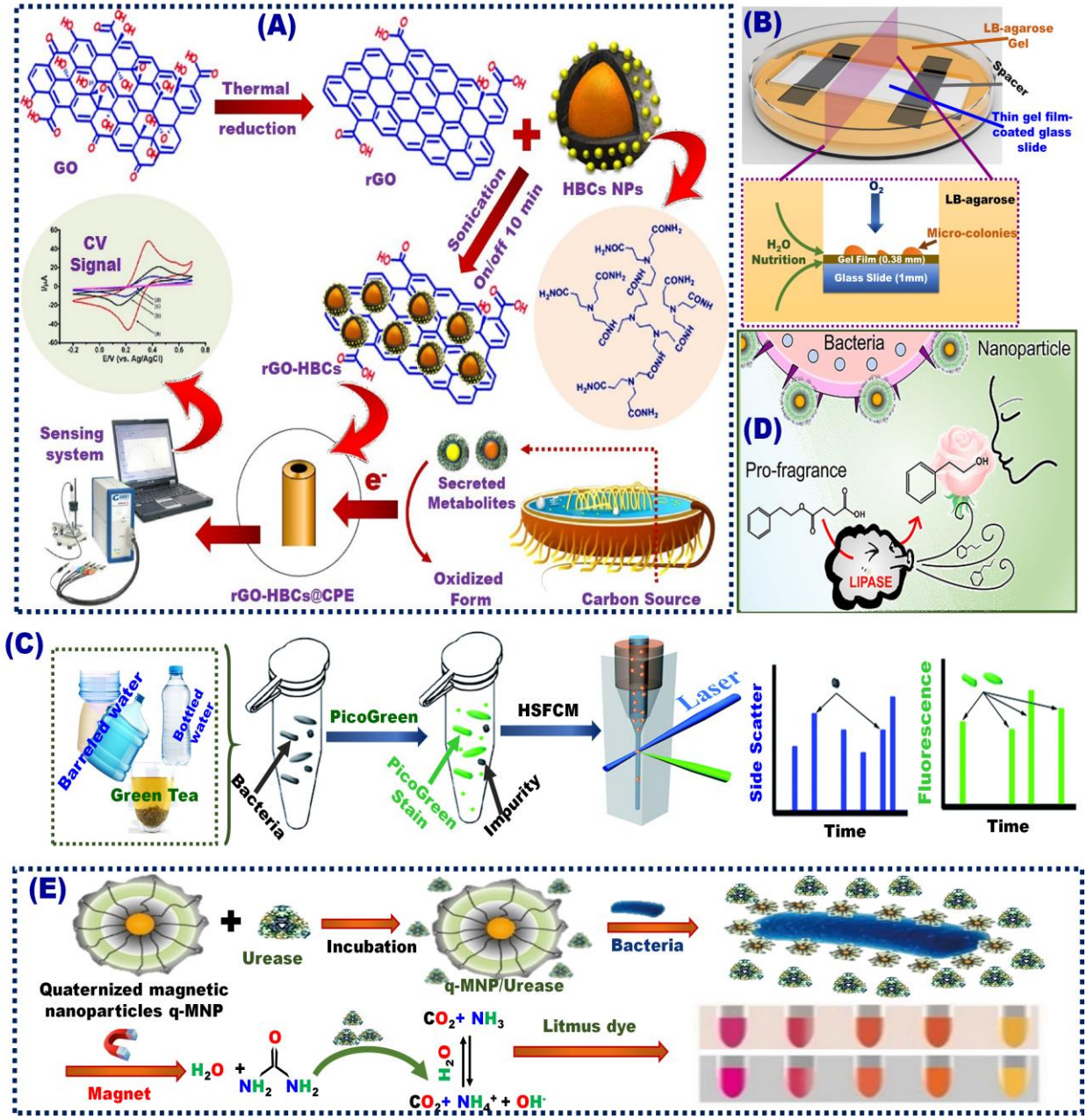
(A)
GO
Thermal reduction
rGO
HBCs NPs
Sonication
On/off 10 min
rGO-HBCs
CV Signal
Sensing system
rGO-HBCs@CPE
e-
Secreted Metabolites
Oxidized Form
Carbon Source
(B)
LB-agarose Gel
Spacer
Thin gel film-coated glass slide
LB-agarose
Micro-colonies
H2O Nutrition
Gel Film (0.38 mm)
Glass Slide (1mm)
(D)
Bacteria
Nanoparticle
Pro-fragrance
LIPASE
(C)
Barreled water
Bottled water
Green Tea
Bacteria
PicoGreen
PicoGreen Stain
Impurity
HSFCM
Laser
Side Scatter
Time
Fluorescence
Time
(E)
Quaternized magnetic nanoparticles q-MNP
Urease
Incubation
q-MNP/Urease
Bacteria
Magnet
H2O
CO2+ NH3
CO2+ NH4+ + OH-
Litmus dye

Scheme 17

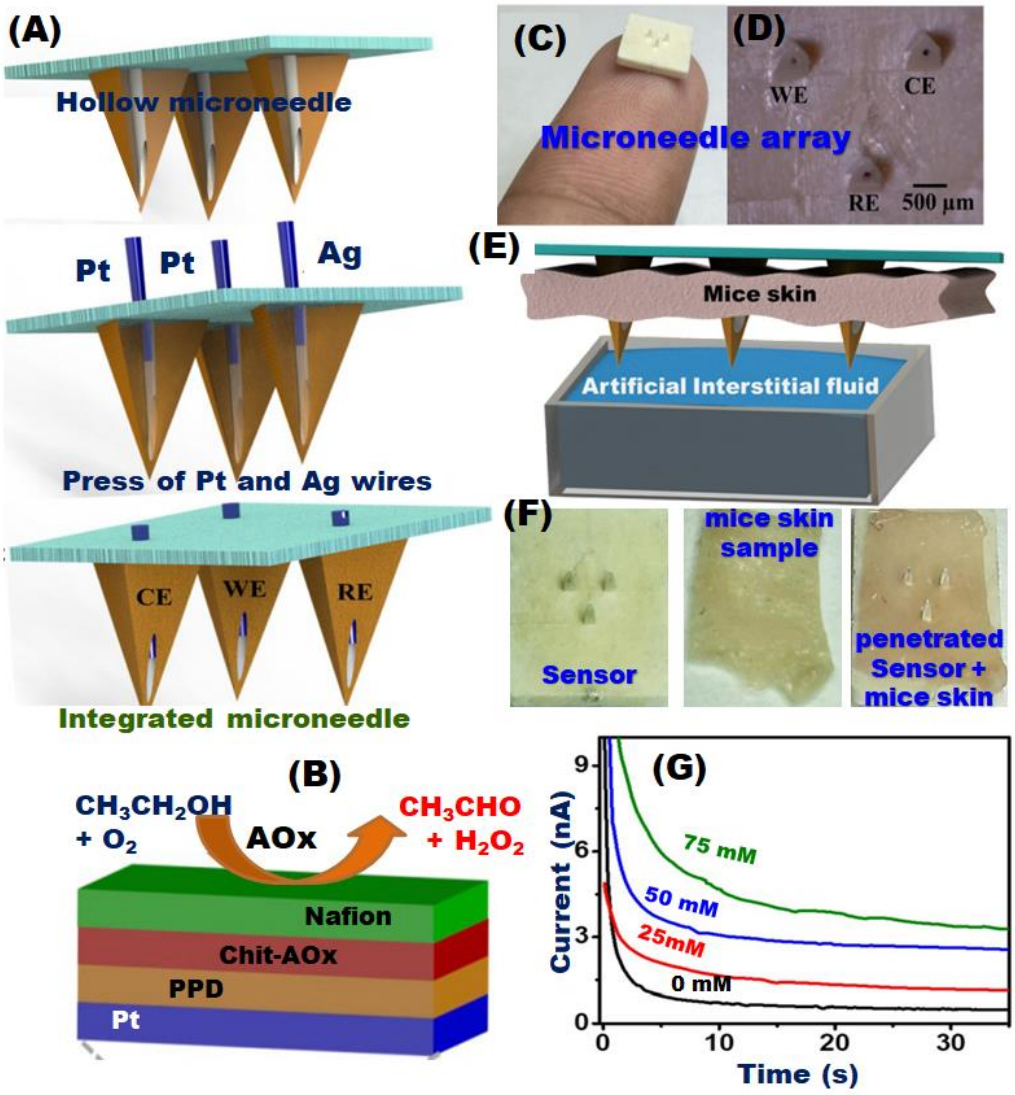
(A)
Hollow microneedle
Pt
Pt
Ag
Press of Pt and Ag wires
CE
WE
RE
Integrated microneedle
(B)
CH3CH2OH
+ O2
AOx
CH3CHO
+ H2O2
Nafion
Chit-AOx
PPD
Pt
(C)
Microneedle array
(D)
WE
CE
RE
500 µm
(E)
Mice skin
Artificial Interstitial fluid
(F)
Sensor
mice skin
sample
penetrated
Sensor +
mice skin
(G)
Current (nA)
Time (s)
75 mM
50 mM
25mM
0 mM
0
3
6
9
0
10
20
30

Scheme 18

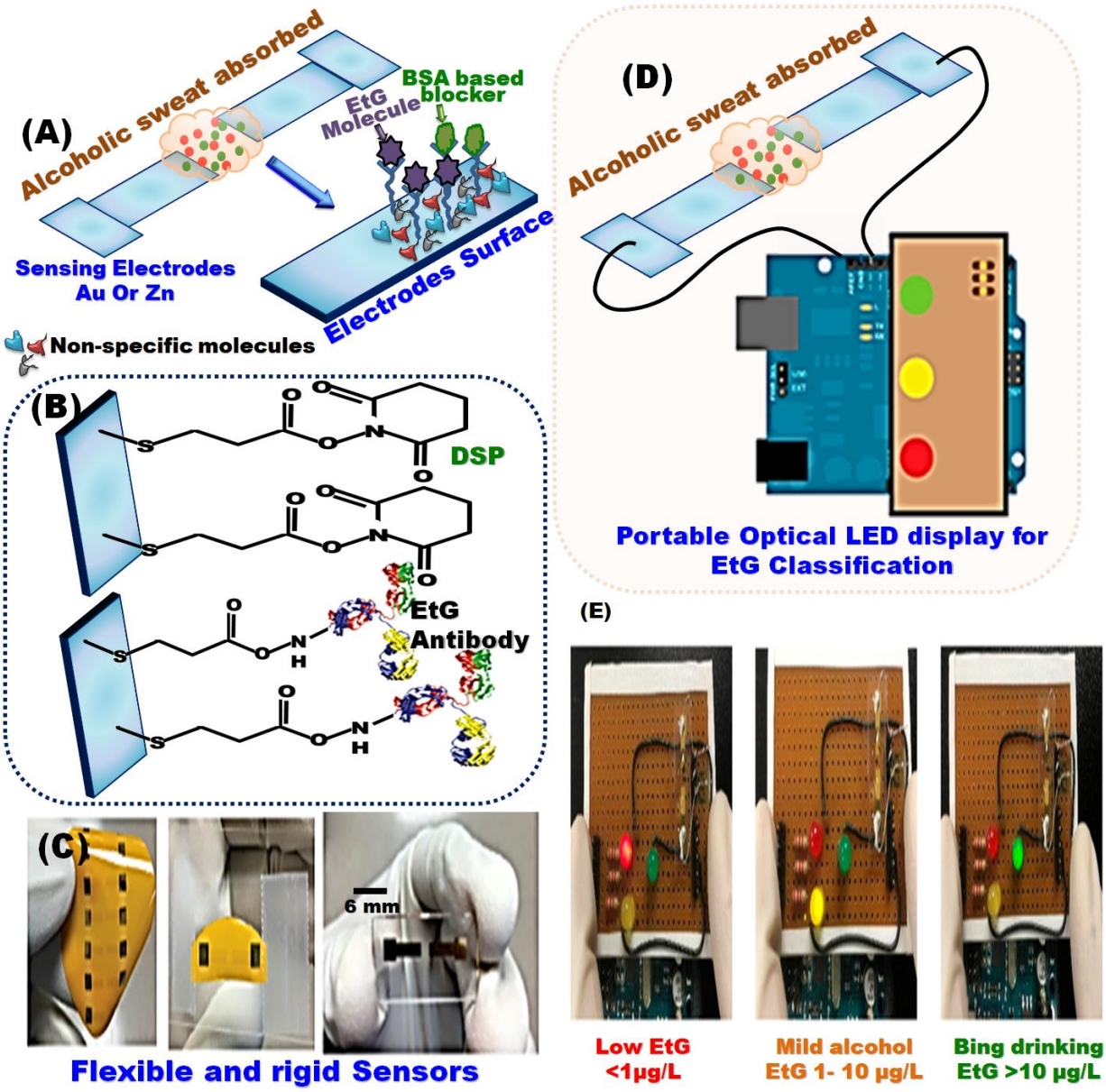
(A)
Alcoholic sweat absorbed
BSA based blocker
EtG Molecule
Sensing Electrodes Au Or Zn
Electrodes Surface
Non-specific molecules
(B)
DSP
EtG Antibody
(C)
6 mm
Flexible and rigid Sensors
(D)
Alcoholic sweat absorbed
Portable Optical LED display for EtG Classification
(E)
Low EtG <1µg/L
Mild alcohol EtG 1- 10 µg/L
Bing drinking EtG >10 µg/L

Scheme 19

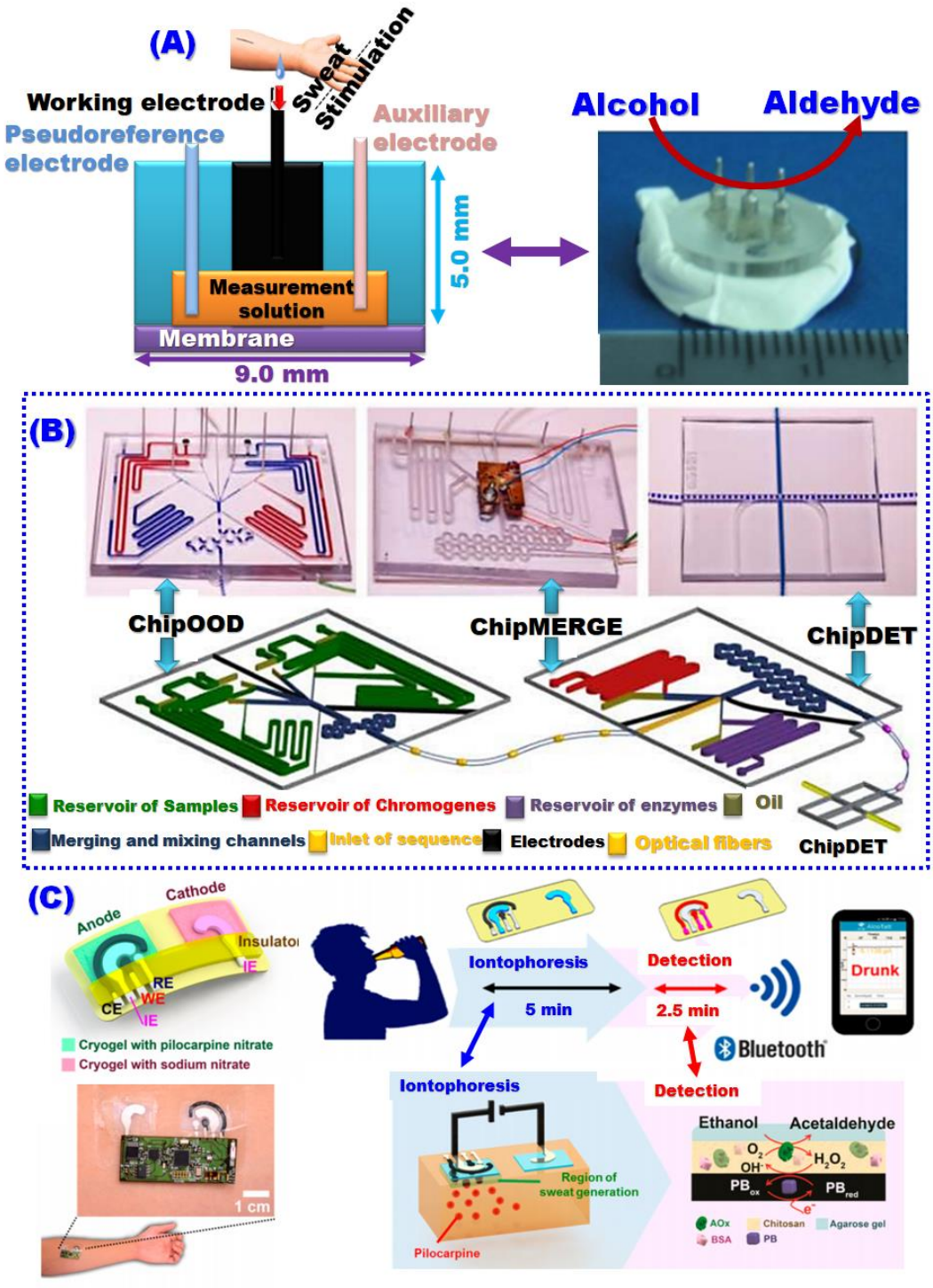
(A)
Sweat Stimulation
Working electrode
Pseudoreference electrode
Auxiliary electrode
Measurement solution
Membrane
5.0 mm
9.0 mm
Alcohol
Aldehyde
(B)
ChipOOD
ChipMERGE
ChipDET
Reservoir of Samples
Reservoir of Chromogenes
Reservoir of enzymes
Oil
Merging and mixing channels
Inlet of sequence
Electrodes
Optical fibers
ChipDET
(C)
Anode
Cathode
Insulator
RE
IE
CE
WE
IE
Cryogel with pilocarpine nitrate
Cryogel with sodium nitrate
1 cm
Iontophoresis
5 min
Detection
2.5 min
Bluetooth
Drunk
Iontophoresis
Detection
Region of sweat generation
Pilocarpine
Ethanol
Acetaldehyde
AOx
Chitosan
Agarose gel
BSA
PB

Scheme 20

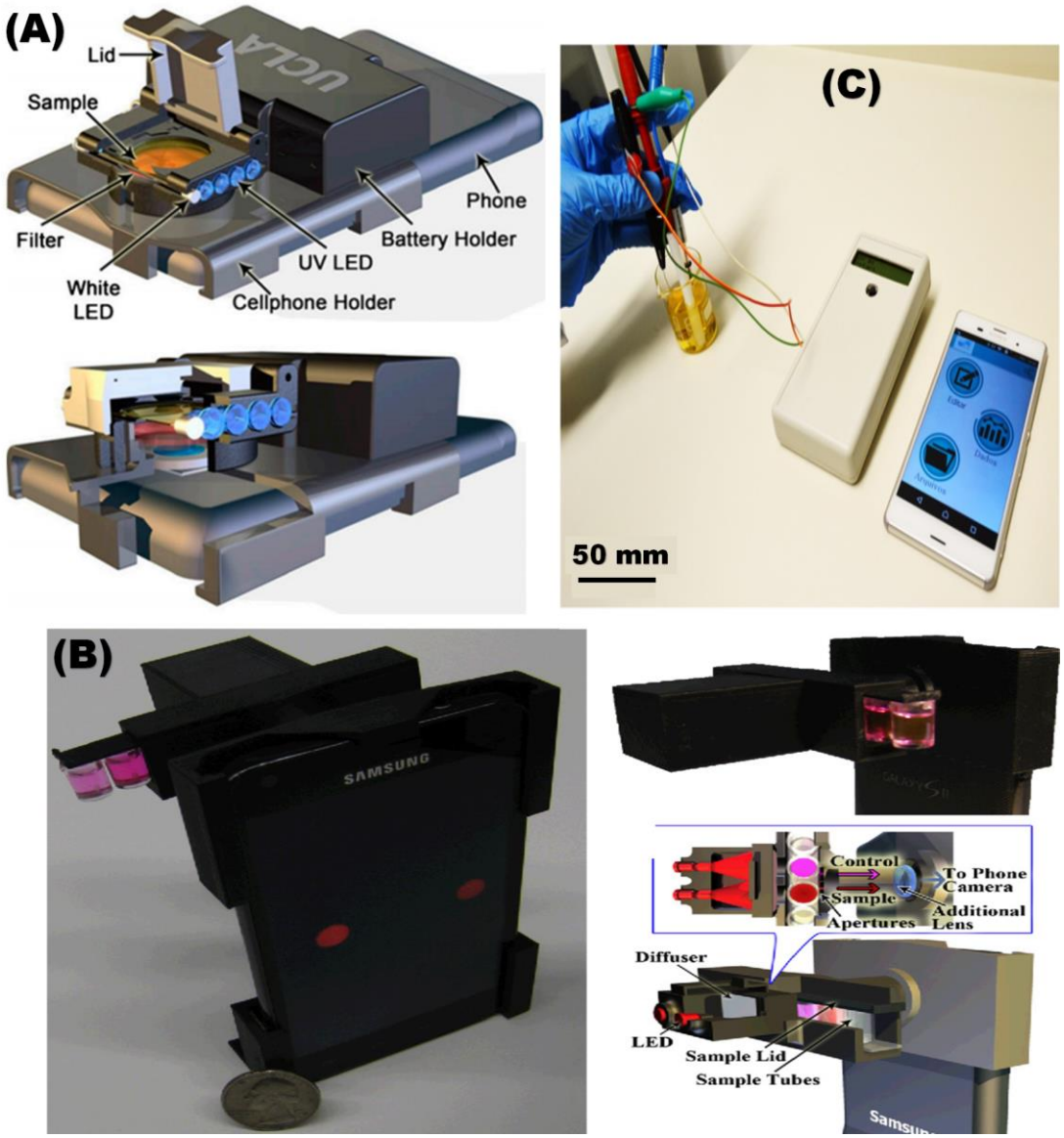
(A)
Lid
Sample
Phone
Filter
Battery Holder
UV LED
White LED
Cellphone Holder
(C)
50 mm
(B)
SAMSUNG
Control
To Phone Camera
Sample
Additional Lens
Apertures
Diffuser
LED
Sample Lid
Sample Tubes

Scheme 21

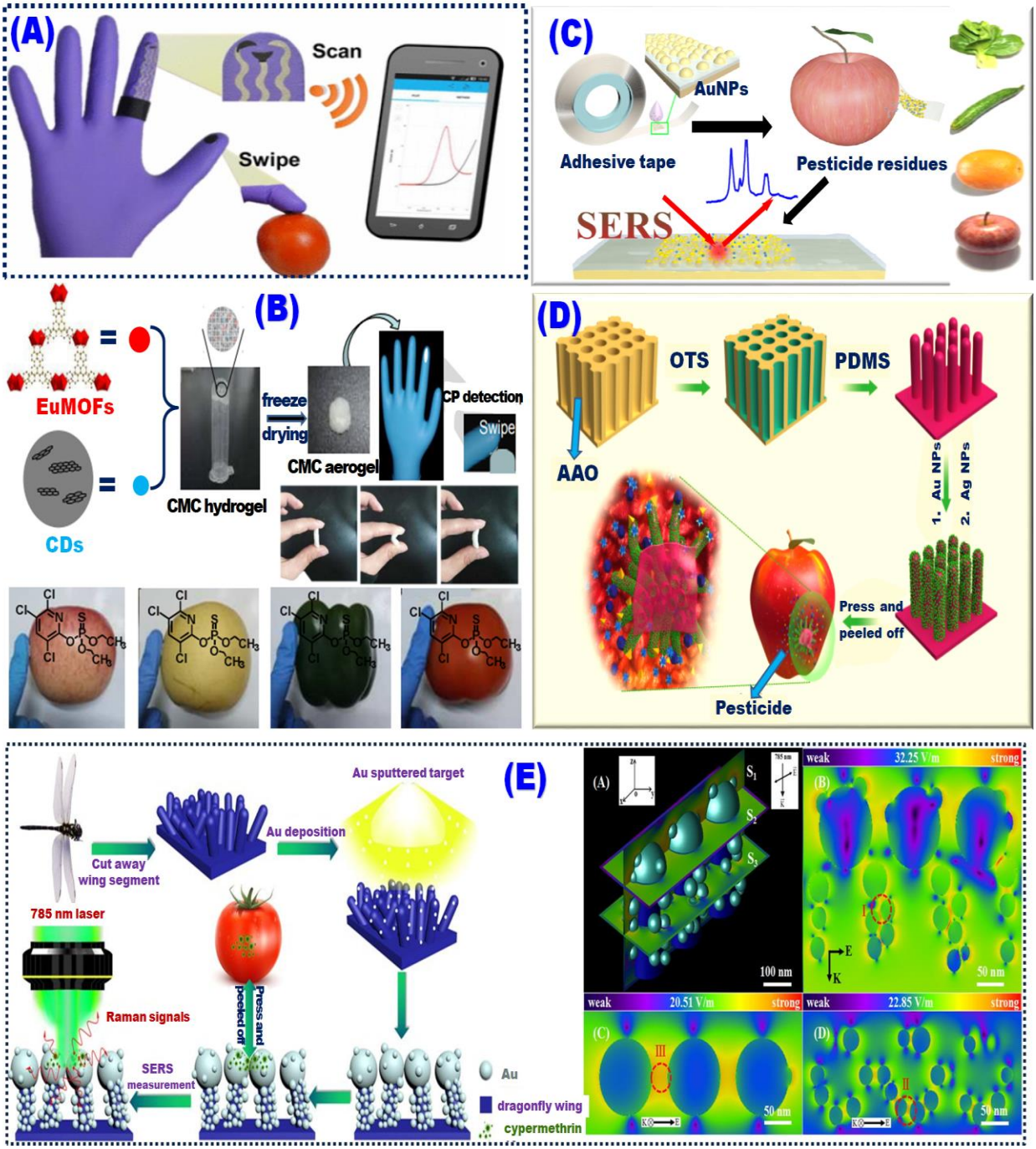
(A)
Scan
Swipe
(C)
AuNPs
Adhesive tape
Pesticide residues
SERS
(B)
EuMOFs
CDs
CMC hydrogel
freeze
drying
CMC aerogel
CP detection
Swipe
(D)
OTS
PDMS
AAO
1. Au NPs
2. Ag NPs
Press and
peeled off
Pesticide
(E)
Au sputtered target
Au deposition
Cut away
wing segment
785 nm laser
Raman signals
SERS
measurement
Press and
peeled off
Au
dragonfly wing
cypermethrin
weak
32.25 V/m
strong
20.51 V/m
22.85 V/m
100 nm
50 nm

Scheme 22

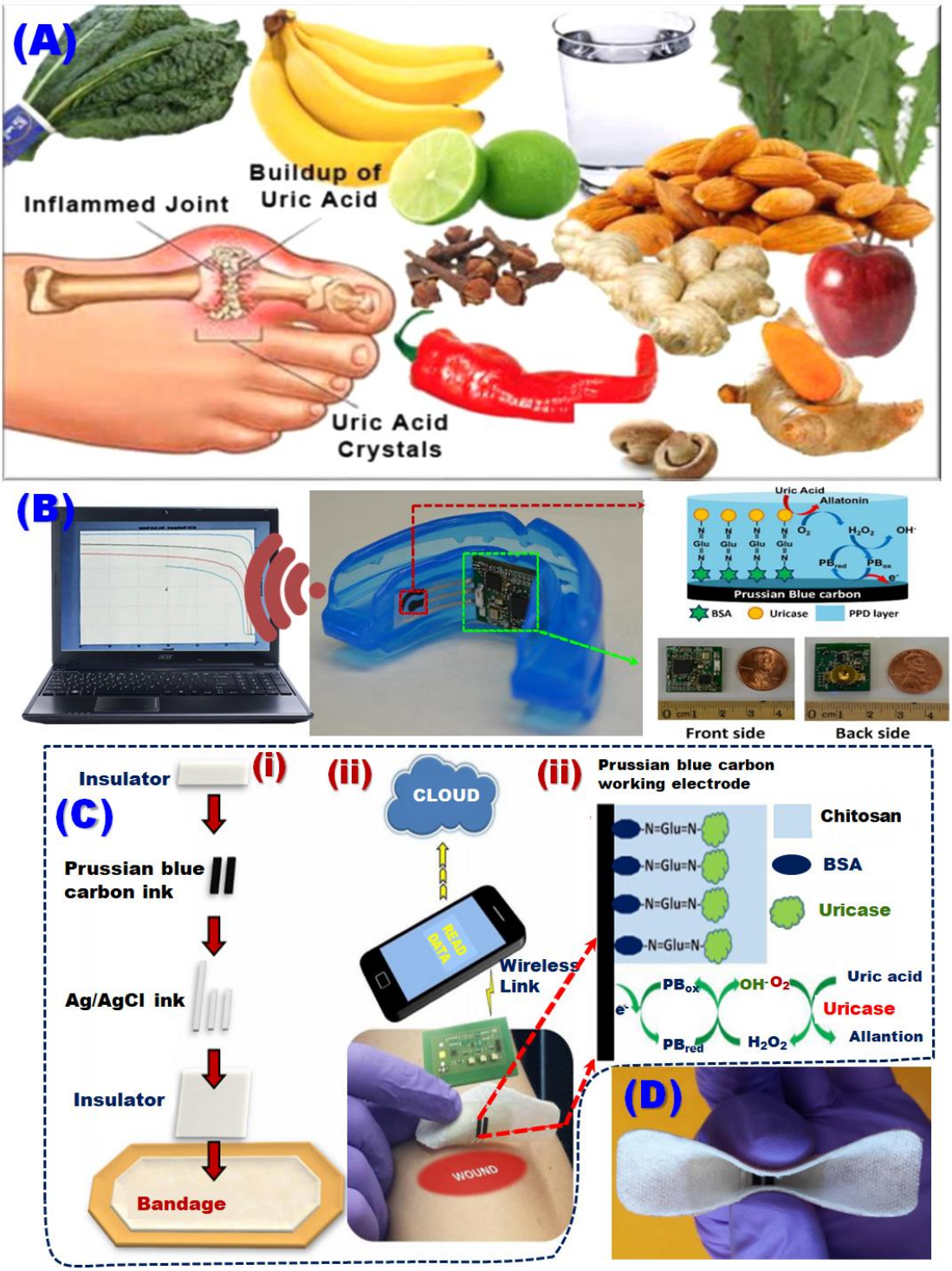
(A)
Buildup of Uric Acid
Inflammed Joint
Uric Acid Crystals
(B)
Uric Acid
Allatonin
Prussian Blue carbon
BSA
Uricase
PPD layer
Front side
Back side
(C)
Insulator
Prussian blue carbon ink
Ag/AgCl ink
Insulator
Bandage
(i)
(ii)
CLOUD
READ DATA
Wireless Link
WOUND
(ii)
Prussian blue carbon working electrode
Chitosan
BSA
Uricase
Uric acid
Uricase
Allantion
(D)

Scheme 23

List of Tables:

Table 1 Various nanoscale sensory systems, and sensing protocols, and analytical techniques reported for sensitive detection of AA targets

AA sensor protocols and designs based materials	Techniques	LOD (µM)	Linear Range (µM)	Ref.
AgNPs	**SERS**	20	20 – 10000	[90]
AgNPs		0.04	15.18 – 23.48	[93]
SiNPs/BSA/MnO_2	**Fluorescence**	0.102	1 – 400	[95]
Carbon nanocages		0.0972	2 – 12	[96]
N, S-CDs		4.69	10–200	[110]
GQDs		0.094	0.3 – 10	[97]
polypyrrole/GQDs		0.005	0.02–5.66	[104]
CDs		0.136	0.136 – 0.23	[105]
GQDs		0.32	1.11 – 300	[106]
N-CDs		0.3	1 – 750	[107]
P-, N-, doped CQDs		1.35	5 – 200	[108]
N-, S- doped CDs		0.17	0.57 – 264	[109]
polyallylamine-AuNCs/MnO_2 nanosheets		0.0032	0.01 – 200	[101]
SiQDs		0.57	2 – 200	[102]
o-phenylenediamine/ CDs		0.009	0.6 – 40	[103]
AuNPs/Luminol	**Chemiluminescence**	20000	10000 – 1	[115]
Cu^{2+}/NGQDs/H_2O_2		0.5	1 – 100	[117]
CdSe/CdS QDs		0.0067	10 – 100	[118]
NiO/GR	**Electrochemical**	0.0167	0.05 – 1100	[120]
NPC/Co_3O_4		0.02	2 – 240	[121]
Carbon fibers/ZnO			600 – 2000	[122]
AgNPs		14.63	150 – 2000	[124]
PEDOT:PSS/OEXTS		0.1	0.01 –10000	[125]
MIPs (o-phenylenediamine and pyrrole)		0.263	1– 1000	[127]
poly(o-phenylenediamine-co-o-aminophenol) (PoPDoAP)		36.4	0.1 – 10000	[128]
TiO2/rGO		1.19	25– 725	[129]
pNR/rGO		1.4	0.05 – 0.75	[130]
graphene-iron oxide-polyvinyl alcohol		0.234	40 – 4100	[132]

Table 2. Various nanoscale sensory systems, and sensing protocols, and analytical techniques reported for sensitive detection of H_2O_2 molecules

H_2O_2 sensor protocols and designs based materials	**Techniques**	**LOD (µM)**	**Linear Range (µM)**	**Ref.**
MP-11/Tb@mesoMOFs/CHIT-AuNPs/3D-KSCs	**Electrochemical**	0.996	3.02 – 640	[113]
PtPb/G		0.05	0.05 – 30	[172]
MP-11/ SnO_2		0.996	3.02 – 640	[173]
α-Fe_2O_3/rGO		0.002	0.002– 2500	[133]
Fe_2O_3/ITO		1	5-4495	[181]
Co_3O_4-MCNFs		0.3	1-360	[182]
Co_3O_4/ SPCE		0.5	1-2580	[179]
Co_3O_4/MWCNTs		0.145	0.1-50	[178]
Co_3O_4 nanowalls/GCE		2.46	20-430	[177]
3D GO–Co_3O_4 PHs/SPCE		10	0-5350	[168]
MP-11 /PCN-333 (Al)/ 3D-KSC		0.7664	250–4750	[166]
3D GO-Co_3O_4		0.015	0.05–400	[167]
Cytochrome C/Ni-Foam		0.127	0.387 – 1725	[174]
Co_9S_8 hollow spheres		0.02	0.1 -11110	[183]
Au@C-Co3O4		0.2	50 – 128000	[175]
$Ni(OH)_2$/RGO/Cu_2O		0.143	1 –30000	[189]
MoS_2/CN NWs [9]		0.35	0.5 – 7500	[186]
Ag NPs	**Colorimetry**	0.0294	0.01–10000	[140]
Ag-NPs/optical fiber		10	10 – 10000	[139]
Au-Ag/C NC		0.00864	1 – 120	[147]
GO-PtNi-3,3′,5,5′-tetramethylbenzidine		0.3	0.8–90	[148]
Chitosan		5	8 – 1500	[150]
HRP/BSA/glutraldehyde	**Fluorescence**	1.55	10 – 10000	[146]
Coumarin		0.5	0.5 –100	[143]
Iodophenol blue-luminole	**Chemiluminescence**	0.01	0 –80	[157]
Ag (I)-Luminol-$CoFe_2O_4$		0.014	0.025–10	[152]
Bovine serum albumin (BSA) caped silver nanoclusters (Ag NCs)		0.15	0.5 –100	[161]
Luminol/H_2O_2/GNPs CL		0.14	0.14 –100	[162]
GO–CdS nanocrystal nanocomposites		1.7 µM	5 µM–1 mM	[164]
Hexythiazox (HXTZ)		0.011 µg mL^{-1}	0.017-0.42 µg mL^{-1}	[165]

Table 3. Various nanoscale sensory systems, and sensing protocols, and analytical techniques reported for sensitive and selective detection of food ingredients and additives of nitrite and sulfite species

Sensor protocols and designs based materials	Techniques	LOD (µM)	Linear Range (µM)	Ref.
Detection of nitrite species				
AgNPs	**Colorimetry**	0.1	0.1 – 50	[219]
Carbon dots (C-dots) and neutral red		0.196	0.145 –4.34	[220]
N-(1-naphthyl)ethylenediamine/PEG		10	10 – 5000	[222]
CoOx/CNT/GCE	**Electrochemical**	0.3	0.5-249	[231]
CoNS/GO/PPy/GCE		0.015	1-3200	[232]
Pd/rGO/GCE		23	1–1000	[233]
Ag-rGO/GCE		0.012	0.1–120	[234]
Ag/HNT/MoS_2/CPE		0.7	2 - 425	[235]
rGO-C60/AuNPs		0.013	0.05–1175.32	[236]
Au-HNTs-GO		0.03	0.1 - 6330	[237]
a-Fe_2O_3 NAs/CF		0.12	0.5 - 1000	[238]
Detection of sulfite species				
TSP [10]	**Fluorescence**	0.2	0.5–150	[248]
Naphthofluorescein		1.74	0–300	[252]
Carbon-dots		0.35	10 – 50	[255]
CPE/Au-Si4Pic+Cl	**Electrochemical**	0.88	2.54 – 48.6	[256]
n-CoNP/CPE		40	1 – 59, 2000 – 8000	[257]
PrHCF		2.15	600 – 8000	[258]
CoHCF/ graphitic carbon		1.7	4 –128	[259]
PTZ-IL/MWCNT/GCE		9.3	30–1177	[260]
CTAB-chitosan-CNTs		9.6	30 – 800	[261]

Table 4. Various nanoscale sensory systems, and sensing protocols, and analytical techniques reported for sensitive detection of hazardous organic and inorganic species such as heavy metals and bisphenol A.

Sensor protocols and designs based materials	Target	Techniques	LOD (μM)	Linear Range (μM)	Ref.
SWCNT- Thiophenol (PhSH)/Au electrode	Hg (II)	Electrochemical	0.003	0.005 – 0.09	[303]
$GSH@Fe_3O_4$ Glutathione functionalized magnetic nanocomposite	Pb (II)		0.00087	0.0024 – 0.5	[275]
	Cd (II)		0.0015	0.004 – 0.9	
GQDs/ Au electrode	Hg (II)		0.00002	0.00002 – 0.0015	[274]
	Cu (II)		0.00005	0.00005 – 0.5	
$CDs@g\text{-}C_3N_4$ Carbon dots@graphitic-carbon nitride	Cr (VI)	Fluorescence	0.00054	--	[273]
	Cu (II)		0.00018	--	
	Pb (II)		0.00002	--	
PVDF-g-PAA-CDs	Cu (II)		0.001	--	[272]
	Hg (II)		0.001	--	
	Fe (III)		1	--	
Ratiometric fluorescent chemosensors (RFCs)/Zr-MOF	Zn (II)		0.000447	--	[296]
S1/Zr-MOF [1]	Zn (II)		0.001	0.008 – 31	[294]
PHBS-sensor [2]	Fe (III)		17		[293]
BTSIXO [3]	Bisphenol A	Colorimetry	0.0876	0.4 –657	[321]
38-mer and 12-mer aptamers/ AuNPs			7.6×10^{-6}	--	[322]
			14.41×10^{-6}	--	
24-bp aptamer/ AuNPs			0.004	0.000004 – 4	[323]
BSA-spescific aptamer/AuNPs			0.0015	--	[324]
ZnFe2O4 and cellulose fibers/MIP			0.0618	0.01 – 1	[325]
DNA–QD_{655}/ magnetic beads (MBs)		Fluorescence	0.74×10^{-9}	--	[327]
FAM-ssDNA/GO			0.02	0.4 – 40	[329]
CdTe QDs/ AuNPs			0.008	0.004 – 0.35	[330]
Boron-doped diamond		Electrochemical	0.005	0.1 – 50	[331]
β-cyclodextrin/MWCNTs			0.006	0.05 – 5	[332]
Tyrosinase/MWCNTs			0.03	0.05 – 3	[333]
TiO_2			0.003	0.01 – 20	[335]
Carboxylic acid functionalized carbon black (CB)/f-MWCNTs			0.08	0.1 – 130	[336]
Cu−Zn/GO/GCE			0.00088	0.003 – 0.1	[337]
TiO_2/Au NTAs			0.0062	0.1 – 28.9	[338]

[1] (2,2′-((1Z,12Z)-5,9-dithia-2,12-diazatrideca-1,12-diene-1,13 diyl) diphenol), (S1)/Zr-MOF

[2] 4-(2-(3-Methyl-5-oxo-1-tosyl-1H-pyrazol-4(5H)-ylidene) hydrazinyl)-N-(pyrimidin-2-yl) benzenesulfonamide (PHBS-sensor)

[2] 3′, 6′- bis(diethylamino) -2- ((3,4,5 trimethyl benzylidene) amino) spiro [isoindoline-1,9′-xanthen] -3-one

Table 5. A list of commercial mobile sensor devices used in the assessment of food quality.

Sensor devices	Target	Ref.	Device image
Food / Hygiene ATP Testing Meter PCE-ATP 1 KIT	Rapid detection food microorganism bacteria detection instrument	https://www.pce-instruments.com/english/measuring-instruments/test-meters/food-hygiene-pce-instruments-food-hygiene-atp-testing-meter-pce-atp-1-kit-det_5855674.htm	
Handheld ATP fluorescence detector	Rapid detection food microorganism bacteria detection instrument	https://www.aliexpress.com/item/4001269652463.html	
RapidChek®	High Performance Food Pathogen Detection Automated Pathogen Detection	https://www.biomerieux-industry.com/products/vidas-high-performance-food-pathogen-detection	
RapidChek® E. coli O157	E. coli O157	https://www.romerlabs.com/en/analytes/food-pathogens/e-coli/	
Livermore Lab and LexaGene's LX6	A Rapid and Sensitive Pathogen Detection System	https://federallabs.org/successes/success-stories/livermore-lab-and-lexagene%E2%80%99s-lx6-a-rapid-and-sensitive-pathogen-detection	
HD Pesticide residue detector	Detection of pesticides invegetable, fruit, meat, tea, household food safety, heavy metal rapid test instrument	https://www.aliexpress.com/item/1005001389512206.html?spm=a2g0o.detail.1000023.3.2d48141ded8XHS	
GeneDisc® Rapid Microbiology System	Pathogen detection	https://www.pall.com/en/food-beverage/quality-control.html	
BD Veritor™ instruments	Rapid COVID-19 test	https://www.prnewswire.com/news-releases/bd-launches-portable-rapid-point-of-care-antigen-test-to-detect-sars-cov-2-in-15-minutes-dramatically-expanding-access-to-covid-19-testing-301088216.html	
Food / Hygiene Temperature Meter PCE-ST 1	Food / hygiene temperature	https://www.pce-instruments.com/english/measuring-instruments/test-meters/food-hygiene-kat_42003.htm	
Abbott's ID NOWTM platform	Rapid test for COVID-19	https://www.abbott.com/corpnewsroom/diagnostics-testing/detect-covid-19-in-as-little-as-5-minutes.html	
Ascorbic Acid Portable Test Kits (Hach)	Ascorbic Acid	https://www.weberscientific.com/ascorbic-acid-portable-test-kits-hach	

HI 767	Marine checker Low concentration nitrite nitrogen	https://hanna.co.jp/item-hi767.html	
HI 3854	Zinc test kit	https://www.e-hanna.info/cart/shop/HI3854.html	
HI 3850	Ascorbic acid (vitamin C) test kit	https://www.e-hanna.info/cart/shop/HI3850.html	
HI 3822	Sulfite test kit	https://www.e-hanna.info/cart/shop/HI3822.html	
HI 3844	Hydrogen peroxide test kit	https://www.e-hanna.info/cart/shop/HI3844.html	
HI 3847	Copper test ki	https://www.e-hanna.info/cart/shop/HI3847.html	
HI 3864	Phenol test kit	https://www.e-hanna.info/cart/shop/HI3864.html	
Lancets Lanceting Device	Uric Acid Mete	https://cnzhizao.en.alibaba.com/product/60814874977-804571538/Uric_Acid_Meter_Monitor_Detector_UA_Monitoring_System_Test_Strips_Paper_Lancets_Lanceting_Device.html	
BFD-100	Meat quality assessment	https://www.innovationnewsnetwork.com/portable-measurement-device-food-quality/430/